

## **Distribution Agreement**

In presenting this thesis or dissertation as a partial fulfillment of the requirements for an advanced degree from Emory University, I hereby grant to Emory University and its agents the non-exclusive license to archive, make accessible, and display my thesis or dissertation in whole or in part in all forms of media, now or hereafter known, including display on the world wide web. I understand that I may select some access restrictions as part of the online submission of this thesis or dissertation. I retain all ownership rights to the copyright of the thesis or dissertation. I also retain the right to use in future works (such as articles or books) all or part of this thesis or dissertation

Signature:

---

Bejan J. Saeedi

---

Date

**Gut-Resident Microbes Modulate Hepatic Metabolism and Susceptibility to Disease**

By

Bejan J. Saeedi  
Doctor of Philosophy

Graduate Division of Biological and Biomedical Science  
Biochemistry, Cell and Developmental Biology

---

Andrew S. Neish, MD  
Advisor

---

Paul Dawson, PhD  
Committee Member

---

Michael Koval, PhD  
Committee Member

---

Ken Moberg, PhD  
Committee Member

---

Eric Ortlund, PhD  
Committee Member

Accepted:

---

Lisa A. Tedesco, PhD  
Dean of the James T. Laney School of Graduate Studies

---

Date

**Gut-Resident Microbes Modulate Hepatic Metabolism and Susceptibility to Disease**

By

Bejan J. Saeedi

B.S., Colorado State University, 2010

Advisor: Andrew S. Neish, MD

An abstract of

A dissertation submitted to the Faculty of the

James T. Laney School of Graduate Studies of Emory University

In partial fulfillment of the requirements for the degree of

Doctor of Philosophy

In Biological and Biomedical Science: Biochemistry, Cell and Developmental Biology

2020

## ABSTRACT

### **Gut-Resident Microbes Modulate Hepatic Metabolism and Susceptibility to Disease**

By Bejan J. Saeedi

The microbes that reside within the intestine are powerful modifiers of host fitness and susceptibility to disease. In the past 20 years, advances in 16S sequencing have allowed for a more thorough investigation of the community architecture of the gut microbiome. Germ-free or antibiotic treated model organisms, coupled with metabolomics, proteomics, and metagenomics, have provided some insight into the functional consequences of perturbations within these communities. While significant progress has been made, the vast majority of these studies have scrutinized the effects of the microbiome within the context of host intestinal health. Recent research, however, has identified profound impacts of the microbiome on organs distal to the gut, with implications for cardiovascular, immunological, and even neurological health. However, the pace of phenotypic characterization has outstripped that of mechanistic understanding. In the studies that follow, we pair big data approaches (small molecule metabolomics and RNA sequencing) with validation in experimentally tractable systems (cell lines, transgenic mice, and *Drosophila*) to assess the effects and underlying molecular mechanisms of the gut microbiome on hepatic metabolism and susceptibility to disease. We identify a microbiome-derived small molecule,  $\delta$ -valerobetaine, that is absorbed systemically and acts to lower carnitine levels and inhibit fatty acid oxidation. We characterize the effect of microbial colonization on hepatic signaling, and observe that the master regulator of the cellular antioxidant response Nrf2 is tonically activated by the presence of a microbiome. Furthermore, we narrow down the contributing microbial genera, and demonstrate that exogenous administration of Lactobacilli can augment this signaling in conventional mice with consequences for oxidative liver injury. Finally,

we develop and validate a novel model of oxidative liver injury in *Drosophila*. These studies together contribute some mechanistic understanding to our burgeoning appreciation of the systemic effects of the microbiome.

**Gut-Resident Microbes Modulate Hepatic Metabolism and Susceptibility to Disease**

By

Bejan J. Saeedi

B.S., Colorado State University, 2010

Advisor: Andrew S. Neish, MD

A dissertation submitted to the Faculty of the

James T. Laney School of Graduate Studies of Emory University

In partial fulfillment of the requirements for the degree of

Doctor of Philosophy

In Biological and Biomedical Science: Biochemistry, Cell and Developmental Biology

2020

## Acknowledgements

I could double the length of this dissertation in an attempt to adequately thank all of the mentors, colleagues, friends, and family that made this document possible. For the sanity of the reader and author alike, I will try to keep it brief. My deepest thanks to those that follow for shaping the arc of my career to this point.

First, I want to thank my mentors at Emory. Dr. Andrew Neish, my PhD advisor, has helped me become an independent scientist. His mentorship gave me the freedom to pursue my own interests and helped me realize my own abilities. He also has an innate sense of where the field is headed, and I hope some of that rubbed off on me. “Skate where the puck is going, not where it’s been” could just as well be attributed to Andy Neish as Wayne Gretzky.

Dr. Michael Koval, my program director and committee member, has always been there for me, particularly in some of my darkest times in graduate school. I likely wouldn’t be writing these acknowledgements without his selfless and unwavering support. The other members of my committee have been similarly supportive. My thanks for all of the time and effort Dr. Eric Ortlund and Dr. Ken Moberg put into my education. Also, thanks to Dr. Saul Karpen, my MD-PhD advisor, for all of his advice over the years.

I cannot adequately express my gratitude to Dr. Paul Dawson. He has been a mentor and friend throughout my PhD. He served on my committee, acted as a co-sponsor for my grant application, gave me myriad opportunities to travel to meetings and courses across the country, and even crewed me at my trail races. When I think of the ideal scientist and all that that entails, including intellect, rigor, and mentorship, I think of Paul Dawson.

A huge thanks to all of the mentors that guided me before I entered the MD-PhD program. Dr. Brian Geiss, my first PI, for giving me the opportunity to fall in love with basic science

research. Dr. Louise Glover for shaping my technical and critical thinking skills. Dr. Sean Colgan for his unflagging support and mentorship without which I would most definitely not have pursued an education as a physician scientist.

When I joined Dr. Colgan's lab, I knew what MD-PhD was, but didn't necessarily know what it looked like. Two people fundamentally shaped my view of MD-PhDs: Caleb Kelly and Dan Kao. Without these two, I would likely have gone straight to medical school and tried to pursue research as a resident or fellow. But Caleb was so immersed and excited about his work, knew all of the literature so well, and was a pretty good chess player (I have beaten him a few times). He impressed on me the importance of time. Time to read, time to tinker, time to fret over minute details. PhD training allows you this time. As a resident, I would never have that same amount of time to hone my skills as a scientist. Dan Kao was next. He was (and is) piercingly brilliant, hard working, and yet even-keeled with an easy sense of humor. In short, all that I aspired to be. He and Caleb had a raw confidence about them that was infectious. The final straw came when I went to Dr. Colgan's office and he told me I should apply to MD-PhD programs. "Look at Caleb and Dan," he said, "You've got the phenotype." I've never looked back.

At Emory, another MD-PhD would reinforce these views: Dr. Brian Robinson. Brian Robinson is a brilliant and hardworking scientist that I had the privilege to work alongside in Dr. Neish's lab. He was instrumental in providing scientific support, career advice, and in acting as a general scientific sounding board for all of my various projects over the years. Perhaps most importantly, he is an incredibly loyal friend. Thank you, Dr. Robinson, for everything. I also want to thank Joshua Owens, who I had the privilege of working alongside every day. Watching Josh develop into an incredibly adept young scientist has been a joy.

Dr. Ken Liu and I worked side by side to develop the projects that make up the bulk of both of our dissertations. Dr. Liu never hesitated to share data or resources or ideas, and it allowed us to form a remarkable collaboration that has resulted in multiple co-first author papers. Thank you, Dr. Liu.

I also want to thank my fellow students, those in my MD-PhD cohort as well as those in the biochemistry, cell and developmental biology graduate program. This journey is not possible without community, and I couldn't have hoped for a better community than you all provided.

Finally, I want to thank all of the family and friends that supported me, encouraged me, and distracted me during this process. I want to thank in particular my wife, Brittney, for pushing me to do this in the first place. Thank you for always believing in me.

# Table of Contents

<b>THE MICROBIOME-LIVER AXIS IN HEALTH AND DISEASE .....</b>	<b>1</b>
1.1 INTRODUCTION.....	2
1.2 STRUCTURE AND FUNCTION OF THE GUT MICROBIOME .....	2
1.3 SYSTEMIC EFFECTS OF THE MICROBIOME .....	3
1.4 THE PORTAL CIRCULATION .....	4
1.5 DETOXIFICATION ACTIVITIES OF THE LIVER .....	5
1.6 LIVER DISEASE AND THE MICROBIOME .....	7
1.7 THE MICROBIOME AS A THERAPEUTIC MODALITY .....	8
1.8 PROBIOTICS AND LIVER DISEASE .....	11
1.9 <i>DROSOPHILA</i> AS A MODEL FOR THE MICROBIOME-LIVER AXIS .....	12
1.10 CONCLUSION .....	14
1.11 REFERENCES.....	17
<b>THE MICROBIOME-DERIVED METABOLITE <math>\delta</math>-VALEROBETAIN INHIBITS HEPATIC MITOCHONDRIAL FATTY ACID OXIDATION AND EXACERBATES HEPATIC STEATOSIS.....</b>	<b>30</b>
2.1 INTRODUCTION .....	32
2.2 RESULTS .....	34
2.2.1 <i>Identification of the microbiome-derived mitochondrial metabolite <math>\delta</math>-valerobetaine (VB)</i> .....	34
2.2.2 <i>The gut microbiome produces VB</i> .....	37
2.2.3 <i><math>\delta</math>-valerobetaine (VB) decreases cellular carnitine in cultured HepG2 cells</i> .....	39
2.2.4 <i><math>\delta</math>-valerobetaine (VB) decreases palmitate-dependent mitochondrial respiration in HepG2 cells</i> .....	41
2.2.5 <i>VB decreases formation of labeled acetyl-CoA production from labeled palmitic acid</i> .....	41
2.2.6 <i>VB decreases carnitine and decreases mitochondrial fatty acid oxidation in conventional mice</i> .....	44
2.2.7 <i>VB is associated with the severity of hepatic steatosis in adolescents and with visceral adiposity in adults</i> .....	48
2.3 DISCUSSION.....	50
2.4 METHODS .....	53
2.5 REFERENCES .....	62
<b>A <i>DROSOPHILA</i> MODEL OF ACETAMINOPHEN TOXICITY .....</b>	<b>71</b>
3.1 INTRODUCTION .....	73
3.2 RESULTS .....	75
3.2.1 <i>Acetaminophen Accumulates in Drosophila</i> .....	75
3.2.2 <i>Acetaminophen exposure results in dose-dependent mortality in WT Drosophila</i> .....	77
3.2.3 <i>APAP Administration Increases ROS in the Drosophila Fat Body and Depletes Systemic Glutathione</i> .....	78
3.2.4 <i>Fat body-specific depletion of Cyp18a1 attenuates APAP toxicity</i> .....	80
3.2.5 <i>Genetic and pharmacologic modifiers of APAP toxicity in Drosophila</i> .....	81
3.2.6 <i>The microbiome protects against acetaminophen toxicity in Drosophila</i> .....	83
3.2.7 <i>Effects of age on APAP-induced mortality</i> .....	84
3.3 DISCUSSION.....	86
3.4 METHODS .....	88
3.5 REFERENCES .....	91
<b>GUT-RESIDENT <i>LACTOBACILLI</i> ACTIVATE HEPATIC NRF2 AND PROTECT AGAINST OXIDATIVE LIVER INJURY .....</b>	<b>95</b>
4.1 INTRODUCTION .....	97
4.2 RESULTS .....	100
4.2.1 <i>Conventionalization of germ-free mice alters the hepatic metabolome</i> .....	100

4.2.2 Conventionalization of germ-free mice induces the hepatic Nrf2 antioxidant response pathway .....	102
4.2.3 Symbiotic <i>Lactobacilli</i> sp. activate the Nrf2 pathway in the <i>Drosophila melanogaster</i> fat body .....	104
4.2.4 Oral administration of <i>Lactobacillus rhamnosus</i> GG activates Nrf2 signaling in the murine liver .....	106
4.2.5 <i>Lactobacillus rhamnosus</i> GG protects the <i>Drosophila</i> fat body against toxicity in a Nrf2-dependent manner .....	108
4.2.6 <i>Lactobacillus rhamnosus</i> GG administration attenuates acetaminophen hepatotoxicity in conventional mice.....	111
4.2.7 Hepatic Nrf2 mediates <i>Lactobacillus rhamnosus</i> GG protection against acetaminophen hepatotoxicity .....	114
4.2.8 Hepatic Nrf2 mediates <i>Lactobacillus rhamnosus</i> GG protection against acute alcohol induced injury.....	116
4.2.9 <i>Lactobacillus rhamnosus</i> GG alters the small molecule milieu of portal serum. ....	118
4.2.10 <i>Lactobacillus rhamnosus</i> GG mediated generation of 5-methoxyindoleacetic acid activates hepatic Nrf2 .....	119
4.2.11 <i>Lactobacilli</i> produce 5-MIAA <i>in vitro</i> .....	122
4.3 DISCUSSION.....	124
4.4 METHODS .....	128
4.5 REFERENCES .....	135
<b>DISCUSSION AND FUTURE DIRECTIONS.....</b>	<b>141</b>
5.1 DISCUSSION.....	142
5.2 FUTURE DIRECTIONS .....	144
5.3 REFERENCES .....	148

# List of Figures

Figure 2.1: Identification of the gut microbiome derived metabolite, $\delta$ -valerobetaine (VB) in mouse liver and liver mitochondria. ....	35
Figure 2.2: 160.1332 m/z identified in CV mice is $\delta$ -valerobetaine. ....	36
Figure 2.3: Intestinal microbes produce $\delta$ -valerobetaine. ....	38
Figure 2.4: Effects of VB on the metabolome of HepG2 cells. ....	40
Figure 2.5: Effects of VB on mitochondrial respiration and fatty acid oxidation. ....	43
Figure 2.6: Effects of VB on carnitine levels in mice. ....	46
Figure 2.7: Effect of VB administration of hepatic steatosis. ....	47
Figure 2.8: Clinical phenotypes associated with circulating VB. ....	49
Figure 3.1: Accumulation of Acetaminophen in <i>Drosophila</i> observed using CLARITY. ....	76
Figure 3.2: Acetaminophen results in dose-dependent mortality in adult <i>Drosophila</i> . ....	77
Figure 3.3: APAP Administration Increases ROS in the <i>Drosophila</i> Fat Body and Depletes Systemic Glutathione. ....	79
Figure 3.4: Fat body-specific depletion of Cyp18a1 attenuates APAP toxicity. ....	80
Figure 3.5: Genetic and pharmacologic modifiers of APAP toxicity in <i>Drosophila</i> . ....	82
Figure 3.6: The microbiome protects against acetaminophen toxicity in <i>Drosophila</i> . ....	84
Figure 3.7: Effects of age on APAP-induced mortality. ....	85
Figure 4.1: Conventionalization of germ-free mice alters the hepatic metabolome. ....	101
Figure 4.2: Conventionalization of germ-free mice induces the hepatic Nrf2 antioxidant response pathway. ....	103
Figure 4.3: Symbiotic <i>Lactobacilli</i> sp. activate the Nrf2 pathway in the <i>Drosophila melanogaster</i> fat body. ....	105
Figure 4.4: Oral administration of <i>Lactobacillus rhamnosus</i> GG activates Nrf2 signaling in murine liver. ....	107
Figure 4.5: <i>Drosophila</i> model of oxidative liver injury. ....	109
Figure 4.6 <i>Lactobacillus rhamnosus</i> GG protects the <i>Drosophila</i> fat body against toxicity in a Nrf2 dependent manner. ....	110
Figure 4.7: <i>Lactobacillus rhamnosus</i> GG administration attenuates acetaminophen hepatotoxicity in conventional mice. ....	112
Figure 4.8: Steady-state mRNA levels of acetaminophen metabolizing enzymes. ....	113
Figure 4.9: Hepatic Nrf2 mediates <i>Lactobacillus rhamnosus</i> GG protection against acetaminophen hepatotoxicity. ....	115
Figure 4.10: Hepatic Nrf2 mediates <i>Lactobacillus rhamnosus</i> GG protection against acute alcohol induced injury. ....	117
Figure 4.11: <i>Lactobacillus rhamnosus</i> GG alters the small molecule milieu of portal serum. ..	118
Figure 4.12: Effect of LGG-induced small molecules on Nrf2 activity in HepG2 cells. ....	120
Figure 4.13: LGG-derived 5-methoxyindoleacetic acid activates hepatic Nrf2. ....	121
Figure 4.14: 5-MIAA quantification in portal serum of LGG treated mice. ....	122
Figure 4.15: Lactobacilli produce 5-MIAA <i>in vitro</i> . ....	123

# **Chapter 1:**

## **The microbiome-liver axis in health and disease**

## 1.1 Introduction

The microbes that reside within the human intestine outnumber human cells by ten-fold<sup>1</sup> and harbor twice the genetic potential of the host<sup>2</sup>. Once considered inert scavengers of indigestible foodstuffs, it has become increasingly evident that these microbes have developed their niche within the host through millions of years of coevolution<sup>3,4</sup>. In this introduction, we will explore what is known about the impact of the microbiome on the host, specifically as it relates to the susceptibility to liver disease. Furthermore, we will explore the current therapeutic approaches being utilized in an attempt to modulate the microbiome and fine-tune human health.

## 1.2 Structure and Function of the Gut Microbiome

The intestinal microbial community is collectively referred to as the “gut microbiome,” and has several characteristic features. First, different microbes tend to colonize different parts of the gastrointestinal tract. The small intestine, with its rapid flow rate and high concentration of bile acids and oxygen, is dominated by facultative anaerobes such as Gram-positive *Lactobacilli*, *Enterococci*, and *Streptococci*, and Gram-negative *Proteobacteria* and *Bacteroides*<sup>5-7</sup>. The cecum and colon are the most densely populated regions of the gastrointestinal tract, with a microbial community dominated by strict and facultative anaerobes that thrive in the anoxic lumen<sup>7,8</sup>.

In addition to being taxonomically distinct, the microbial communities of each region of the gastrointestinal tract are functionally distinct. Microaerophilic bacteria in the small intestine such as *Lactobacilli* tend to be fast growing and tolerant of bile acids, oxygen, and antimicrobial peptides. In the colon, fermentation of undigested carbohydrates results in the production of short-chain fatty acids that can be utilized by the host<sup>9-11</sup>.

### 1.3 Systemic Effects of the Microbiome

Given these myriad metabolic and signaling properties, it is not surprising that the microbiome has a significant influence on the intestinal mucosa. Indeed, studies of the microbiome have demonstrated that certain bacterial microbes can elicit profound changes in signaling within the intestinal epithelium<sup>12</sup>, mucosal immune system<sup>13</sup>, and enteric nervous system<sup>14</sup>.

Dysbiosis, or a deviation in composition and diversity of the microbiome from a “normal” set point, has been correlated with diverse intestinal diseases, including inflammatory bowel diseases<sup>15–18</sup>, irritable bowel syndromes<sup>19</sup>, and susceptibility to intestinal pathogens<sup>20</sup>. While the effect of the microbiome on the intestinal mucosa has been extensively investigated, questions remain regarding the extent and mechanism of microbial influence on organs beyond the alimentary tract. Germ-free mice, which are raised in sterile isolators and are completely devoid of a microbiome, are critical tools for investigating the influence of the microbiome on systemic host tissues.

Many studies using germ-free or antibiotic-treated mice have implicated the microbiome in altering systemic signaling, susceptibility to disease/injury, and modification of host metabolism. These effects have been identified in nearly every organ, with implications for cardiovascular<sup>21</sup>, immunologic<sup>22</sup>, and even neurological health<sup>23</sup>. However, this trove of phenotypic information is at present unmatched by mechanistic understanding.

Mechanistic investigation of these processes is complicated by several key characteristics of the microbiome. First, the gut microbiome is incredibly complex, heterogenous, and widely divergent from species to species<sup>3</sup>, and even individual to individual<sup>24</sup>. Second, each individual microbial species has distinct metabolic activities which can alter the small molecule milieu obtained from dietary intake<sup>24,25</sup>. Third, the mechanisms by which the microbiome *as a whole* may

impact systemic diseases are likely multifactorial, precluding straight-forward implications of a single molecular pathway.

Nevertheless, several breakthrough studies have begun to untangle these diverse mechanisms and explain the profound effects that gut microbes have on systemic host physiology.

An elegant example is a study published in 2011 that elucidated a discrete molecular mechanism for microbiome-mediated atherosclerosis<sup>26</sup>. The authors performed unbiased small molecule metabolomics on human serum obtained from patients with coronary vascular disease. They identified microbe-derived trimethylamine, and the subsequent trimethylamine oxide produced by the host, as a key risk factor in the formation of atherosclerotic plaques. Beyond the mechanistic implications of this study, the authors provided a roadmap for the future elucidation of discrete microbiome-mediated effects on the host.

This study and others like it serve to demonstrate that small molecules, either derived from microbial metabolism or produced by host cells in response to microbial signaling, can travel systemically and affect host processes in distant organs. To understand this, we must take a closer look at how small molecules produced in the gut are absorbed and trafficked to the rest of the body.

#### **1.4 The Portal Circulation**

Ingested substances travel down the alimentary canal and are digested by both host and microbial activities. This breaks down and metabolizes the more complex molecules present in the diet to easily absorbable small molecules, lipids, and peptides. These are then absorbed by the host, either by diffusion through the tight junctions and into the basolateral compartment, or by active transport into the intestinal epithelium. If not utilized by the epithelium or other cellular components of the submucosa, they are then transported systemically via one of two systems. The

lymphatics absorb processed lipids from the basolateral aspect of the intestinal epithelium via specialized structures called lacteals. These lipids travel from the intestine to the thoracic duct, where they are emptied into the subclavian vein to join the systemic circulation.

The majority of the small molecules and peptides absorbed in the intestine are transported via the portal circulation, a specialized circulatory system that connects the majority of the intestine with the liver. Foreign substances, or “xenobiotics,” arriving from the gut via the portal circulation are filtered through the liver as blood moves from the portal vein, through the sinusoids, and into the central vein. Throughout this process, hepatocytes absorb, metabolize, and detoxify any caustic compounds before they find their way into the systemic circulation. The liver, therefore, serves a critical gatekeeper function, preventing harmful metabolites from flooding the general circulation and disseminating to the rest of the body. The importance of the liver is apparent in diseases that alter liver function, such as cirrhotic liver disease. Patients afflicted with these diseases exhibit a range of debilitating symptoms, from bleeding abnormalities to progressive neurologic dysfunction and death<sup>27,28</sup>. These sequela are primarily due to the inability of the damaged liver to effectively filter and detoxify xenobiotics arriving from the gut. Maintaining the metabolic capability of the liver is therefore critical to organismal health.

### **1.5 Detoxification Activities of the Liver**

The liver is in a unique and precarious physiologic position. It sits at the interface between a flood of foreign substances and a finely tuned systemic circulation. To cope with this onslaught of xenobiotics and to prevent toxins from reaching the body, the liver utilizes several key detoxification and antioxidant responses. These are broadly categorized into two types of metabolic activities, phase 1 and phase 2 detoxification.

Phase 1 detoxification responses involve the enzymatic modification of the structure of a small molecule. For example, the addition or removal of a hydroxy group, which may render the small molecule less reactive. These reactions are generally carried out by the Cytochrome P450 family of enzymes<sup>29</sup>.

Subsequent detoxication of small molecules occurs via Phase II metabolism, in which small molecules are conjugated to other chemical moieties. Examples of this include sulfonylation (addition of a sulfhydryl group), glucuronidation (addition of a glucuronide group), or glutathionylation (addition of a glutathione moiety). These conjugations render reactive small molecules inert, and often increase their solubility, thus facilitating their excretion<sup>29</sup>.

Transcriptional control of the majority of the xenobiotic response falls to a set of transcription factors including pregnane-x-receptor (PXR), constitutive-active androstane receptor (CAR), and Aryl hydrocarbon receptor (AHR). These transcription factors are critical for the regulation of the expression of the cytochrome P450 enzymes and are reviewed in detail elsewhere<sup>30,31</sup>. Another transcription factor that is essential both for Phase II metabolism of xenobiotics and for cytoprotection against potentially caustic small molecules arriving from the intestine is the basic leucine zipper transcription factor Nuclear factor erythroid-derived 2 (Nrf2)<sup>32–34</sup>.

Under homeostatic conditions Nrf2 is bound by an E3 ubiquitin ligase adaptor Kelch-like ECH associated protein 1 (Keap1) which promotes the degradation of Nrf2<sup>35</sup>. Inhibition of Keap1 by reactive oxygen species (ROS) or certain electrophilic xenobiotics results in Nrf2 release and subsequent nuclear translocation where it is responsible for the induction of its transcriptional program<sup>36</sup>. Because this pathway is regulated post-translationally, it can be rapidly activated under conditions of cell stress or xenobiotic exposure. Given the liver's extensive exposure to absorbed

intestinal contents, including microbial products, it is possible that the microbiome plays a role in fine-tuning this response. Indeed, several studies have described vast differences in the expression and activity of enzymes involved in xenobiotic metabolism in the absence of a microbiome<sup>37</sup>.

## **1.6 Liver Disease and the Microbiome**

A puzzling aspect of the pathogenesis of hepatic disease is that there is significant inter-individual variability in severity and disease progression<sup>38</sup>. While some of these differences can be accounted for by the genetic makeup of an affected individual, there remain a significant number of patients for whom genetics cannot explain their altered susceptibility to disease. For example, non-alcoholic fatty liver disease (NAFLD) is characterized by the accumulation of lipids within the liver<sup>39</sup>. Over time, this lipid deposition will result in an inflammatory response and development of more severe liver injury known as non-alcoholic steatohepatitis (NASH)<sup>40</sup>. However, it is not clear why some patients with NAFLD will progress to NASH, while other patients with equally severe steatosis will never mount an inflammatory response<sup>41</sup>. Analysis of patients with hepatic steatosis revealed significant shifts in the makeup of the gut microbiome between those with and without NASH<sup>42,43</sup>.

Alcoholic liver disease (ALD) is another example. While much is known about the molecular and genetic basis of susceptibility to alcohol exposure in the liver, severity of disease is, again, often determined by factors we do not yet understand. Here too, it has been speculated that the microbiome may play a role<sup>44</sup>. Indeed, transfer of fecal material from patients with severe alcoholic liver disease into germ-free mice exacerbated their hepatic phenotype after exposure to alcohol compared to mice that acquired a control microbiome<sup>45</sup>.

In addition to NAFLD and ALD, drug-induced liver injury (DILI) is also extremely variable<sup>38</sup>. Acetaminophen overdose, the most common cause of DILI in the United States<sup>46</sup>, can cause severe liver damage at relatively low doses in some individuals, while other individuals have a much higher threshold for hepatotoxicity. Again, the microbiome has been proposed as a key factor in this variability<sup>37</sup>.

### **1.7 The Microbiome as a Therapeutic Modality**

Given the potential importance of the microbiome in altering susceptibility to liver injury, clinicians and researchers have begun to explore the possibility of microbiome manipulation as therapy. Currently, three viable clinical approaches exist to alter the makeup of the gut microbiome.

Antibiotics are small molecules that interfere with bacterial processes (biosynthesis of cell wall components, alteration of metabolism, inhibition of protein synthesis, etc). When taken orally, antibiotics can broadly deplete microbial taxa within the intestine<sup>47</sup>. While this may attenuate the replication of pathogenic bacteria or temper bacterial overgrowth, antibiotics also deplete commensal microbes that perform beneficial functions. For example, loss of bacterial abundance after oral amoxicillin opens a niche for the pathogenic *C. difficile* to populate, resulting in bloody diarrhea and other negative sequelae for the patient<sup>48</sup>. In addition, antibiotics are themselves xenobiotic compounds, can be metabolized by the liver, and are in many cases themselves hepatotoxic<sup>49</sup>.

The microbiome-based therapy that has shown the most promise to date is fecal microbiota transplant (FMT). This therapeutic modality involves the wholesale repletion of a dysbiotic microbiome with a eubiotic (or healthy) microbiome. Stool samples are collected from healthy,

screened donors, and subsequently infused into the intestine of patients, either by naso-gastric tube or via endoscopy<sup>50,51</sup>. Given the complexity of the microbiome, the importance of microbe-microbe crosstalk in establishing a community architecture, and the lack of understanding of the mechanistic underpinnings of microbial effects on the host, FMT has been touted as the catch-all therapy for addressing microbiome related issues<sup>52</sup>.

The greatest success story to date is the use of FMT for treatment of recurrent *C. difficile* infection<sup>53</sup>. Most cases of *C. difficile* occur shortly after a patient has completed an oral dose of antibiotics, particularly amoxicillin, clindamycin, ampicillin, cephalosporins, and fluoroquinolones<sup>48</sup>. This effectively wipes out several critical bacterial taxa in the gut, leaving an empty niche for *C. diff* to populate. FMT is thought to provide benefit by rapidly repopulating that empty niche with normal commensals<sup>48</sup>. Indeed, clinical use of FMT for recurrent *C. diff* has increased dramatically, with a 92 percent cure rates<sup>54</sup> and an 11% recurrence rate (relative to 24% after traditional antibiotic therapy)<sup>55</sup>. Due to the efficacy of FMT against this focused clinical problem, researchers and clinicians have attempted to utilize FMT in other contexts<sup>52</sup>.

Although its role as a causative agent has been elusive, dysbiosis of the gut microbiome has been shown in a diverse array of disease, from IBD<sup>15–18</sup> to obesity<sup>56</sup> to Parkinson’s disease<sup>57,58</sup>. Preclinical studies have demonstrated that fecal microbiota transplant of affected individuals into germ-free mice can result in phenotypic features of disease. Restoration of a normal gut flora via FMT can, in many cases, rescue these phenotypes. Unfortunately, the success of FMT in the clinical setting beyond the narrow indication of *C. difficile* infection has been mixed<sup>52</sup>.

Another approach to modifying the gut microbiome is through the administration of exogenous commensal microbes, or “probiotics<sup>59</sup>.” Conceptually, probiotics are thought to work by “balancing” the intestinal microbial population, presumably by acting as keystone species and

providing substrates for the bloom of other beneficial bugs<sup>60</sup>. For example, administration of *Lactobacilli* is thought to increase the concentration of luminal lactate, which can be metabolized by *Clostridial* species. Therefore, *Lactobacilli* supplementation can result in a bloom of *Clostridia* *sp.* which have known trophic and signaling properties within the intestinal tissue<sup>61,62</sup>. Due to this hypothetical mechanism of action, it has now become common clinical practice to prescribe probiotics after or concurrent with a course of antibiotics<sup>63</sup>. This is done in an attempt to more rapidly replete the gut microbiome, without the cost and invasiveness of FMT.

A recent study, however, demonstrated that the use of probiotics immediately following a round of antibiotics may actually inhibit the reconstitution of the microbiome<sup>64</sup>. Indeed, probiotic supplementation resulted in a significant decrease in the diversity of the microbiome after antibiotic use. Given the conventional knowledge that a more diverse microbiome is a healthier microbiome<sup>2</sup>, these data indicate that probiotic use may actually be at best, ineffective, and at worst, counterproductive. However, no functional outcomes were measured, so it is difficult to draw broad conclusions. Nevertheless, this study underscores the necessity for more investigation into probiotics, despite their acceptance in popular culture and, increasingly, in clinical practice<sup>63</sup>.

Beyond their role as the supposed lynchpin of microbial diversity, probiotics are thought to possess intrinsic activities that directly affect the host. Perhaps the most obvious of these activities is nutrient harvest from the diet. The most widely appreciated example of this is the production of SCFA from dietary fiber<sup>65</sup>. Bacteria in the cecum naturally ferment these indigestible fibers into acetate, butyrate, and propionate<sup>66</sup>. Butyrate, in particular, then serves as the preferred fuel source of the epithelial colonocytes that lie downstream<sup>67,68</sup>. In addition to contributing to energy production, butyrate also serves several critical signaling functions. It is a potent histone deacetylase (HDAC) inhibitor<sup>69</sup>, and therefore alters the epigenetics of colonocytes. Additionally,

butyrate is metabolized via oxidative phosphorylation, which consumes oxygen and increases the hypoxic tone within the cell. This stabilizes the transcription factor hypoxia inducible factor (HIF)<sup>70</sup>, which serves several critical functions within the intestinal mucosa, from production of anti-microbial peptides<sup>71</sup>, to strengthening of the epithelial barrier<sup>72</sup>, to alteration of the mucosal immune system to better target invasive microbes<sup>73</sup>.

Probiotic supplementation has been shown to increase the production of SCFA, and augment the signaling events described above<sup>62</sup>. Additional examples of probiotic-derived small molecules and their subsequent effects on the host abound throughout the literature. Various species of indoles, for example, have been isolated from discrete microbial species and found to activate host AHR<sup>74</sup> and Nrf2<sup>75</sup>, among others. These effects have been primarily observed in the intestine, but microbe-derived small molecules are absorbed through the intestinal barrier and transported into the portal blood and on to the liver, where they can affect host signaling. While the exact nature of these small molecules, and their exact source, remains poorly defined in the literature, the effects of probiotics on hepatic health and susceptibility to disease is an active area of research.

## **1.8 Probiotics and Liver Disease**

Myriad studies demonstrate that oral administration of probiotics can attenuate liver disease<sup>76</sup>. For example, several studies have shown that the commercially available probiotic *Lactobacillus rhamnosus* GG (LGG) can attenuate alcoholic liver injury<sup>77-79</sup> and non-alcoholic liver injury<sup>80,81</sup>. However, no clear determination has been made as to how gut microbes influence systemic signaling and susceptibility to disease.

The argument can be made that if these probiotics elicit hepatoprotective effects, what does the mechanism really matter? After all, the most important property of a therapeutic is the functional response, not the mechanism of action. Some of our most widely used drugs are derived from plants that were used for thousands of years, long before we had a molecular understanding of disease. Indeed, ingestion of fecal material was described by Ge Hong in 4<sup>th</sup> century China as a treatment for diarrhea<sup>82</sup>. Fecal microbiota transplant as we now know it for *C. difficile* was first performed in 1958<sup>82</sup>, decades before we appreciated the complex social structures residing in our intestines. Does it matter if we understand how something works, as long as it works?

The trouble occurs when the findings observed in mice and other preclinical models do not reproduce in humans. Due to the complex, multifactorial nature of the mechanisms involved, it is difficult to replicate the conditions necessary for microbiome-based therapies outside the laboratory. Every individual patient has a unique set of variables including diet, exercise, underlying disease, genetic predispositions, and so on, all of which are precisely controlled in animal experiments. Without knowing *how* a specific microbiome-based therapeutic modality works, it is nearly impossible to predict if it *will* work. Indeed, this has been painfully borne out in the past decade as researchers have struggled to bring promising therapeutics from mice to humans with mixed and inconclusive results<sup>84</sup>. Therefore, a critical need exists to discover the specific mechanisms by which individual probiotics mediate their effects on the host.

### **1.9 *Drosophila* as a Model for the Microbiome-Liver Axis**

The difficulty in approaching these questions lies in the very same reason why many probiotic therapies fail in human cohorts. The complexity of the microbiome makes it difficult to isolate a single bacterial species, demonstrate the effects of a discrete microbe-derived small

molecule, or investigate the genetic modifications that alter sensitivity to a therapeutic modality. These studies can be undertaken in mice, but generation of germ-free mice is costly and burdened with its own set of confounding variables (altered immune function<sup>13</sup>, defective nutrient harvesting<sup>25</sup>, impaired development of the gastrointestinal tract<sup>85</sup>, etc.). Genetic knockouts in murine models are possible, but time-consuming and expensive. These issues raise a significant barrier to performing critical pilot or screening studies to begin to home in on the exact molecular mechanisms at play. Additionally, *in vitro* models do not adequately reproduce the necessary 3-dimensional architecture of the microbiome-gut-liver axis in a physiologically relevant manner.

A potential solution is the utilization of other model organisms. *Drosophila*, for example, have a gastrointestinal tract similar to that observed in vertebrates, with defined regions that perform different physiologic functions and a single monolayer of epithelium encasing the intestinal lumen<sup>86</sup>. While *Drosophila* lack a portal circulation *per se*, they do have a circulatory system that carries metabolites from the gut to other regions of the body. In addition, an organ called the “fat body” behaves similarly to the mammalian liver, performing critical roles in lipid metabolism and production of acute phase reactants<sup>87</sup>. Finally, *Drosophila* have a well-defined microbiome and can easily be made germ-free<sup>86</sup>.

The benefits of utilizing *Drosophila* for researching the effects of the microbiome on the liver are many. Perhaps most critical is the ease of tissue-specific gene knockdown. A library of genetic mutants, interfering-RNA constructs, tissue specific drivers, and reporter lines already exists and can be procured quickly and inexpensively. Genetic screens of the entire *Drosophila* genome can be done relatively easily, and can help identify potential genetic polymorphisms that alter susceptibility to liver injury. Additionally, *Drosophila* can be used for high-throughput screens of small molecules in an attempt to identify novel therapeutics for liver injury. As the

current standard of care for many liver diseases, particularly drug and alcohol induced liver injury, are mainly supportive<sup>88</sup>, a need for this sort of drug discovery platform is desperately needed.

*Drosophila* are also incredibly useful for the study of the gut microbiome<sup>86</sup>. In addition to the reasons listed above, *Drosophila* can also be used to quickly and easily pilot germ-free studies because they can be very easily generated germ-free. To accomplish this, *Drosophila* eggs are simply washed in bleach and placed on sterile food. This can be done with wild-type flies or any type of genetically altered *Drosophila*. The resulting flies lack any microbiome and can be monocolonized with individual bacteria to try to home in on the specific gut microbes eliciting host effects. Given the immense expense of generating and utilizing germ-free mice, this is a major advantage.

Despite these advantages, there remains a critical need for fat-body specific models of injury in *Drosophila*. Various toxins have been used in an attempt to poison the fat-body, for example malathion<sup>89</sup>, but the relevance of these toxins in mammalian systems is unclear. A robust, clinically relevant, translatable model of fat body injury would make *Drosophila* a tractable model of liver disease and bring to the study of the gut-liver axis a whole host of new tools.

## **1.10 Conclusion**

In the chapters that follow, we attempt to fill these gaps in our current understanding of the microbiome-liver axis.

In Chapter 2, we perform unbiased, small molecule metabolomics on hepatic tissue from germ-free and conventionalized (microbiome-replete) mice. From these data, we identify and characterize a discrete small molecule,  $\delta$ -valerobetaine, that is derived from the microbiota and completely absent in germ-free animals. This molecule is structurally similar to butyrobetaine,

with the exception of being one carbon longer. As butyrobetaine is the direct molecular precursor of carnitine, we hypothesized that  $\delta$ -valerobetaine may alter cellular carnitine levels. Indeed,  $\delta$ -valerobetaine is inversely correlated with carnitine abundance in the liver, and exogenous administration of  $\delta$ -VB resulted in a dramatic decrease in circulating carnitine. This, in turn, prevents the proper oxidation of long-chain fatty acids in hepatic mitochondria, and results in an increase in hepatic steatosis after overnight fast. This small molecule, therefore, may help explain the fact that germ-free mice fail to gain weight or develop liver disease in response to a high fat diet<sup>90</sup>.

In Chapter 3, we develop and validate a *Drosophila* model of drug-induced liver injury. We demonstrate that administration of acetaminophen to *Drosophila* results in a dose dependent increase in mortality. Acetaminophen exposure causes reactive oxygen production within the *Drosophila* fat body and a depletion of systemic glutathione, similar to that observed in mammals. This toxicity can be attenuated by overexpression of *Drosophila* Nrf2 in the fat body, and augmented by its depletion. We also demonstrate that fat-body specific knockdown of the Cyp2e1 analog Cyp18a1, which is responsible for the bioconversion of APAP to its toxic metabolite NAPQI, results in an increase in native APAP and a decrease in overall toxicity. Therefore, we demonstrate that the mechanisms by which *Drosophila* succumb to APAP toxicity are conserved to humans and provide a novel model for the study of acute oxidative liver injury.

In Chapter 4, we again utilized small molecule metabolomics coupled with RNAseq in germ-free and conventionalized mice to identify the broad contours of the effects of the microbiome on hepatic signaling. These data demonstrate that the presence of a gut microbiome increases the activation of Nrf2, the master regulator of the host xenobiotic and antioxidant response. *Lactobacilli* appear to be most adept at eliciting this response, and administration of

exogenous *Lactobacilli* to conventional mice can augment Nrf2 activation in the liver even above that observed by the microbiome as a whole. Furthermore, we demonstrate the functional importance of this activation by challenging *Lactobacillus*-fed mice with two different models of acute liver injury, acetaminophen overdose and acute alcohol exposure. In both instances, *Lactobacillus* administration protects against injury in a Nrf2-dependent manner. Finally, we identify a small molecule, 5-methoxyindole acetic acid, that is increased in the portal circulation of *Lactobacillus*-gavaged animals. Further characterization of this metabolite revealed that it is capable of activating Nrf2 both *in vivo* and *in vitro*, and is produced specifically by *Lactobacilli*.

These studies serve to advance our understanding of the microbiome by uncovering the discrete small molecules and molecular pathways that mediate communication between the microbiome and liver. Perhaps more importantly, they aid in honing the tools necessary to move microbiome and probiotic research forward in a meaningful manner.

## 1.11 References

1. Xu J, Gordon JI. Honor thy symbionts. *Proc Natl Acad Sci USA*. 2003 Sep 2;100(18):10452–10459. PMID: PMC193582
2. Human Microbiome Project Consortium. Structure, function and diversity of the healthy human microbiome. *Nature*. 2012 Jun 13;486(7402):207–214. PMID: PMC3564958
3. Ley RE, Hamady M, Lozupone C, Turnbaugh PJ, Ramey RR, Bircher JS, Schlegel ML, Tucker TA, Schrenzel MD, Knight R, Gordon JI. Evolution of mammals and their gut microbes. *Science*. 2008 Jun 20;320(5883):1647–1651. PMID: PMC2649005
4. Ley RE, Lozupone CA, Hamady M, Knight R, Gordon JI. Worlds within worlds: evolution of the vertebrate gut microbiota. *Nat Rev Microbiol*. 2008;6(10):776–788. PMID: PMC2664199
5. Zoetendal EG, Raes J, van den Bogert B, Arumugam M, Booijink CCGM, Troost FJ, Bork P, Wels M, de Vos WM, Kleerebezem M. The human small intestinal microbiota is driven by rapid uptake and conversion of simple carbohydrates. *ISME J*. 2012 Jul;6(7):1415–1426. PMID: PMC3379644
6. Booijink CCGM, El-Aidy S, Rajilić-Stojanović M, Heilig HGJ, Troost FJ, Smidt H, Kleerebezem M, De Vos WM, Zoetendal EG. High temporal and inter-individual variation detected in the human ileal microbiota. *Environ Microbiol*. 2010 Dec;12(12):3213–3227. PMID: 20626454
7. Gu S, Chen D, Zhang J-N, Lv X, Wang K, Duan L-P, Nie Y, Wu X-L. Bacterial community mapping of the mouse gastrointestinal tract. *PLoS ONE*. 2013;8(10):e74957. PMID: PMC3792069

8. Donaldson GP, Lee SM, Mazmanian SK. Gut biogeography of the bacterial microbiota. *Nat Rev Microbiol*. 2016 Jan;14(1):20–32. PMID: PMC4837114
9. Cummings JH. Fermentation in the human large intestine: evidence and implications for health. *Lancet*. 1983 May 28;1(8335):1206–1209. PMID: 6134000
10. Lee W-J, Hase K. Gut microbiota-generated metabolites in animal health and disease. *Nat Chem Biol*. 2014 Jun;10(6):416–424. PMID: 24838170
11. Pryde SE, Duncan SH, Hold GL, Stewart CS, Flint HJ. The microbiology of butyrate formation in the human colon. *FEMS Microbiol Lett*. 2002 Dec 17;217(2):133–139. PMID: 12480096
12. Wells JM, Rossi O, Meijerink M, van Baarlen P. Epithelial crosstalk at the microbiota-mucosal interface. *Proc Natl Acad Sci USA*. 2011 Mar 15;108 Suppl 1:4607–4614. PMID: PMC3063605
13. Round JL, Mazmanian SK. The gut microbiota shapes intestinal immune responses during health and disease. *Nat Rev Immunol*. 2009 May;9(5):313–323. PMID: PMC4095778
14. Endres K, Schäfer K-H. Influence of Commensal Microbiota on the Enteric Nervous System and Its Role in Neurodegenerative Diseases. *J Innate Immun*. 2018;10(3):172–180. PMID: PMC6757170
15. Chassaing B, Darfeuille-Michaud A. The commensal microbiota and enteropathogens in the pathogenesis of inflammatory bowel diseases. *Gastroenterology*. 2011 May;140(6):1720–1728. PMID: 21530738
16. Andoh A, Imaeda H, Aomatsu T, Inatomi O, Bamba S, Sasaki M, Saito Y, Tsujikawa T, Fujiyama Y. Comparison of the fecal microbiota profiles between ulcerative colitis and

- Crohn's disease using terminal restriction fragment length polymorphism analysis. *J Gastroenterol.* 2011 Apr;46(4):479–486. PMID: 21253779
17. Hansen R, Russell RK, Reiff C, Louis P, McIntosh F, Berry SH, Mukhopadhyaya I, Bisset WM, Barclay AR, Bishop J, Flynn DM, McGrogan P, Loganathan S, Mahdi G, Flint HJ, El-Omar EM, Hold GL. Microbiota of de-novo pediatric IBD: increased *Faecalibacterium prausnitzii* and reduced bacterial diversity in Crohn's but not in ulcerative colitis. *Am J Gastroenterol.* 2012 Dec;107(12):1913–1922. PMID: 23044767
  18. Man SM, Kaakoush NO, Mitchell HM. The role of bacteria and pattern-recognition receptors in Crohn's disease. *Nat Rev Gastroenterol Hepatol.* 2011 Mar;8(3):152–168. PMID: 21304476
  19. Parkes GC, Brostoff J, Whelan K, Sanderson JD. Gastrointestinal microbiota in irritable bowel syndrome: their role in its pathogenesis and treatment. *Am J Gastroenterol.* 2008 Jun;103(6):1557–1567. PMID: 18513268
  20. Kim S, Covington A, Pamer EG. The intestinal microbiota: Antibiotics, colonization resistance, and enteric pathogens. *Immunol Rev.* 2017 Sep;279(1):90–105. PMID: PMC6026851
  21. Tang WHW, Li DY, Hazen SL. Dietary metabolism, the gut microbiome, and heart failure. *Nat Rev Cardiol.* 2019;16(3):137–154. PMID: PMC6377322
  22. Brown EM, Kenny DJ, Xavier RJ. Gut Microbiota Regulation of T Cells During Inflammation and Autoimmunity. *Annu Rev Immunol.* 2019 26;37:599–624. PMID: 31026411
  23. Cryan JF, O'Riordan KJ, Cowan CSM, Sandhu KV, Bastiaanssen TFS, Boehme M, Codagnone MG, Cussotto S, Fulling C, Golubeva AV, Guzzetta KE, Jaggar M, Long-Smith

- CM, Lyte JM, Martin JA, Molinero-Perez A, Moloney G, Morelli E, Morillas E, O'Connor R, Cruz-Pereira JS, Peterson VL, Rea K, Ritz NL, Sherwin E, Spichak S, Teichman EM, van de Wouw M, Ventura-Silva AP, Wallace-Fitzsimons SE, Hyland N, Clarke G, Dinan TG. The Microbiota-Gut-Brain Axis. *Physiol Rev.* 2019 01;99(4):1877–2013. PMID: 31460832
24. Healey GR, Murphy R, Brough L, Butts CA, Coad J. Interindividual variability in gut microbiota and host response to dietary interventions. *Nutr Rev.* 2017 Dec 1;75(12):1059–1080. PMID: 29190368
25. Krajmalnik-Brown R, Ilhan Z-E, Kang D-W, DiBaise JK. Effects of gut microbes on nutrient absorption and energy regulation. *Nutr Clin Pract.* 2012 Apr;27(2):201–214. PMID: PMC3601187
26. Wang Z, Klipfell E, Bennett BJ, Koeth R, Levison BS, Dugar B, Feldstein AE, Britt EB, Fu X, Chung Y-M, Wu Y, Schauer P, Smith JD, Allayee H, Tang WHW, DiDonato JA, Lusis AJ, Hazen SL. Gut flora metabolism of phosphatidylcholine promotes cardiovascular disease. *Nature.* 2011 Apr 7;472(7341):57–63. PMID: PMC3086762
27. Bernal W, Wendon J. Acute liver failure. *N Engl J Med.* 2013 Dec 26;369(26):2525–2534. PMID: 24369077
28. Asrani SK, O'Leary JG. Acute-on-chronic liver failure. *Clin Liver Dis.* 2014 Aug;18(3):561–574. PMID: PMC4411558
29. Zanger UM, Schwab M. Cytochrome P450 enzymes in drug metabolism: regulation of gene expression, enzyme activities, and impact of genetic variation. *Pharmacol Ther.* 2013 Apr;138(1):103–141. PMID: 23333322
30. Larigot L, Juricek L, Dairou J, Coumoul X. AhR signaling pathways and regulatory functions. *Biochim Open.* 2018 Dec;7:1–9. PMID: PMC6039966

31. Timsit YE, Negishi M. CAR and PXR: the xenobiotic-sensing receptors. *Steroids*. 2007 Mar;72(3):231–246. PMID: PMC1950246
32. Itoh K, Chiba T, Takahashi S, Ishii T, Igarashi K, Katoh Y, Oyake T, Hayashi N, Satoh K, Hatayama I, Yamamoto M, Nabeshima Y. An Nrf2/small Maf heterodimer mediates the induction of phase II detoxifying enzyme genes through antioxidant response elements. *Biochem Biophys Res Commun*. 1997 Jul 18;236(2):313–322. PMID: 9240432
33. Moi P, Chan K, Asunis I, Cao A, Kan YW. Isolation of NF-E2-related factor 2 (Nrf2), a NF-E2-like basic leucine zipper transcriptional activator that binds to the tandem NF-E2/AP1 repeat of the beta-globin locus control region. *Proc Natl Acad Sci USA*. 1994 Oct 11;91(21):9926–9930. PMID: PMC44930
34. Wu KC, Cui JY, Klaassen CD. Effect of graded Nrf2 activation on phase-I and -II drug metabolizing enzymes and transporters in mouse liver. *PLoS ONE*. 2012;7(7):e39006. PMID: PMC3395627
35. McMahon M, Thomas N, Itoh K, Yamamoto M, Hayes JD. Dimerization of substrate adaptors can facilitate cullin-mediated ubiquitylation of proteins by a “tethering” mechanism: a two-site interaction model for the Nrf2-Keap1 complex. *J Biol Chem*. 2006 Aug 25;281(34):24756–24768. PMID: 16790436
36. Dinkova-Kostova AT, Holtzclaw WD, Cole RN, Itoh K, Wakabayashi N, Katoh Y, Yamamoto M, Talalay P. Direct evidence that sulfhydryl groups of Keap1 are the sensors regulating induction of phase 2 enzymes that protect against carcinogens and oxidants. *Proc Natl Acad Sci USA*. 2002 Sep 3;99(18):11908–11913. PMID: PMC129367

37. Klaassen CD, Cui JY. Review: Mechanisms of How the Intestinal Microbiota Alters the Effects of Drugs and Bile Acids. *Drug Metab Dispos.* 2015 Oct;43(10):1505–1521. PMID: PMC4576672
38. McGill MR, Jaeschke H. Metabolism and disposition of acetaminophen: recent advances in relation to hepatotoxicity and diagnosis. *Pharm Res.* 2013 Sep;30(9):2174–2187. PMID: PMC3709007
39. Marchesini G, Bugianesi E, Forlani G, Cerrelli F, Lenzi M, Manini R, Natale S, Vanni E, Villanova N, Melchionda N, Rizzetto M. Nonalcoholic fatty liver, steatohepatitis, and the metabolic syndrome. *Hepatology.* 2003 Apr;37(4):917–923. PMID: 12668987
40. Suzuki A, Diehl AM. Nonalcoholic Steatohepatitis. *Annu Rev Med.* 2017 14;68:85–98. PMID: 27732787
41. Sanyal AJ, Harrison SA, Ratziu V, Abdelmalek MF, Diehl AM, Caldwell S, Shiffman ML, Aguilar Schall R, Jia C, McColgan B, Djedjos CS, McHutchison JG, Subramanian GM, Myers RP, Younossi Z, Muir AJ, Afdhal NH, Bosch J, Goodman Z. The Natural History of Advanced Fibrosis Due to Nonalcoholic Steatohepatitis: Data From the Simtuzumab Trials. *Hepatology.* 2019 Dec;70(6):1913–1927. PMID: 30993748
42. Zhu L, Baker SS, Gill C, Liu W, Alkhoury R, Baker RD, Gill SR. Characterization of gut microbiomes in nonalcoholic steatohepatitis (NASH) patients: a connection between endogenous alcohol and NASH. *Hepatology.* 2013 Feb;57(2):601–609. PMID: 23055155
43. Boursier J, Mueller O, Barret M, Machado M, Fizanne L, Araujo-Perez F, Guy CD, Seed PC, Rawls JF, David LA, Hunault G, Oberti F, Calès P, Diehl AM. The severity of nonalcoholic fatty liver disease is associated with gut dysbiosis and shift in the metabolic function of the gut microbiota. *Hepatology.* 2016 Mar;63(3):764–775. PMID: PMC4975935

44. Szabo G. Gut-liver axis in alcoholic liver disease. *Gastroenterology*. 2015 Jan;148(1):30–36.  
PMCID: PMC4274189
45. Llopis M, Cassard AM, Wrzosek L, Boschat L, Bruneau A, Ferrere G, Puchois V, Martin JC, Lepage P, Le Roy T, Lefèvre L, Langelier B, Cailleux F, González-Castro AM, Rabot S, Gaudin F, Agostini H, Prévot S, Berrebi D, Ciocan D, Jousse C, Naveau S, Gérard P, Perlemuter G. Intestinal microbiota contributes to individual susceptibility to alcoholic liver disease. *Gut*. 2016 May;65(5):830–839. PMID: 26642859
46. Yoon E, Babar A, Choudhary M, Kutner M, Pysopoulos N. Acetaminophen-Induced Hepatotoxicity: a Comprehensive Update. *J Clin Transl Hepatol*. 2016 Jun 28;4(2):131–142.  
PMCID: PMC4913076
47. Becattini S, Taur Y, Pamer EG. Antibiotic-Induced Changes in the Intestinal Microbiota and Disease. *Trends Mol Med*. 2016;22(6):458–478. PMCID: PMC4885777
48. Leffler DA, Lamont JT. Clostridium difficile infection. *N Engl J Med*. 2015 Apr 16;372(16):1539–1548. PMID: 25875259
49. Stine JG, Lewis JH. Hepatotoxicity of antibiotics: a review and update for the clinician. *Clin Liver Dis*. 2013 Nov;17(4):609–642, ix. PMID: 24099021
50. Woodworth MH, Neish EM, Miller NS, Dhere T, Burd EM, Carpentieri C, Sitchenko KL, Kraft CS. Laboratory Testing of Donors and Stool Samples for Fecal Microbiota Transplantation for Recurrent Clostridium difficile Infection. *J Clin Microbiol*. 2017;55(4):1002–1010. PMCID: PMC5377826
51. Tauxe WM, Dhere T, Ward A, Racsá LD, Varkey JB, Kraft CS. Fecal microbiota transplant protocol for clostridium difficile infection. *Lab Med*. 2015;46(1):e19-23. PMID: 25805532

52. D'Haens GR, Jobin C. Fecal Microbial Transplantation for Diseases Beyond Recurrent Clostridium Difficile Infection. *Gastroenterology*. 2019;157(3):624–636. PMID: 31220424
53. Kassam Z, Lee CH, Yuan Y, Hunt RH. Fecal microbiota transplantation for Clostridium difficile infection: systematic review and meta-analysis. *Am J Gastroenterol*. 2013 Apr;108(4):500–508. PMID: 23511459
54. Quraishi MN, Widlak M, Bhala N, Moore D, Price M, Sharma N, Iqbal TH. Systematic review with meta-analysis: the efficacy of faecal microbiota transplantation for the treatment of recurrent and refractory Clostridium difficile infection. *Aliment Pharmacol Ther*. 2017;46(5):479–493. PMID: 28707337
55. Hui W, Li T, Liu W, Zhou C, Gao F. Fecal microbiota transplantation for treatment of recurrent C. difficile infection: An updated randomized controlled trial meta-analysis. *PLoS ONE*. 2019;14(1):e0210016. PMID: 31220424
56. Turnbaugh PJ, Ley RE, Mahowald MA, Magrini V, Mardis ER, Gordon JI. An obesity-associated gut microbiome with increased capacity for energy harvest. *Nature*. 2006 Dec 21;444(7122):1027–1031. PMID: 17183312
57. Petrov VA, Saltykova IV, Zhukova IA, Alifirova VM, Zhukova NG, Dorofeeva YB, Tyakht AV, Kovarsky BA, Alekseev DG, Kostryukova ES, Mironova YS, Izhboldina OP, Nikitina MA, Perevozchikova TV, Fait EA, Babenko VV, Vakhitova MT, Govorun VM, Sazonov AE. Analysis of Gut Microbiota in Patients with Parkinson's Disease. *Bull Exp Biol Med*. 2017 Apr;162(6):734–737. PMID: 28429209
58. Hill-Burns EM, Debelius JW, Morton JT, Wissemann WT, Lewis MR, Wallen ZD, Peddada SD, Factor SA, Molho E, Zabetian CP, Knight R, Payami H. Parkinson's disease and

Parkinson's disease medications have distinct signatures of the gut microbiome. *Mov Disord.* 2017;32(5):739–749. PMID: PMC5469442

59. Hill C, Guarner F, Reid G, Gibson GR, Merenstein DJ, Pot B, Morelli L, Canani RB, Flint HJ, Salminen S, Calder PC, Sanders ME. Expert consensus document. The International Scientific Association for Probiotics and Prebiotics consensus statement on the scope and appropriate use of the term probiotic. *Nat Rev Gastroenterol Hepatol.* 2014 Aug;11(8):506–514. PMID: 24912386
60. Plaza-Diaz J, Ruiz-Ojeda FJ, Gil-Campos M, Gil A. Mechanisms of Action of Probiotics. *Adv Nutr.* 2019 01;10(suppl\_1):S49–S66. PMID: PMC6363529
61. Flint HJ, Duncan SH, Scott KP, Louis P. Links between diet, gut microbiota composition and gut metabolism. *Proc Nutr Soc.* 2015 Feb;74(1):13–22. PMID: 25268552
62. Tyagi AM, Yu M, Darby TM, Vaccaro C, Li J-Y, Owens JA, Hsu E, Adams J, Weitzmann MN, Jones RM, Pacifici R. The Microbial Metabolite Butyrate Stimulates Bone Formation via T Regulatory Cell-Mediated Regulation of WNT10B Expression. *Immunity.* 2018 18;49(6):1116-1131.e7. PMID: PMC6345170
63. Draper K, Ley C, Parsonnet J. Probiotic guidelines and physician practice: a cross-sectional survey and overview of the literature. *Benef Microbes.* 2017 Aug 24;8(4):507–519. PMID: 28618862
64. Suez J, Zmora N, Zilberman-Schapira G, Mor U, Dori-Bachash M, Bashardes S, Zur M, Regev-Lehavi D, Ben-Zeev Brik R, Federici S, Horn M, Cohen Y, Moor AE, Zeevi D, Korem T, Kotler E, Harmelin A, Itzkovitz S, Maharshak N, Shibolet O, Pevsner-Fischer M, Shapiro H, Sharon I, Halpern Z, Segal E, Elinav E. Post-Antibiotic Gut Mucosal Microbiome

- Reconstitution Is Impaired by Probiotics and Improved by Autologous FMT. *Cell*. 2018 06;174(6):1406-1423.e16. PMID: 30193113
65. Bergman EN. Energy contributions of volatile fatty acids from the gastrointestinal tract in various species. *Physiol Rev*. 1990 Apr;70(2):567–590. PMID: 2181501
66. Macfarlane S, Macfarlane GT. Regulation of short-chain fatty acid production. *Proc Nutr Soc*. 2003 Feb;62(1):67–72. PMID: 12740060
67. Hamer HM, Jonkers D, Venema K, Vanhoutvin S, Troost FJ, Brummer R-J. Review article: the role of butyrate on colonic function. *Aliment Pharmacol Ther*. 2008 Jan 15;27(2):104–119. PMID: 17973645
68. Donohoe DR, Garge N, Zhang X, Sun W, O’Connell TM, Bunker MK, Bultman SJ. The microbiome and butyrate regulate energy metabolism and autophagy in the mammalian colon. *Cell Metab*. 2011 May 4;13(5):517–526. PMCID: PMC3099420
69. Davie JR. Inhibition of histone deacetylase activity by butyrate. *J Nutr*. 2003;133(7 Suppl):2485S-2493S. PMID: 12840228
70. Kelly CJ, Zheng L, Campbell EL, Saeedi B, Scholz CC, Bayless AJ, Wilson KE, Glover LE, Kominsky DJ, Magnuson A, Weir TL, Ehrentraut SF, Pickel C, Kuhn KA, Lanis JM, Nguyen V, Taylor CT, Colgan SP. Crosstalk between Microbiota-Derived Short-Chain Fatty Acids and Intestinal Epithelial HIF Augments Tissue Barrier Function. *Cell Host Microbe*. 2015 May 13;17(5):662–671. PMCID: PMC4433427
71. Kelly CJ, Glover LE, Campbell EL, Kominsky DJ, Ehrentraut SF, Bowers BE, Bayless AJ, Saeedi BJ, Colgan SP. Fundamental role for HIF-1 $\alpha$  in constitutive expression of human  $\beta$  defensin-1. *Mucosal Immunol*. 2013 Nov;6(6):1110–1118. PMCID: PMC3740147

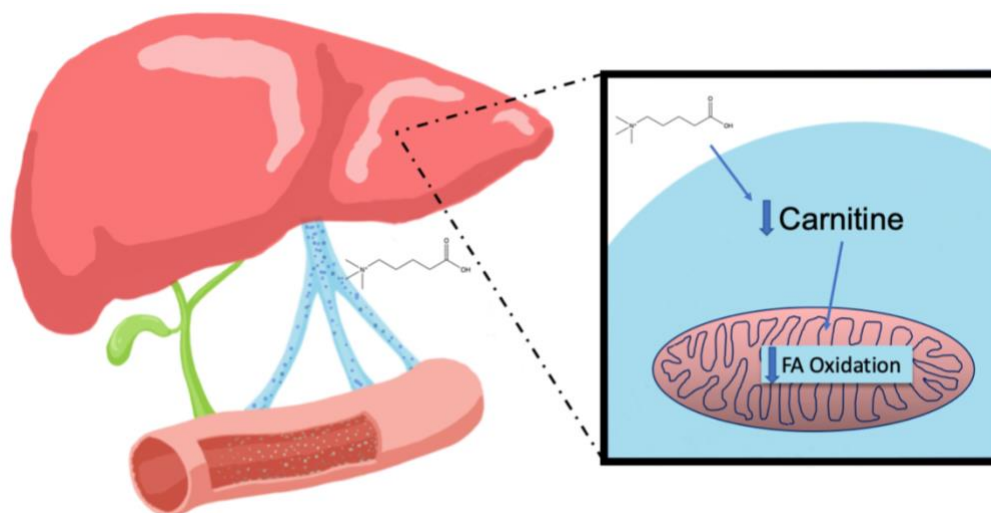
72. Saeedi BJ, Kao DJ, Kitzenberg DA, Dobrinskikh E, Schwisow KD, Masterson JC, Kendrick AA, Kelly CJ, Bayless AJ, Kominsky DJ, Campbell EL, Kuhn KA, Furuta GT, Colgan SP, Glover LE. HIF-dependent regulation of claudin-1 is central to intestinal epithelial tight junction integrity. *Mol Biol Cell*. 2015 Jun 15;26(12):2252–2262. PMID: PMC4462943
73. Dang EV, Barbi J, Yang H-Y, Jinasena D, Yu H, Zheng Y, Bordman Z, Fu J, Kim Y, Yen H-R, Luo W, Zeller K, Shimoda L, Topalian SL, Semenza GL, Dang CV, Pardoll DM, Pan F. Control of T(H)17/T(reg) balance by hypoxia-inducible factor 1. *Cell*. 2011 Sep 2;146(5):772–784. PMID: PMC3387678
74. Zelante T, Iannitti RG, Cunha C, De Luca A, Giovannini G, Pieraccini G, Zecchi R, D'Angelo C, Massi-Benedetti C, Fallarino F, Carvalho A, Puccetti P, Romani L. Tryptophan catabolites from microbiota engage aryl hydrocarbon receptor and balance mucosal reactivity via interleukin-22. *Immunity*. 2013 Aug 22;39(2):372–385. PMID: 23973224
75. Wlodarska M, Luo C, Kolde R, d'Hennezel E, Annand JW, Heim CE, Krastel P, Schmitt EK, Omar AS, Creasey EA, Garner AL, Mohammadi S, O'Connell DJ, Abubucker S, Arthur TD, Franzosa EA, Huttenhower C, Murphy LO, Haiser HJ, Vlamakis H, Porter JA, Xavier RJ. Indoleacrylic Acid Produced by Commensal *Peptostreptococcus* Species Suppresses Inflammation. *Cell Host Microbe*. 2017 Jul 12;22(1):25-37.e6. PMID: PMC5672633
76. Wiest R, Albillos A, Trauner M, Bajaj JS, Jalan R. Targeting the gut-liver axis in liver disease. *J Hepatol*. 2017;67(5):1084–1103. PMID: 28526488
77. Forsyth CB, Farhadi A, Jakate SM, Tang Y, Shaikh M, Keshavarzian A. *Lactobacillus GG* treatment ameliorates alcohol-induced intestinal oxidative stress, gut leakiness, and liver injury in a rat model of alcoholic steatohepatitis. *Alcohol*. 2009 Mar;43(2):163–172. PMID: PMC2675276

78. Wang Y, Liu Y, Sidhu A, Ma Z, McClain C, Feng W. Lactobacillus rhamnosus GG culture supernatant ameliorates acute alcohol-induced intestinal permeability and liver injury. *Am J Physiol Gastrointest Liver Physiol*. 2012 Jul;303(1):G32-41. PMID: PMC3404581
79. Chen R-C, Xu L-M, Du S-J, Huang S-S, Wu H, Dong J-J, Huang J-R, Wang X-D, Feng W-K, Chen Y-P. Lactobacillus rhamnosus GG supernatant promotes intestinal barrier function, balances Treg and TH17 cells and ameliorates hepatic injury in a mouse model of chronic-binge alcohol feeding. *Toxicol Lett*. 2016 Jan 22;241:103–110. PMID: 26617183
80. Kim B, Park K-Y, Ji Y, Park S, Holzapfel W, Hyun C-K. Protective effects of Lactobacillus rhamnosus GG against dyslipidemia in high-fat diet-induced obese mice. *Biochem Biophys Res Commun*. 2016 Apr 29;473(2):530–536. PMID: 27018382
81. Ritze Y, Bárdos G, Claus A, Ehrmann V, Bergheim I, Schwiertz A, Bischoff SC. Lactobacillus rhamnosus GG protects against non-alcoholic fatty liver disease in mice. *PLoS ONE*. 2014;9(1):e80169. PMID: PMC3903470
82. Zhang F, Luo W, Shi Y, Fan Z, Ji G. Should we standardize the 1,700-year-old fecal microbiota transplantation? *Am J Gastroenterol*. 2012 Nov;107(11):1755; author reply p.1755-1756. PMID: 23160295
83. Eiseman B, Silen W, Bascom GS, Kauvar AJ. Fecal enema as an adjunct in the treatment of pseudomembranous enterocolitis. *Surgery*. 1958 Nov;44(5):854–859. PMID: 13592638
84. Suez J, Zmora N, Segal E, Elinav E. The pros, cons, and many unknowns of probiotics. *Nat Med*. 2019;25(5):716–729. PMID: 31061539
85. Hooper LV, Gordon JI. Commensal host-bacterial relationships in the gut. *Science*. 2001 May 11;292(5519):1115–1118. PMID: 11352068

86. Douglas AE. The *Drosophila* model for microbiome research. *Lab Anim (NY)*. 2018;47(6):157–164. PMID: PMC6586217
87. Baker KD, Thummel CS. Diabetic larvae and obese flies-emerging studies of metabolism in *Drosophila*. *Cell Metab*. 2007 Oct;6(4):257–266. PMID: PMC2231808
88. Stine JG, Lewis JH. Current and future directions in the treatment and prevention of drug-induced liver injury: a systematic review. *Expert Rev Gastroenterol Hepatol*. 2016;10(4):517–536. PMID: PMC5074808
89. Misra JR, Horner MA, Lam G, Thummel CS. Transcriptional regulation of xenobiotic detoxification in *Drosophila*. *Genes Dev*. 2011 Sep 1;25(17):1796–1806. PMID: PMC3175716
90. Bäckhed F, Ding H, Wang T, Hooper LV, Koh GY, Nagy A, Semenkovich CF, Gordon JI. The gut microbiota as an environmental factor that regulates fat storage. *Proc Natl Acad Sci USA*. 2004 Nov 2;101(44):15718–15723. PMID: PMC524219

# Chapter 2:

## The microbiome-derived metabolite $\delta$ -valerobetaine inhibits hepatic mitochondrial fatty acid oxidation and exacerbates hepatic steatosis.



This chapter is adapted from:

Liu KH<sup>1\*</sup>, Saeedi BJ<sup>2\*</sup>, Cioffi C<sup>3</sup>, Bellissimo MP<sup>5</sup>, Owens JA<sup>3</sup>, Druzak S<sup>4</sup>, Orr M<sup>1</sup>, Hu X<sup>1</sup>, Fernandes J<sup>1</sup>, Camacho MC<sup>2</sup>, Hunter-Chang S<sup>2</sup>, van Insberghe D<sup>2</sup>, Ma C<sup>1</sup>, Darby T<sup>3</sup>, Ganesh T<sup>6</sup>, Yeligar S<sup>1</sup>, Uppal K<sup>1</sup>, Go Y<sup>1</sup>, Alvarez JA<sup>5</sup>, Vos MB<sup>3</sup>, Ziegler TR<sup>5</sup>, Jones RM<sup>3</sup>, Ortlund EA<sup>4</sup>, Neish AS<sup>2</sup>, & Jones DP<sup>1</sup> (in preparation)

<sup>1</sup>Division of Pulmonary, Allergy, Critical Care and Sleep Medicine, <sup>2</sup>Department of Pathology, <sup>3</sup>Department of Pediatrics, <sup>4</sup>Department of Biochemistry, <sup>5</sup>Division of Endocrinology, Metabolism, and Lipids, <sup>6</sup>Department of Pharmacology and Chemical Biology, Emory University School of Medicine, Atlanta GA

Denotes equal contribution\*, Denotes Corresponding Author(s)

## ABSTRACT

Dysregulation of the intestinal microbiome is linked to an epidemic of human metabolic disorders involving energy metabolism. Here, we identify the microbial-derived small molecule,  $\delta$ -valerobetaine (VB), a structural analog of the carnitine precursor  $\gamma$ -butyrobetaine. VB is absent in germ-free mice and derived liver mitochondria but was present in conventionalized mice and mitochondria. When supplemented to cells *in vitro*, VB decreased mitochondrial fatty acid oxidation by lowering intracellular carnitine. *In vivo*, VB administered to fasted mice lowered carnitine, decreased fatty acid oxidation and exacerbated hepatic steatosis elicited by overnight fasting. In addition, circulating VB in humans was associated with the severity of hepatic steatosis, hepatic insulin resistance, and visceral adiposity. These results demonstrate that VB is a gut microbe-derived small molecule that modulates mitochondrial energy metabolism and may contribute to fatty liver disease and other metabolic disorders.

## 2.1 INTRODUCTION

Emerging evidence links the epidemic of human metabolic disorders to unfavorable changes in the composition and activity of the intestinal microbiota (dysbiosis)<sup>1-6</sup>. Indeed, studies in germ-free mice have demonstrated that the presence of an intact intestinal microbiome is necessary for the development of many metabolic disorders, including non-alcoholic fatty liver disease, type II diabetes, and high-fat diet induced obesity. Given the complexity of the microbiome, no singular mechanism has been elucidated. These effects have been primarily attributed to changes in fat absorption and nutrient harvest, because the intestinal microbiota possess remarkable metabolic functions for digestion of dietary macromolecules. However, they are also responsible for the synthesis of diverse metabolites that directly impact human metabolism<sup>7,8</sup>. For example, epidemiological and experimental evidence show that microbial products such as lipopolysaccharide (LPS)<sup>9,10</sup>, phenylacetic acid<sup>11</sup>, and methylamines<sup>12-14</sup> contribute to the development of insulin resistance, hepatic steatosis, and cardiovascular disease. Of note, metabolomic analyses of germ-free (GF) and conventional (C) mouse tissues reveal that approximately 10% of the circulating mammalian metabolome are metabolites of microbial origin<sup>15</sup>. Unfortunately the majority of these are unidentified<sup>16</sup> and their functional importance in modulating host metabolism is unknown.

Mitochondrial dysfunction is commonly associated with human metabolic disorders. Studies have shown that microbial metabolites can directly influence host mitochondrial functions and metabolism<sup>18,19</sup>.

In this study, we identify and functionally characterize a microbiome-derived small molecule,  $\delta$ -valerobetaine (VB), that alters host fatty acid oxidation in the liver. Small molecule metabolomics on germ-free (GF) and conventionalized (CV) mouse liver revealed a dramatic shift

in the hepatic metabolome in response to intestinal microbiota colonization. The top discriminatory metabolite detected in liver and liver mitochondria of CV mice was  $\delta$ -valerobetaine (VB). VB is absent in GF mice and structurally resembles  $\gamma$ -butyrobetaine, the immediate biosynthetic precursor to carnitine, which is required for mitochondrial fatty acid oxidation. Exogenous administration of VB *in vitro* and *in vivo* resulted in a decrease in cellular carnitine, inhibition of mitochondrial fatty acid oxidation, and an increase in hepatic lipid accumulation. These results establish VB as a link between the gut microbiome and systemic fatty acid oxidation. Furthermore, analysis of a human cohort revealed that circulating VB is positively correlated with visceral adipose tissue (VAT) and hepatic steatosis. Taken together, these data demonstrate that the microbiome-derived small molecule VB acts systemically to modulate host fatty acid metabolism, and may account, in part, for the effects of the microbiome on clinical phenotypes linked to adiposity and hepatic steatosis.

## 2.2 RESULTS

### 2.2.1 Identification of the microbiome-derived mitochondrial metabolite $\delta$ -valerobetaine (VB)

To characterize the impact of the microbiome on the hepatic metabolome, we performed small molecule metabolomics on livers from sex-matched littermate germ-free (GF) and CV (microbiome-replete) mice. As shown in Figure 1A, the presence of a gut microbiome resulted in significant alterations in the hepatic metabolic profile relative to the GF condition.

To identify discrete microbial metabolites present in systemic tissues, we looked for features which were present only in conventionalized liver and liver mitochondria and absent in GF animals. The top-ranked differentially expressed feature in both CV liver ( $p$ -FDR =  $2.3e-6$ ) (**Figure 2.1A, 2.1C**) and CV liver mitochondria ( $p < 0.05$ ) (**Figure 2.1B**) was a metabolite with an  $m/z$  of 160.1332 and elemental composition  $C_8H_{18}NO_2$ . In addition, 160.1332  $m/z$  was present in portal serum (**Figure 2.1D**) and cecal contents (**Figure 2.1E**) obtained from CV but not GF mice. Authentic standard co-elution and MS/MS experiments show the identity of 160.1332  $m/z$  to be  $\delta$ -valerobetaine (VB) (**Figure 2.2A-B**). Estimated concentrations of VB in conventional mice ranged from 51-90 ng/mg in the cecum, 19-70 ng/mg in the colon, 9-26  $\mu$ M in the portal vein, 12-31 ng/mg in the liver, and 2-10  $\mu$ M in peripheral serum of CV animals.

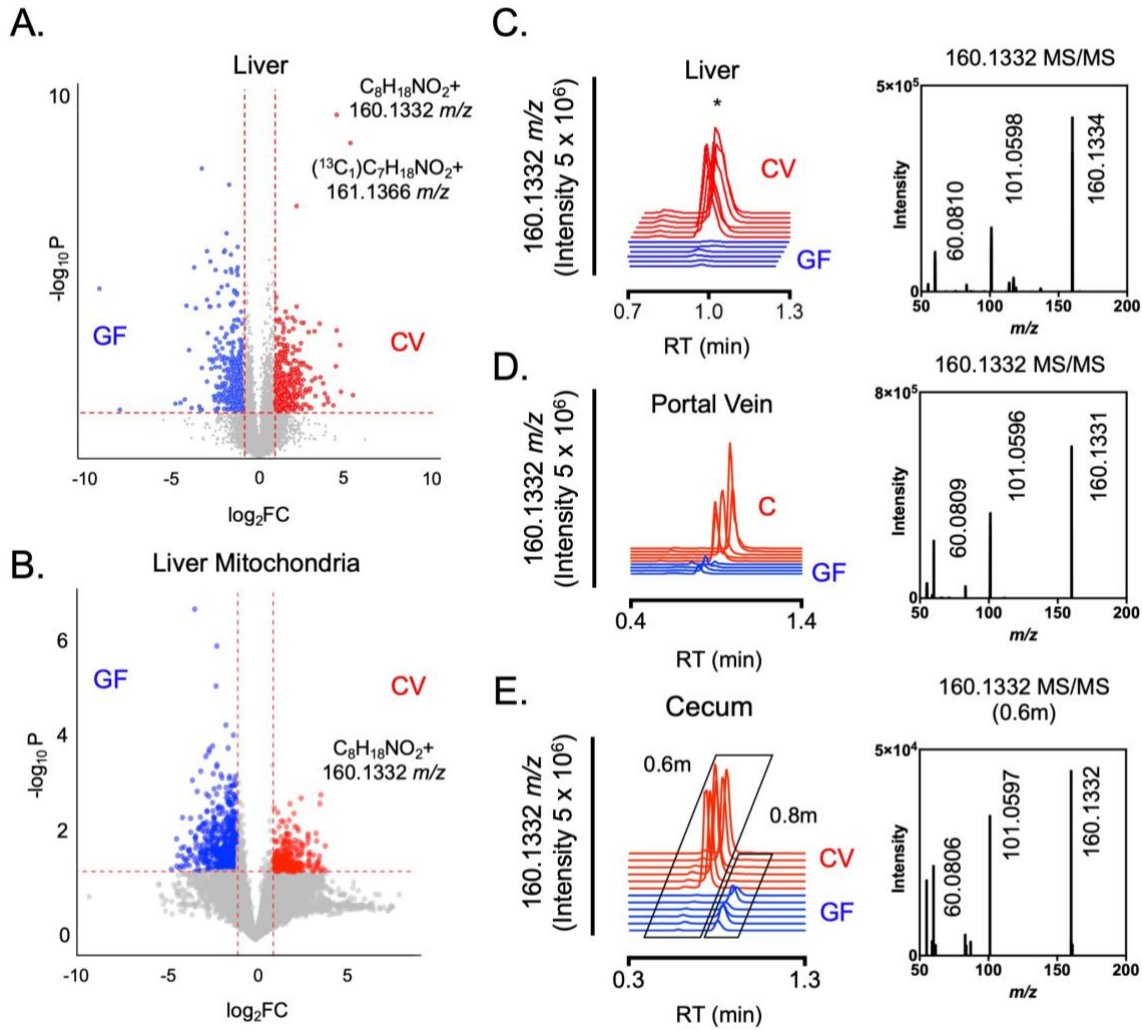


**Figure 2.1: Identification of the gut microbiome derived metabolite,  $\delta$ -valerobetaine (VB) in mouse liver and liver mitochondria.**

Volcano-plots of features from germ-free (GF, blue) and conventionalized (CV, red) mouse tissue reveal A) liver and B) liver mitochondria. Note the top-ranked differentially expressed feature in both is 160.1332 m/z with the elemental composition  $C_8H_{18}NO_2$ . High-resolution mass spectral analysis of C) liver, D) portal vein-derived serum, and E) cecal contents shows the absence of 160.1332 m/z in GF mouse tissues. High-resolution tandem mass spectral analysis shows the characteristic fragmentation pattern of 160.1332 m/z and the presence of a quaternary ammonium group.

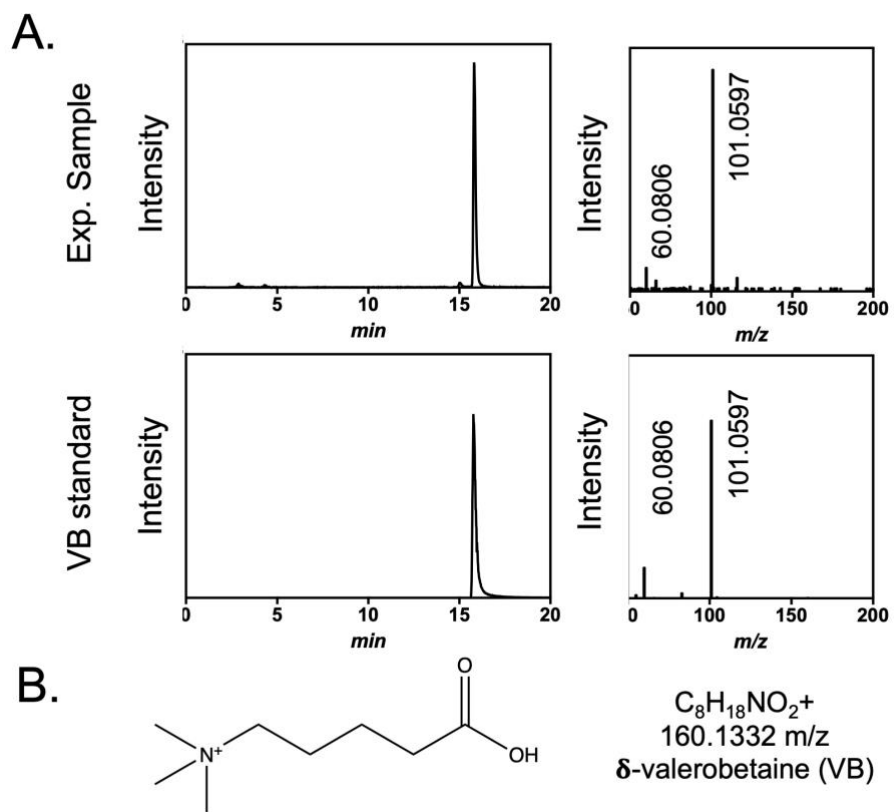


**Figure 2.2: 160.1332 m/z identified in CV mice is  $\delta$ -valerobetaine.**

A) Experimental confirmation of VB using synthesized standard and experimental samples. **B)** Chemical structure of VB.

### **2.2.2 The gut microbiome produces VB**

To determine whether microbial activity was responsible for intestinal production of VB in mice, we performed *ex vivo* cultures of cecal contents from conventional and GF mice (**Figure 2.3A**) and analyzed the culture supernatant for VB by LC-MS/MS. These data demonstrate that cultures of conventional cecal contents could produce VB independently of host factors. Additionally, GF cecal contents were incapable of generating VB, demonstrating that VB is derived from the gut microbiome. To determine if specific bacterial taxa are responsible for this production, we performed a metabolic screen of the culture supernatant of several candidate commensal and pathogenic microbes. Interestingly, several taxonomically distinct bacteria, including a commensal *Escherichia coli* (gram-negative), pathogenic *Salmonella typhimurium* (SL1344, gram-negative), and commensal *Lactobacillus rhamnosus* (LGG, gram-positive) were capable of producing produce VB *ex vivo* (**Figure 2.3B**). These data suggest that production of VB is not specific to individual classes of bacteria and may be relatively widespread within the microbial community. Taken together, these data demonstrate that intestinal production of VB requires microbial activity and therefore, the presence of VB in conventional animals reflects microbial production, followed by absorption and distribution into mouse tissues.

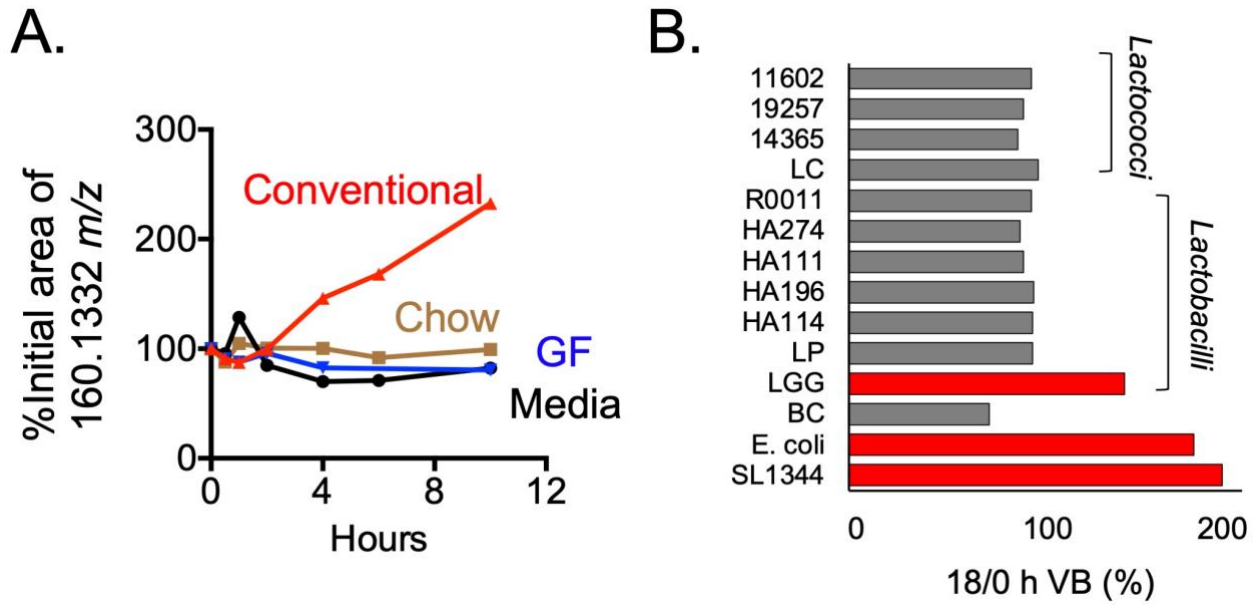


**Figure 2.3: Intestinal microbes produce  $\delta$ -valerobetaine.**

(A) Metabolomic assessment of VB abundance in culture supernatant from *ex vivo* incubations of cecal contents from GF and conventional mice. (B) VB abundance in *ex vivo* culture supernatants of commensal and pathogenic bacteria 18 hours after inoculation.

### **2.2.3 *δ*-valerobetaine (VB) decreases cellular carnitine in cultured HepG2 cells**

We next sought to characterize the functional importance of VB on host tissue. To this end, we treated HepG2 cells with VB for 12 hours, and assessed changes to the intracellular metabolome. The top metabolic pathway changed by VB-treatment was carnitine-shuttle metabolism (**Figure 2.4A**). More specifically, VB-treatment caused a dose-dependent decrease in cellular carnitine, short-chain and long-chain acylcarnitines (**Figure 2.4B**). At 10  $\mu$ M, a concentration of VB equivalent to that present in conventional mouse portal circulation, the observed carnitine peak intensity was half of the observed carnitine peak intensity in control cells. This effect was similar to that observed by treatment with meldonium, a competitive inhibitor of membrane carnitine-reuptake and inhibitor of BBOX-mediated carnitine biosynthesis (**Figure 2.4C**). Propionylcholine, an ester with the identical elemental composition as VB, did not elicit a carnitine-lowering effect in HepG2 cells (**Figure 2.4C**). Cellular carnitine levels could be rescued by addition of exogenous carnitine to the cell media (**Figure 2.4D**).

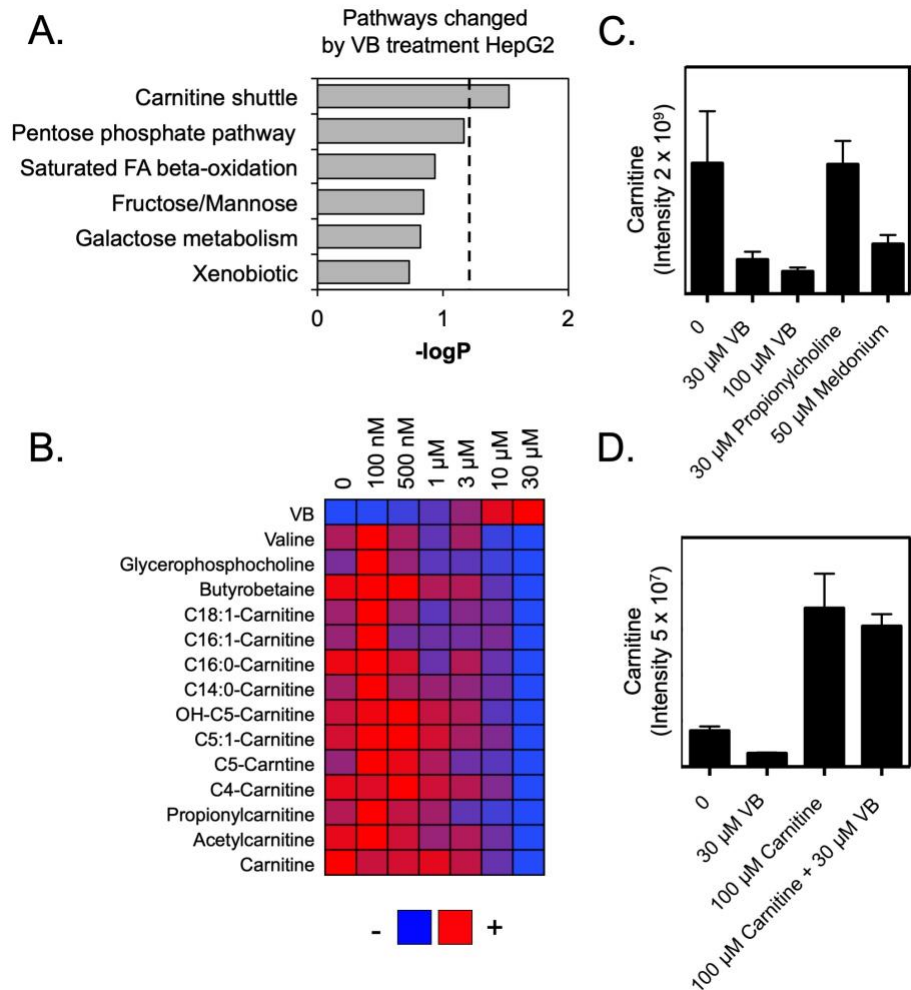


**Figure 2.4: Effects of VB on the metabolome of HepG2 cells.**

(A) *Mummichog* metabolic pathway enrichment of untargeted metabolomic profiling of HepG2 cells treated with physiologically relevant concentrations of VB (0-30  $\mu$ M, n = 4 biological replicates). (B) Dose-dependent effects of VB treatment on the cellular abundance of carnitine, acylcarnitines, and the carnitine precursor butyrobetaine (linear scale). (C) Effect of VB on cellular carnitine (n = 3 biological replicates) compared to propionylcholine, an ester with the same molecular weight as VB, and meldonium, an inhibitor of carnitine biosynthesis (BBOX) and uptake. Data are displayed as mean  $\pm$  standard deviation. (D) Rescue of VB-mediated carnitine depletion with exogenous carnitine treatment (n = 3 biological replicates).

#### ***2.2.4 $\delta$ -valerobetaine (VB) decreases palmitate-dependent mitochondrial respiration in HepG2 cells***

Carnitine is required for transport of long-chain fatty acyl chains into mitochondria for fatty acid oxidation. To determine the consequences of VB-mediated cellular carnitine depletion, we assessed the effects of VB treatment on basal respiratory rate, ATP production, and spare capacity of HepG2 cells. Under culture conditions where glucose, glutamine, and pyruvate were present in the culture media, VB did not elicit major changes to the basal respiratory rate, ATP-production, spare capacity, or non-mitochondrial respiration (**Figure 2.5A**). These data suggest that VB does not alter cellular metabolism and oxidative phosphorylation directly. In contrast, when cells were provided palmitate as a fuel source under conditions of glucose, glutamine, and pyruvate deprivation, VB elicited a dose-dependent decrease in respiration following injection of the uncoupling agent FCCP (**Figure 2.5B**). The observed decrease in spare capacity for fatty acid oxidation in HepG2 cells was similar to that observed with etomoxir, an irreversible inhibitor of carnitine palmitoyltransferase (CPT1). These data demonstrate that VB alters cellular respiration by inhibiting fatty acid oxidation specifically, with no effect on oxidative phosphorylation in the presence of excess glucose, glutamine, or pyruvate.

#### ***2.2.5 VB decreases formation of labeled acetyl-CoA production from labeled palmitic acid***

Palmitate, as well as other long-chain fatty acids, must be conjugated to cellular carnitine in the cytosol in order to be transported into the mitochondria for beta-oxidation. The end product of mitochondrial beta-oxidation is acetyl-CoA. We performed a stable isotope tracer study to determine the effect of VB treatment on the beta-oxidation of  $^{13}\text{C}_{16}$ -palmitate to  $^{13}\text{C}_2$ -acetyl-CoA in HepG2 cells (Figure 2.5C). 50  $\mu\text{M}$  VB-pretreatment for 24 hours prior to the introduction of labeled palmitate decreased labeled  $^{13}\text{C}_2$ -acetyl-CoA relative to vehicle at all time points. This

effect was rescued by carnitine supplementation. VB added concurrently with labeled palmitate led to a moderate decrease in formation of labeled acetyl-CoA compared to vehicle treated cells. Etomoxir was included as a positive control and completely blocked formation of acetyl-CoA from labelled palmitate. These results indicate that VB decreases mitochondrial fatty acid oxidation by decreasing the availability of free cellular carnitine. Of note, VB did not alter the uptake of cellular  $^{13}\text{C}_{16}$ -palmitate or the formation of  $^{13}\text{C}_{16}$ -palmitoyl-CoA (**Figure 2.5D**).

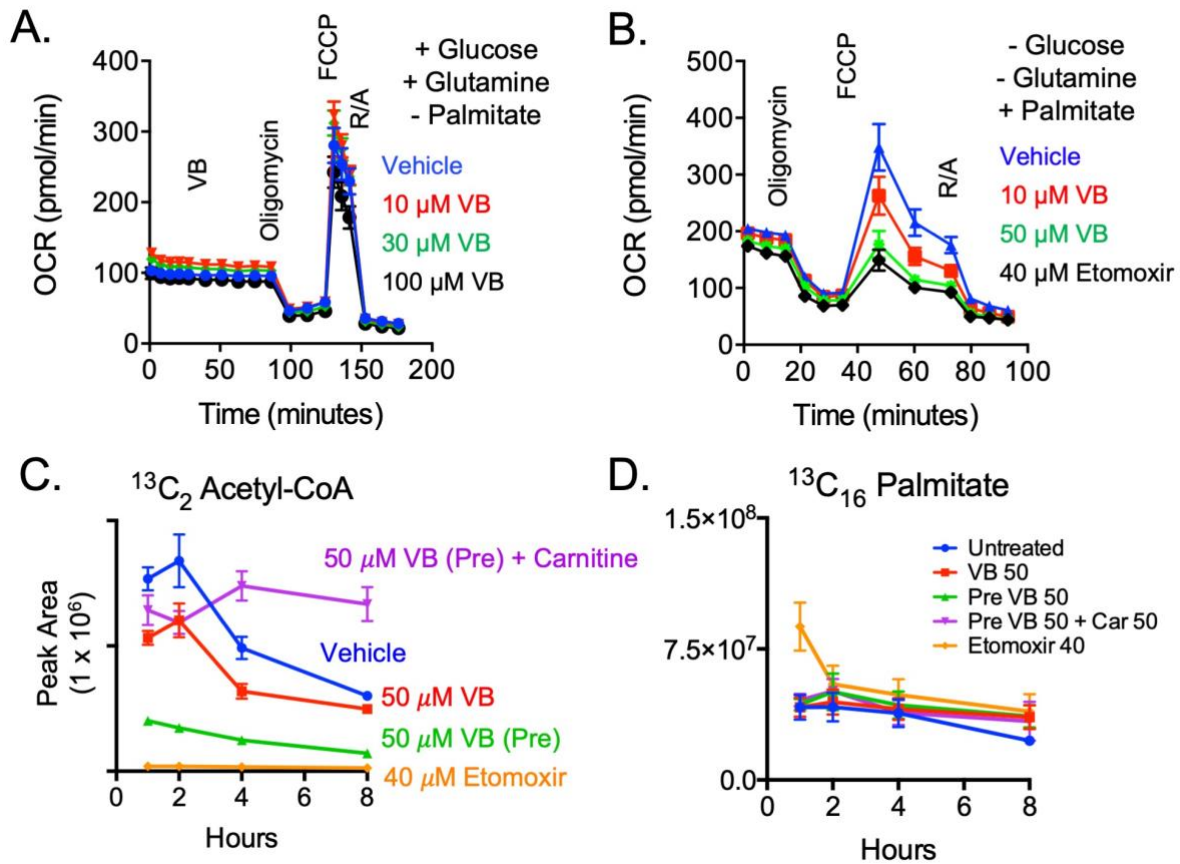


**Figure 2.5: Effects of VB on mitochondrial respiration and fatty acid oxidation.**

(A) Mitochondrial respiration in serum starved HepG2 cells supplemented with glucose, glutamine and pyruvate +/- VB. (B) Mitochondrial respiration after 12 hour treatment with VB in serum starved HepG2 cells supplemented with palmitate and without glucose, glutamine, or pyruvate. (C) Production of  $^{13}\text{C}_2$  Acetyl-CoA from labelled  $^{13}\text{C}_{16}$  palmitate over the course of 8 hours with concurrent VB treatment (Red), 12 hr VB pre-treatment (Green), 12 hr VB pretreatment with addition of exogenous carnitine (Purple), or treatment with etomoxir (Yellow). (D) Effect of VB on  $^{13}\text{C}_{16}$  Palmitate uptake into HepG2 cells. Data are represented as the average of 3 biological replicates  $\pm$  SD.

### ***2.2.6 VB decreases carnitine and decreases mitochondrial fatty acid oxidation in conventional mice***

We used conventional mice to determine whether the effects of VB *in vitro* were reproducible *in vivo*. First, we assessed the effect of VB dosing on circulating and cellular carnitine. Mice were dosed daily by intraperitoneal injection of either vehicle (PBS), 10 mg/kg VB, or 100 mg/kg VB. After one-week of treatment, mice were sacrificed and serum and liver were collected for mass spectrometry analysis. After one week of treatment, VB decreased circulating carnitine levels in serum in a dose-dependent manner in both males and females (Figure 2.6A). In the liver, however, VB significantly reduced cellular carnitine only in females, with male hepatic carnitine levels trending down (Figure 2.6B).

Again, given the critical role of cellular carnitine in facilitating beta-oxidation, we hypothesized that exogenous VB administration would impair the ability of the liver to metabolize long-chain fatty acids. To test this, we again pretreated mice with either vehicle (PBS) or 100 mg/kg VB by IP for 1 week, followed by an overnight fast. In this experimental model, mice will develop acute hepatic steatosis. This is thought to occur due to the rapid mobilization of fatty acid stores from the adipose tissue to the liver for metabolism in times of starvation. We hypothesized that VB would exacerbate hepatic steatosis in this context, because the liver would be unable to oxidize the incoming LCFA.

In agreement with data from fed mice, VB administration decreased circulating carnitine in the peripheral serum in a dose dependent manner (Figure 2.6C). VB also significantly lowered hepatic cellular carnitine levels in these fasted mice in both males and females (Figure 2.6D). Histologic analysis of liver tissue reveals an accumulation of neutral lipids (as observed by Oil red O staining) after overnight fast, relative to that observed in fed animals (Figure 2.7A, 2.7C). Under fed conditions, VB does not significantly increase the amount of steatosis observed (Figure 2.7A-

B). However, under fasted conditions, VB results in a significant increase in hepatic steatosis in both male and female mice (Figure 2.7C-D). Accordingly, VB treatment increased hepatic triglyceride content relative to vehicle controls (Figure 2.7E). Taken together, these data demonstrate that VB decreases hepatic fatty acid oxidation.

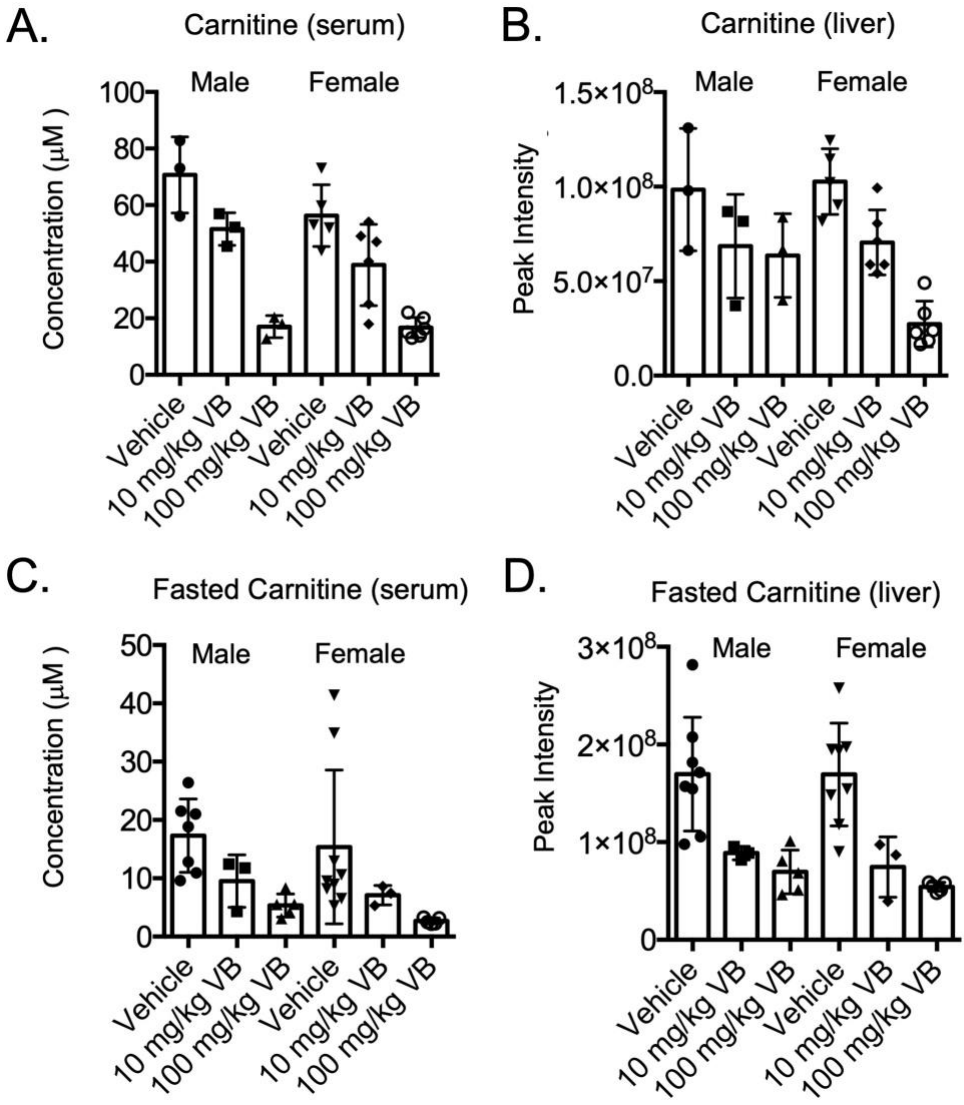


**Figure 2.6: Effects of VB on carnitine levels in mice.**

Measurement of carnitine levels in male and female mice after 1 week IP injection of either vehicle (PBS), 10 mg/kg VB, or 100 mg/kg VB. **(A)** Circulating carnitine levels in fed mice. **(B)** Hepatic carnitine levels in fed mice. **(C)** Circulating carnitine levels in fasted mice. **(D)** Hepatic carnitine levels in fasted mice. n=at least 3 mice per group.

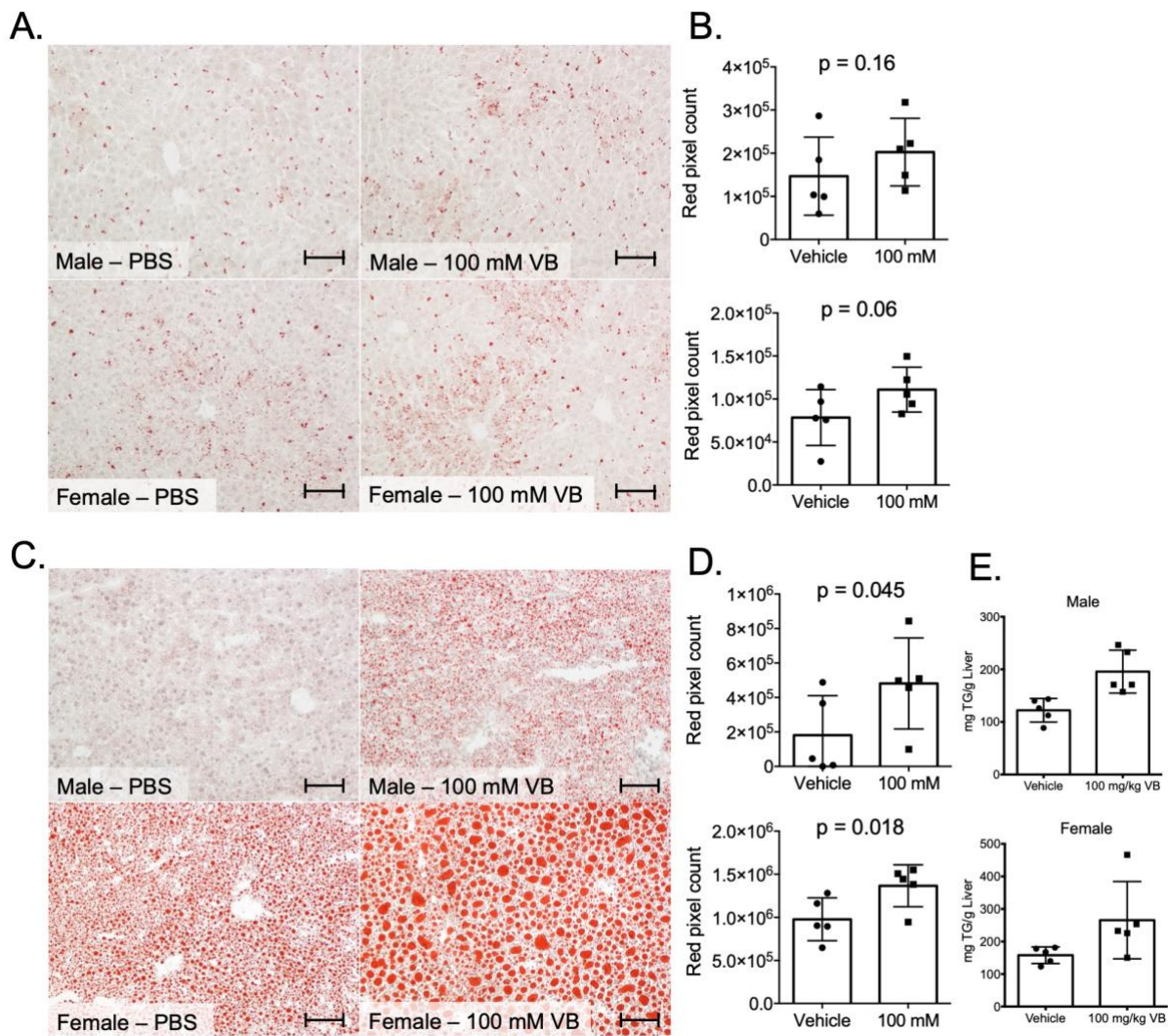


**Figure 2.7: Effect of VB administration of hepatic steatosis.**

(A) Representative Oil Red O stains of fed mouse liver with vehicle or VB treatment. (B) Quantification of red pixel count in Oil Red O staining in fed mice (n = 5 per treatment). (C) Representative Oil Red O stains of fasted mouse liver with vehicle or VB treatment. (D) Quantification of red pixel count in Oil Red O staining in fasted mice (n = 5 per treatment). (E) Quantification of liver triglycerides in VB treated animals after fasting. Scale bar represents 100  $\mu$ m under 20x magnification. Data were analyzed using a one-tailed t-test.

### ***2.2.7 VB is associated with the severity of hepatic steatosis in adolescents and with visceral adiposity in adults***

To further characterize the importance of VB in altering host systemic metabolism, we determined the correlation between circulating VB levels and the degree of hepatic steatosis and visceral adipose tissue weight (VAT) in humans. Data from two separate studies were used for this analysis – one focused on identification of plasma metabolites associated with the severity of hepatic steatosis (mild (<33% steatosis), moderate (33-66% steatosis), to severe (>66% steatosis) in children and adolescents with biopsy-proven NAFLD<sup>21</sup> and the other re-examined a previously published dataset<sup>22</sup> focused on identification of plasma metabolites associated with body composition parameters in fasted, actively working adults who were mostly full-time employees of Emory University, Atlanta. In the cohort of youth with clinically diagnosed NAFLD (n = 74, mean age 14 years, males = 54, females = 20), circulating VB levels were significantly higher in participants with severe steatosis compared to mild steatosis ( $\beta = 0.328$ ,  $p = 0.03$ , linear regression adjusted for age, sex, and race) (**Figure 2.8A**). In adults (n = 179, mean age 50 years, males = 63, females = 116), plasma VB was positively correlated with VAT ( $\beta = 3.7E+04 \pm 1.1E+04$ ,  $p = 0.0006$ ), independent of age, race, and sex (**Figure 2.8B**). This relationship held when additionally controlling for total body fat.

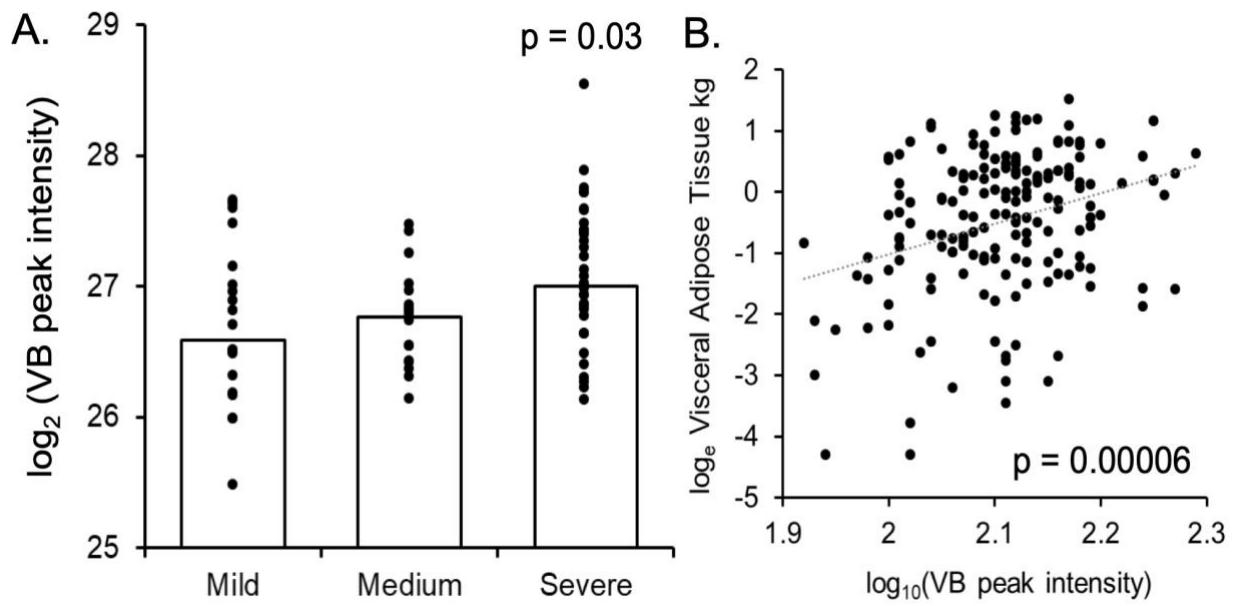


**Figure 2.8: Clinical phenotypes associated with circulating VB.**

(A) Plasma VB levels in adolescents with mild, medium, or severe hepatic steatosis. ( $n = 74$ ,  $\beta = 0.345$ ,  $p < 0.02$ ). (B) Plasma VB correlated with central adiposity in adults (VAT – log kg visceral adipose tissue) ( $n = 179$ ,  $p < 0.0006$ ).

## 2.3 DISCUSSION

Phylogenetic and evolutionary evidence indicate that eukaryotic mitochondria are descended from an ancient bacterial endosymbiont <sup>23</sup>, and there is increasing recognition of the holobiont – the eukaryotic host and its associated microbiome – function as the biological unit subject to evolutionary pressures. The present results suggest that VB is a microbiome-derived metabolite through which intestinal microbes modulate the activity of host mitochondria to influence collective bioenergetics. VB regulates fatty acid oxidation through modulation of systemic and hepatic carnitine abundance, which decreases long-chain fatty acid transport and metabolism by mitochondria. This may allow enhanced utilization of short-chain fatty acids by the eukaryotic host since short-chain fatty acids do not require the carnitine shuttle to be oxidized by host mitochondria <sup>24</sup>. This, in turn, could benefit members of the intestinal microbiota since accumulation of fermentation byproducts of the microbiome has been shown to be toxic to microbes <sup>25</sup>. Additionally, evolutionarily conserved benefits of microbiome-mitochondria cross-talk could involve energy conservation. In calorie-restricted states, microbial production of VB could promote survival of the holobiont/symbiont by functioning as a brake on host fatty acid oxidation, thereby preserving collective nutritional resources. In support of this, germ-free mice succumb more quickly following prolonged fasting periods compared to conventional mice <sup>26</sup>. Thus, these results establish a novel molecular communication between the microbiome and mitochondria, which could underlie aspects of microbiome-host symbiosis.

Recent studies also show VB can be obtained from dietary sources <sup>34-36</sup>, and recently published reports describe potential beneficial effects of VB on human health. VB is produced by ruminant microbes in water buffalo and is associated with increased acylcarnitines and the nutritional value of water buffalo milk <sup>36,37</sup>. Whole grain diets, which are associated with

decreased risk of cardiometabolic disorders, type 2 diabetes, and weight gain <sup>38</sup>, have been shown to increase circulating VB in humans <sup>34</sup>. Whole grains do not contain VB but have pre-biotic effects on gut microbial composition <sup>38</sup> (e.g. increasing *Bacteroidetes/Firmicutes* ratio) and increases in *Lactobacillus* and *Bifidobacterium*. These changes are negatively correlated with markers of obesity and dyslipidaemia and suggest that microbial products (such as VB) produced by beneficial diets and probiotic-associated bacteria could elicit beneficial effects on human metabolic health.

VB regulation of the host carnitine pool has likely impacts on human health due to the importance of carnitine homeostasis in preventing metabolic disorders of humans. Carnitine regulates glucose and lipid metabolism <sup>39,40</sup>, and previous studies have convincingly demonstrated that attenuating cellular carnitine levels results in mitochondrial dysfunction, decreases in hepatic fatty acid oxidation, and hepatic toxicities including steatosis <sup>41-45</sup>. Furthermore, a decline in free carnitine has been shown to accompany an accumulation of medium and long-chain acylcarnitines in muscle and associated obesity in aging <sup>46</sup>. Furthermore, carnitine supplementation is beneficial for treatment of obesity and fatty liver and augments glucose utilization in humans and mice <sup>47-51</sup>. However, excessive fatty acid oxidation and the accumulation of incompletely oxidized acylcarnitines are also associated with obesity and insulin resistance <sup>52</sup>. For example, excessive fatty acid oxidation (and decreased glucose utilization) is observed in insulin-resistant heart tissues <sup>53</sup>. Limiting carnitine-dependent fatty acid oxidation under these conditions can improve metabolic flexibility by driving an increase in glucose utilization (the Randle cycle). While VB was observed in brains, lungs, and hearts of conventional mice, the contribution of the microbial metabolite VB to extrahepatic metabolism is not currently known.

In conclusion, the present results show that  $\delta$ -valerobetaine, a structural analogue of the carnitine precursor  $\gamma$ -butyrobetaine, is a gut microbe-derived small molecule that alters mitochondrial energy metabolism. A key focus on prebiotic and probiotic management of VB production may help guide the management of the critical microbiome-host symbiotic relationship and its implications for the current epidemic of human metabolic disorders.

## 2.4 METHODS

### *Animals*

Germ-free (GF) male and female Swiss-Webster mice (Taconic Biosciences) were raised in germ-free isolators and fed sterilized mouse chow (Envigo 2019S Teklad Global 19% Protein Extruded Rodent Diet) and sterilized water *ad libitum* at the Emory University Gnotobiotic Animal Research Facility. Conventionalized (CV) mice were transferred to bedding from conventional Swiss-Webster (S) mice at three weeks of age, and maintained for 3 weeks while paired GF mice were maintained in germ-free isolators. After three weeks, luminal contents from the cecum and colon, portal vein serum, and intact livers were collected for mitochondrial isolation, RNA-sequencing and metabolomics. Data for GF and conventional C57BL6J ([jax.org/strain/000664](http://jax.org/strain/000664)) mice (Jackson laboratories, identical housing as Swiss-Webster) are provided as indicated.

### *High-resolution metabolomics (HRM)*

Cytosolic and mitochondrial fractions from GF/CV liver (n = 12) were prepared by differential centrifugation<sup>54</sup>. Serum and fractionated cytosol and mitochondria were mixed with 2x volume of ice-cold acetonitrile-internal standard solution. Liver and luminal contents were weighed and mixed with 10x volume of ice-cold 20% water/80% acetonitrile-internal standard solution. Tissue samples were homogenized using a pellet pestle prior to the next step. Samples were vortexed, and placed on ice for 30 minutes prior to centrifugation at 14,000g for 10 minutes at 4°C to precipitate proteins. Supernatants were transferred to autosampler vials and stored at -70°C prior to instrumental analysis.

Untargeted high-resolution mass spectrometric profiling was performed using a Dionex Ultimate 3000 UHPLC system coupled to a Thermo Scientific Velos LTQ-Orbitrap (metabolite identification studies), Thermo Scientific High-Field Q-Exactive (HFQE) (liver, liver

mitochondria, liver cytosol, portal vein) or Thermo Scientific Fusion (cecum, colon, *ex vivo* incubations, isotope tracer) <sup>55</sup>. Briefly on the Fusion and HFQE, an LC column switching method using a reversed phase C18 column (Higgins Targa C18 2.1 mm x 50 mm, 3  $\mu$ M particle size) and a HILIC column (Waters XBridge BEH Amide XP HILIC column 2.1 mm x 50 mm, 2.6  $\mu$ M particle size) were used for the analytical separation of extracts prior to high-resolution mass spectrometry analysis with HILIC/ESI+ and C18/ESI- at 120k resolution while of ions between 85-1,275 *m/z*. A similar LC column switching method 10 minute and 20 minute reversed phase C18 and HILIC separation methods with 10 cm columns with ESI+ was used on the Velos-Orbitrap for confirmation.

#### *Data processing, statistics, and feature selection*

Spectral features were extracted and aligned using optimized parameters for apLCMS <sup>56,57</sup>, with downstream quality control performed by xMSanalyzer <sup>58</sup>. Each metabolic feature was characterized by its *m/z* ratio, retention time, and peak intensity. Statistical analysis was performed using R-packages *limma* <sup>59</sup> for differential expression analysis and *diffexp* for linear regression analysis in xmsPANDA (<https://github.com/kuppal2/xmsPANDA>). Differentially expressed metabolites with a raw p-value of less than 0.05 were used for pathway enrichment analysis in *mummichog* <sup>60</sup>. Pathway enrichment significance in *mummichog* was based permutation testing with a  $p < 0.05$ . Metabolite names in *mummichog* were converted to KEGG IDs using <http://csbg.cnbc.csic.es/mbrole/conversion.jsp>.

#### *Metabolite Identification and Quantification*

Detected metabolites were referenced against an in-house reference library established with authentic chemical standards and matched within 5 ppm of the confirmed mass and within 10 s of the confirmed retention time. Features of interest were visually inspected to ensure

chromatographic and spectral peak quality. When no standard was available, MS isotopic ratios and MS/MS spectra were referenced against online spectral libraries or *in silico* ion dissociation spectra. Tandem MS<sub>2</sub> spectra were collected for target features on either Thermo Scientific Velos-Orbitrap, High-Field Q-Exactive, or Fusion mass spectrometers using collisional induced dissociation (CID) or high-energy collisional induced dissociation (HCD). MS<sub>2</sub> spectra were matched to experimental online mass spectral databases mzCloud and METLIN <sup>61</sup> or *in silico* predicted fragmentation patterns from metfrag <sup>62</sup> to identify candidate structures. Standards were purchased when commercially available or synthesized as described below. Reference standardization <sup>63</sup> was used for quantification of identified metabolites.

#### *Synthesis of $\delta$ -valerobetaine and valine betaine*

$\delta$ -Valerobetaine (VB) was synthesized as described previously <sup>64</sup>. Briefly, 5-bromovaleric acid (Sigma-Aldrich) and 1 molar equivalent trimethylamine (20% in EtOH) were stirred for 24h under vacuum at room temperature. The precipitate containing trimethylamine HBr salt was removed by filtration and the filtrate was evaporated under vacuum and recrystallized with cold isopropanol and acetonitrile. Purity was assessed to be greater than 95% with proton NMR and elemental analysis. MS: 160.1332 *m/z* ESI+ (MS<sub>2</sub>: 101.0597, 60.0809). <sup>1</sup>H NMR (**Appendix 3**) (400 MHz, D<sub>2</sub>O)  $\delta$  3.15 (multiplet, 2H),  $\delta$  2.91 (singlet, 9H),  $\delta$  2.27 (triplet, 2H),  $\delta$  1.64 (quintuplet, 2H),  $\delta$  1.46 (quintuplet, 2H). Elemental analysis (as VB-HBr salt) was C 37%, H 8%, N 5%, Br 31%. Valine betaine was synthesized as previously described <sup>65</sup>. L-Valine and methyl iodide were stirred for 48h in anhydrous methanol in the presence of excess potassium bicarbonate. The precipitate was dried and washed with ice-cold methanol. MS: 160.1332 *m/z* ESI+ (MS<sub>2</sub>: 60.0809).

#### *Ex-vivo fermentation*

Cecal contents from conventional or GF mice were collected and immediately placed in either De Man, Rogosa, and Sharpe media (MRS broth – Oxoid, CM0359) or degassed Tryptic Soy Broth (Millipore 22092) in oxygen evacuated headspace vials. Samples were incubated at 37°C were collected in triplicate over a 24-h time period and prepared for metabolomics analysis as above.

#### *Ex-vivo microbial metabolism assays*

Bacteria were purchased from ATCC and/or isolated in our laboratory and were cultured in specified liquid media. Samples were collected at baseline and again at 18 hours after incubation at 37°C. *Lactococcus lactis* Subsp. *cremoris* (LC, ATCC 19257, ATCC 14365, ATCC 11602), *Lactobacillus rhamnosus* GG (LGG, ATCC 53103), *Lactobacillus plantarum* (LP, HA-119), *Lactobacillus paracasei* (HA274), *Lactobacillus rhamnosus* (HA-114, HA-111, R0011), were grown in MRS broth (Oxoid, CM0359). *Bacillus cereus* was grown in brain heart infusion (BHI) media. *E. coli* (K12) and *Salmonella typhimurium* (SL1344) were grown in Luria Broth (LB).

#### *VB dose response experiments in HepG2 cells: metabolomics analysis*

HepG2 cells (ATCC) were used between passages 8-15 and grown in EMEM (ATCC) supplemented with 10% FBS and 0.5% Penicillin/Streptomycin (P/S). Cells were grown to 90% confluence in 3.5 cm cell culture dishes and treated with experimental compounds (VB, meldonium, propionylcholine, carnitine) in EMEM supplemented with 0.5% FBS and 0.5% penicillin/streptomycin. Cells were washed with ice cold Hank's Buffered Salt Solution (HBSS) and harvested by scraping on ice using 200 µL of ice-cold 20:80 water:acetonitrile containing 9 stable isotope internal standards and centrifuged at 14,000g for 10 minutes at 4°C. Supernatants were transferred to autosampler vials and maintained at 4°C until instrumental analysis.

#### *VB dose response experiments in HepG2 cells: Stable Isotope Palmitate Tracer Assay*

$^{13}\text{C}_{16}$ -palmitic acid (Sigma-Aldrich 605573) was dissolved in 150 mM NaCl after heating to 70°C and slowly mixed with prewarmed (37°C) FFA-free BSA (Sigma-Aldrich A4602) solution in 150 mM NaCl with stirring to produce a 1 mM palmitate to 0.17 mM BSA ratio. HepG2 cells were grown in 12-well cell culture plates to 80% confluence. Cell media was replaced with EMEM containing 0.5% FBS for 12 h  $\pm$  VB prior to treatment with labeled palmitic acid. Cells were washed twice with pre-warmed HBSS and media was replaced with EMEM containing 0.5% FBS, 200  $\mu\text{M}$  labeled palmitate, and either vehicle, 50  $\mu\text{M}$  VB, 40  $\mu\text{M}$  etomoxir, or 50  $\mu\text{M}$  carnitine. At each time point, cells were washed once with ice cold HBSS and harvested by scraping on ice using 200  $\mu\text{L}$  of ice-cold 20:80 water:acetonitrile containing 9 stable isotope internal standards and centrifuged at 14,000g for 10 min at 4°C. Supernatants were transferred to autosampler vials and maintained at 4°C until analysis. Data were analyzed using xCalibur QuanBrowser for carnitine and labeled palmitate, palmitoyl-CoA, palmitoylcarnitine, acetyl-CoA, and acetylcarnitine.

*VB dose response experiments in HepG2 cells: Mitochondrial Respiration Assays*

Oxygen consumption (OCR) was measured in the human hepatoma HepG2 cell line using a Seahorse XFe96 analyzer (Agilent Technologies). For assessments of respiration linked to oxidation of glucose and glutamine, cells were cultured on 96-well cell culture microplates and treated overnight with 0, 1, 3, 10, 30, 100  $\mu\text{M}$  VB in DMEM with 0.5% FBS. Cells were then washed 1x with 100  $\mu\text{M}$  pH 7.4 Seahorse XF DMEM (Agilent Technologies) in 0.5% FBS and media was replaced with XF DMEM supplemented with fuel substrates and VB or vehicle. The media was supplemented with 10 mM glucose, 2 mM GlutaMAX, and 1 mM pyruvate  $\pm$  VB.

For assessments of fatty acid oxidation, cells were serum-starved overnight with or without VB. After washing, media was replaced with Krebs Heinsleit Buffer (KHB) containing 200  $\mu\text{M}$

BSA-conjugated palmitate (Agilent Technologies) in the absence of supplemental glucose, GlutaMAX, pyruvate, or carnitine. KHB was prepared from pH 7.4 sterile filtered water containing 111 mM NaCl, 4.7 mM KCl, 2 mM MgSO<sub>4</sub>, and 1.2 mM NaH<sub>2</sub>PO<sub>4</sub>. VB (0, 10, 50 μM final concentration) or etomoxir (40 μM final concentration) were added to the assay medium prior to assessments of oxygen consumption (OCR) and extracellular acidification rate (ECAR).

To evaluate mitochondrial function, a MitoStress test kit (Agilent Technologies) was used with respiration assays. Three consecutive respiration measurements were acquired every 10 minutes for every experimental condition prior to and after injections of Oligomycin (1.5 μM final concentration), FCCP (1 μM final concentration), and Rotenone/Antimycin A (0.5 μM final concentration). Basal respiration (OCR prior to injection of mitochondrial inhibitors), ATP production (difference in OCR after addition of oligomycin), maximal respiration (OCR after addition of FCCP) and spare capacity (difference in OCR between basal and maximal respiration) were calculated using the Seahorse XF Cell Mito Stress Test Report Generator (<https://www.agilent.com/en/products/cell-analysis/cell-analysis-software/data-analysis/seahorse-xf-cell-mito-stress-test-report-generators>).

#### *Animal VB model*

Animal experiments were performed under approved Emory University IACUC animal protocols. For experiments with fed mice, conventional C57BL6J mice (Jackson laboratories) were injected IP with 100 μL saline vehicle, 100 μL 10 mM VB (10 mg/kg), or 100 μL 100 mM VB (100 mg/kg) once a day for one week. For experiments in fasted conventional mice, animals were treated with the same doses for three days and then fasted for 12 hours prior to sample collection. At the end of each treatment period liver, heart, brain, cecal and colonic contents and serum were collected for mass spectrometry, histology analysis, and triglyceride quantification.

### *Histology (Oil Red O) analysis*

Oil red O staining for neutral lipids was performed on 8-10 micron mouse liver sections prepared using a Cryostat. Images were taken on a Nikon Eclipse 50i at 20x magnification and red density was quantified in ImageJ software.

### *Triglyceride quantification*

Triglycerides were quantified in tissues using a triglyceride assay kit (Abcam 65336). 50 mg of liver tissue was homogenized in 1 mL of assay buffer and diluted 100x prior to addition of lipase. After 20 minutes, the triglyceride probe was added. After incubation for 30 minutes, the plate was read fluorometrically (535/587 nm) and quantified using the provided standard calibration curve.

### *Emory Pediatric Liver Biopsy Data Repository*

The Emory Pediatric Liver Biopsy Data Biorepository is an ongoing cross-sectional cohort study of children who provided data and biospecimens prior to undergoing a clinically-indicated liver biopsy for suspected liver disease or monitoring of a liver disease, as previously described.<sup>21</sup> Exclusion criteria were fever within the past two weeks, renal disease or insufficiency, or pregnancy. The analytical sample was a sub-group of 74 participants ages 7-19 years old who were enrolled between 2007 to 2015, had a clinical diagnosis of NAFLD after exclusion of other liver diseases, and a plasma sample available at the time of metabolomics analysis. A physical examination and fasting blood collection were performed prior to liver biopsy. Liver biopsies were reviewed by pathologists in a blinded manner, and were scored based on grade of steatosis (<5% = 0, 5-33% = 1, 34-66% = 2, >66% = 3), steatosis location (Zone 1, Zone 3, azonal, panacinar), lobular inflammation (0 = No foci, 1 = < 2 foci per 200 x field, 2 = 2-4 foci per 200 x field, 3 = > 4 foci per 200 x field), portal inflammation (0 = none, 1 = mild, 2 = more than mild), hepatocyte

ballooning (0 = none, 1 = few, 2 = many), and fibrosis stage (0 = none, 1 = periportal or perisinusoidal, 2 = perisinusoidal and portal/periportal, 3 = bridging fibrosis, 4 = cirrhosis). All study protocols were approved by the Emory University and Children's Healthcare of Atlanta Institutional Review Boards and written informed consent and assent were obtained.

Multiple linear regression adjusted for age (years,), sex, and race/ethnicity were used to examine associations of steatosis grade, based on liver biopsy scores, with plasma VB levels. This was done with steatosis grade as a continuous variable (1, 2, or 3) to assess the dose response, and as a categorical variable to compare VB levels in those with moderate and severe steatosis compared to mild steatosis. VB was log-transformed for analysis. Regression analysis was conducted in R Statistical Software (v3.5.3).<sup>66</sup>

#### *Center for Health Discovery and Well-Being (CHDWB) Cohort*

This cohort includes adults who were primarily employed by Emory University or Emory Healthcare systems at the time of enrollment. Individuals employed for greater than two years were invited to join the study from an alphabetized list and underwent extensive phenotyping as previously described <sup>67</sup>. General exclusion criteria were presence of a poorly controlled chronic disease, an acute illness within 12 weeks of study visit, currently pregnant or breastfeeding, or a history of malignancy within the previous five years <sup>68</sup>. A subset of the cohort (n=179) with high-resolution metabolomics data was included in this study <sup>69</sup>. Body composition and visceral adipose tissue (VAT) were determined using a Lunar iDXA densitometer and CoreScan™ software (GE Healthcare, Madison, WI, USA), which automatically quantifies VAT and has been validated against computed tomography <sup>70</sup>. Peripheral blood samples were drawn by trained nurses and fasting insulin and glucose levels were measured commercially (Quest Diagnostics, Valencia,

CA). The homeostatic model assessment of insulin resistance (HOMA-IR) was calculated as fasting insulin ( $\mu\text{IU/mL}$ ) x fasting glucose (mg/dL) divided by 405 <sup>71</sup>.

Multiple linear regression analyses, adjusting for age, race, and sex, were used to test for associations between VB with VAT and HOMA-IR. VAT and HOMA-IR were log-transformed for analyses. Analyses were conducted in JMP Pro (version 14, SAS Inc, Cary, NC).

### **Acknowledgments**

This work was supported by T32-GM008602, P30-ES019776, R01-ES023485, U2C-ES030163, R2C-DK118619, S10-OD018006, UH2-AI132345, and R01-AI064462.

Additionally, the authors would like to acknowledge support from the Georgia Clinical and Translational Science Alliance UL1 TR002378 and the Emory-Georgia Tech Predictive Health Institute and its Center for Health Discovery and Well Being.

## 2.5 REFERENCES

- 1 Carding, S., Verbeke, K., Vipond, D. T., Corfe, B. M. & Owen, L. J. Dysbiosis of the gut microbiota in disease.
- 2 Holmes, E., Li, J. V., Marchesi, J. R. & Nicholson, J. K. Gut microbiota composition and activity in relation to host metabolic phenotype and disease risk. *Cell metabolism* **16**, 559-564, doi:10.1016/j.cmet.2012.10.007 (2012).
- 3 Dumas, M. B., R. H.; Toye, A.; Cloarec, O.; Blancher, C.; Rothwell, A.; Fearnside, J.; Tatoud, R.; Blanc, V.; Lindon, J. C.; Mitchell, S. C.; Holmes, E.; McCarthy, M. I.; Scott, J.; Gauguier, D., Nicholson, J. K. Metabolic profiling reveals a contribution of gut microbiota to fatty liver phenotype in insulin-resistant mice. *PNAS* **103**, 12511-12516 (2006).
- 4 Rosenbaum, M., Knight, R. & Leibel, R. L. The gut microbiota in human energy homeostasis and obesity. *Trends Endocrinol Metab* **26**, 493-501, doi:10.1016/j.tem.2015.07.002 (2015).
- 5 Ignacio, A. *et al.* Correlation between body mass index and faecal microbiota from children. *Clin Microbiol Infect* **22**, 258 e251-258, doi:10.1016/j.cmi.2015.10.031 (2016).
- 6 Gonzalez, F. J., Jiang, C. & Patterson, A. D. An Intestinal Microbiota-Farnesoid X Receptor Axis Modulates Metabolic Disease. *Gastroenterology* **151**, 845-859, doi:10.1053/j.gastro.2016.08.057 (2016).
- 7 Holmes, E., Li, J. V., Athanasiou, T., Ashrafian, H. & Nicholson, J. K. Understanding the role of gut microbiome-host metabolic signal disruption in health and disease. *Trends Microbiol* **19**, 349-359, doi:10.1016/j.tim.2011.05.006 (2011).

- 8 Spanogiannopoulos, P., Bess, E. N., Carmody, R. N. & Turnbaugh, P. J. The microbial pharmacists within us: a metagenomic view of xenobiotic metabolism. *Nat Rev Microbiol* **14**, 273-287, doi:10.1038/nrmicro.2016.17 (2016).
- 9 Cani, P. D. *et al.* Metabolic Endotoxemia Initiates Obesity and Insulin Resistance. *Diabetes* **56**, 1761-1772, doi:10.2337/db06-1491 (2007).
- 10 Cani, P. D. *et al.* Changes in Gut Microbiota Control Metabolic Endotoxemia-Induced Inflammation in High-Fat Diet-Induced Obesity and Diabetes in Mice. *Diabetes* **57**, 1470-1481, doi:10.2337/db07-1403 (2008).
- 11 Hoyles, L. *et al.* Molecular phenomics and metagenomics of hepatic steatosis in non-diabetic obese women. *Nat Med* **24**, 1070-1080, doi:10.1038/s41591-018-0061-3 (2018).
- 12 Wang, Z. *et al.* Gut flora metabolism of phosphatidylcholine promotes cardiovascular disease. *Nature* **472**, 57-63, doi:10.1038/nature09922 (2011).
- 13 Koeth, R. A. *et al.* Intestinal microbiota metabolism of L-carnitine, a nutrient in red meat, promotes atherosclerosis. *Nat Med* **19**, 576-585, doi:10.1038/nm.3145 (2013).
- 14 Koeth, R. A. *et al.* gamma-Butyrobetaine is a proatherogenic intermediate in gut microbial metabolism of L-carnitine to TMAO. *Cell Metab* **20**, 799-812, doi:10.1016/j.cmet.2014.10.006 (2014).
- 15 Wikoff, W. R. A., A. T.; Liu, J.; Schultz, P. G.; Lesley, S. A.; Peters, E. C.; Siuzdak, G. Metabolomics analysis reveals large effects of gut microflora on mammalian blood metabolites. *PNAS* **106**, 3698-3703 (2009).
- 16 Peisl, B. Y. L., Schymanski, E. L. & Wilmes, P. Dark matter in host-microbiome metabolomics: Tackling the unknowns-A review. *Anal Chim Acta* **1037**, 13-27, doi:10.1016/j.aca.2017.12.034 (2018).

- 17 Bajpai, P., Darra, A. & Agrawal, A. Microbe-mitochondrion crosstalk and health: An emerging paradigm. *Mitochondrion* **39**, 20-25, doi:<https://doi.org/10.1016/j.mito.2017.08.008> (2018).
- 18 Donohoe, D. R. *et al.* The microbiome and butyrate regulate energy metabolism and autophagy in the mammalian colon. *Cell Metab* **13**, 517-526, doi:10.1016/j.cmet.2011.02.018 (2011).
- 19 Mollica, M. P. *et al.* Butyrate Regulates Liver Mitochondrial Function, Efficiency, and Dynamics in Insulin-Resistant Obese Mice. *Diabetes* **66**, 1405-1418, doi:10.2337/db16-0924 (2017).
- 20 Yardeni, T. *et al.* Host mitochondria influence gut microbiome diversity: A role for ROS. *Science Signaling* **12**, eaaw3159, doi:10.1126/scisignal.aaw3159 (2019).
- 21 Cioffi, C. & Vos, M. B. Su1506 - Comparison of Plasma Metabolomics Profiles of Pediatric NASH vs. NAFLD. *Gastroenterology* **154**, S-1161, doi:10.1016/S0016-5085(18)33847-2 (2018).
- 22 Bellissimo, M. P. *et al.* Plasma High-Resolution Metabolomics Differentiates Adults with Normal Weight Obesity from Lean Individuals. *Obesity* **27**, 1729-1737, doi:10.1002/oby.22654 (2019).
- 23 Sagan, L. On the Origin of Mitosing Cells. *J. Theoret. Biol.* **14**, 225-274 (1967).
- 24 Schönfeld, P. W., L. Short- and medium-chain fatty acids in the energy metabolism - the cellular perspective. *J Lipid Res* **57**, 943-954, doi:10.1194/jlr.R067629 (2016).
- 25 Royce, L. A., Liu, P., Stebbins, M. J., Hanson, B. C. & Jarboe, L. R. The damaging effects of short chain fatty acids on Escherichia coli membranes. *Appl Microbiol Biotechnol* **97**, 8317-8327, doi:10.1007/s00253-013-5113-5 (2013).

- 26 Tennant B Fau - Malm, O. J., Malm Oj Fau - Horowitz, R. E., Horowitz Re Fau - Levenson, S. M. & Levenson, S. M. Response of germfree, conventional, conventionalized and E. coli monocontaminated mice to starvation.
- 27 Barcena, C., Mayoral, P. & Quiros, P. M. Mitohormesis, an Antiaging Paradigm.
- 28 Khan, S. A. *et al.* ATGL-Catalyzed Lipolysis Regulates SIRT1 to Control PGC-1 $\alpha$ /PPAR- $\alpha$  Signaling. *Diabetes* **64**, 418, doi:10.2337/db14-0325 (2015).
- 29 Rupp, H., Rupp, T. P. & Maisch, B. Fatty acid oxidation inhibition with PPARalpha activation (FOXIB/PPARalpha) for normalizing gene expression in heart failure? *Cardiovasc Res* **66**, 423-426, doi:10.1016/j.cardiores.2005.03.023 (2005).
- 30 van Vlies, N., Ferdinandusse, S., Turkenburg, M., Wanders, R. J. A. & Vaz, F. M. PPAR $\alpha$ -activation results in enhanced carnitine biosynthesis and OCTN2-mediated hepatic carnitine accumulation. *Biochimica et Biophysica Acta (BBA) - Bioenergetics* **1767**, 1134-1142, doi:10.1016/j.bbablo.2007.07.001 (2007).
- 31 Ringseis, R., Wen, G. & Eder, K. Regulation of Genes Involved in Carnitine Homeostasis by PPARalpha across Different Species (Rat, Mouse, Pig, Cattle, Chicken, and Human). *PPAR Res* **2012**, 868317, doi:10.1155/2012/868317 (2012).
- 32 Montagner, A. *et al.* Liver PPARalpha is crucial for whole-body fatty acid homeostasis and is protective against NAFLD.
- 33 Iemitsu, M. *et al.* Aging-induced decrease in the PPAR-alpha level in hearts is improved by exercise training.
- 34 Karkkainen, O. *et al.* Diets rich in whole grains increase betainized compounds associated with glucose metabolism.

- 35 Yasumoto, T. & Shimuzu, N. Identification of  $\delta$ -Valerobetaine and Other Betaines in the Ovary of a Shellfish *Callista brevisiphonata*. *NIPPON SUISAN GAKKAISHI* **43**, 201-206, doi:10.2331/suisan.43.201 (1977).
- 36 Servillo, L. *et al.* Ruminant meat and milk contain delta-valerobetaine, another precursor of trimethylamine N-oxide (TMAO) like gamma-butyrobetaine. *Food Chem* **260**, 193-199, doi:10.1016/j.foodchem.2018.03.114 (2018).
- 37 Servillo, L. *et al.* Carnitine Precursors and Short-Chain Acylcarnitines in Water Buffalo Milk. *J Agric Food Chem* **66**, 8142-8149, doi:10.1021/acs.jafc.8b02963 (2018).
- 38 Ye, E. Q., Chacko Sa Fau - Chou, E. L., Chou El Fau - Kugizaki, M., Kugizaki M Fau - Liu, S. & Liu, S. Greater whole-grain intake is associated with lower risk of type 2 diabetes, cardiovascular disease, and weight gain.
- 39 Ringseis, R., Keller, J. & Eder, K. Role of carnitine in the regulation of glucose homeostasis and insulin sensitivity: evidence from in vivo and in vitro studies with carnitine supplementation and carnitine deficiency. *Eur J Nutr* **51**, 1-18, doi:10.1007/s00394-011-0284-2 (2012).
- 40 Fritz, I. B. Action of carnitine on long chain fatty acid oxidation by liver. *Am. J. Physiol.* **197**, 297-304 (1959).
- 41 Spaniol, M. *et al.* Mechanisms of liver steatosis in rats with systemic carnitine deficiency due to treatment with trimethylhydraziniumpropionate. *Journal of Lipid Research* **44**, 144-153, doi:10.1194/jlr.M200200-JLR200 (2003).
- 42 Spaniol, M. B., H.; Auer, L.; Zimmermann, A.; Solioz, M.; Stieger, B.; Krähenbühl, S. Development and characterization of an animal model of carnitine deficiency. *Eur. J. Biochem.* **268**, 1876-1887 (2001).

- 43 Krähenbühl, S. M., G.; Kupferschmidt, H.; Meier, P. J.; Krause, M. Plasma and hepatic carnitine and coenzyme A pools in a patient with fatal, valproate induced hepatotoxicity. *Gut* **37**, 140-143 (1995).
- 44 Luef, G. J. *et al.* Valproate therapy and nonalcoholic fatty liver disease.
- 45 Lheureux, P. E. & Hantson, P. Carnitine in the treatment of valproic acid-induced toxicity.
- 46 Noland, R. C. *et al.* Carnitine insufficiency caused by aging and overnutrition compromises mitochondrial performance and metabolic control.
- 47 Bianchi, P. B. L., D. C.; Davis, A. T. Carnitine Supplementation Ameliorates the Steatosis and Ketosis Induced by Pivalate in Rats. *J Nutr* **126**, 2873-2879 (1996).
- 48 Asai, T. *et al.* Combined therapy with PPARalpha agonist and L-carnitine rescues lipotoxic cardiomyopathy due to systemic carnitine deficiency. *Cardiovasc Res* **70**, 566-577, doi:10.1016/j.cardiores.2006.02.005 (2006).
- 49 Ishikawa, H. *et al.* L-carnitine prevents progression of non-alcoholic steatohepatitis in a mouse model with upregulation of mitochondrial pathway. *PLoS One* **9**, e100627, doi:10.1371/journal.pone.0100627 (2014).
- 50 Jiang, F. *et al.* L-carnitine ameliorates the liver inflammatory response by regulating carnitine palmitoyltransferase I-dependent PPAR $\gamma$  signaling. *Molecular Medicine Reports* **13**, 1320-1328, doi:10.3892/mmr.2015.4639 (2016).
- 51 Libert, D. M., Nowacki, A. S. & Natowicz, M. R. Metabolomic analysis of obesity, metabolic syndrome, and type 2 diabetes: amino acid and acylcarnitine levels change along a spectrum of metabolic wellness. *PeerJ* **6**, doi:10.7717/peerj.5410 (2018).

- 52 Koves, T. R. *et al.* Mitochondrial overload and incomplete fatty acid oxidation contribute to skeletal muscle insulin resistance. *Cell metabolism* **7**, 45-56, doi:10.1016/j.cmet.2007.10.013 (2008).
- 53 Lopaschuk, G. D. Fatty Acid Oxidation and Its Relation with Insulin Resistance and Associated Disorders. *Ann Nutr Metab* **68 Suppl 3**, 15-20, doi:10.1159/000448357 (2016).
- 54 Go, Y. M. *et al.* Mitochondrial metabolomics using high-resolution Fourier-transform mass spectrometry. *Methods in molecular biology* **1198**, 43-73, doi:10.1007/978-1-4939-1258-2\_4 (2014).
- 55 Liu, K. H. *et al.* High-Resolution Metabolomics Assessment of Military Personnel: Evaluating Analytical Strategies for Chemical Detection. *J Occup Environ Med* **58**, S53-61, doi:10.1097/JOM.0000000000000773 (2016).
- 56 Yu, T. & Jones, D. P. Improving peak detection in high-resolution LC/MS metabolomics data using preexisting knowledge and machine learning approach. *Bioinformatics* **30**, 2941-2948, doi:10.1093/bioinformatics/btu430 (2014).
- 57 Yu, T., Park, Y., Johnson, J. M. & Jones, D. P. apLCMS--adaptive processing of high-resolution LC/MS data. *Bioinformatics* **25**, 1930-1936, doi:10.1093/bioinformatics/btp291 (2009).
- 58 Uppal, K. *et al.* xMSanalyzer: automated pipeline for improved feature detection and downstream analysis of large-scale, non-targeted metabolomics data. *BMC bioinformatics* **14**, 15, doi:10.1186/1471-2105-14-15 (2013).
- 59 Ritchie, M. E. *et al.* limma powers differential expression analyses for RNA-sequencing and microarray studies. *Nucleic acids research* **43**, e47-e47, doi:10.1093/nar/gkv007 (2015).

- 60 Li, S. *et al.* Predicting network activity from high throughput metabolomics. *PLoS computational biology* **9**, e1003123, doi:10.1371/journal.pcbi.1003123 (2013).
- 61 Smith, C. A. *et al.* METLIN: a metabolite mass spectral database.
- 62 Ruttkies, C., Schymanski, E. L., Wolf, S., Hollender, J. & Neumann, S. MetFrag relaunched: incorporating strategies beyond in silico fragmentation. *J Cheminform* **8**, 3-3, doi:10.1186/s13321-016-0115-9 (2016).
- 63 Go, Y.-M. *et al.* Reference Standardization for Mass Spectrometry and High-Resolution Metabolomics Applications to Exposome Research. *Toxicological Sciences*, doi:10.1093/toxsci/kfv198 (2015).
- 64 Tars, K. *et al.* Targeting Carnitine Biosynthesis: Discovery of New Inhibitors against  $\gamma$ -Butyrobetaine Hydroxylase. *Journal of Medicinal Chemistry* **57**, 2213-2236, doi:10.1021/jm401603e (2014).
- 65 C. M. Chen, F. & Leo Benoiton, N. *A new method of quaternizing amines and its use in amino acid and peptide chemistry*. Vol. 54 (2011).
- 66 R: A language environment for statistical computing (R Foundation for Statistical Computing, Vienna Austria).
- 67 Rask, K. J., Brigham Kl Fau - Johns, M. M. E. & Johns, M. M. Integrating comparative effectiveness research programs into predictive health: a unique role for academic health centers.
- 68 Brigham, K. L. Predictive health: the imminent revolution in health care.
- 69 Soltow, Q. A. *et al.* High-performance metabolic profiling with dual chromatography-Fourier-transform mass spectrometry (DC-FTMS) for study of the exposome. *Metabolomics* **9**, 132-143, doi:10.1007/s11306-011-0332-1 (2011).

- 70 Kaul, S. *et al.* Dual-energy X-ray absorptiometry for quantification of visceral fat.
- 71 Matthews Dr Fau - Hosker, J. P. *et al.* Homeostasis model assessment: insulin resistance and beta-cell function from fasting plasma glucose and insulin concentrations in man.

# Chapter 3

## ***A Drosophila* model of acetaminophen toxicity**

## ABSTRACT

Acetaminophen overdose is the most common cause of acute drug induced liver injury in the United States. Despite its clinical importance, current therapy is limited and mainly supportive. Research into the mechanisms of acetaminophen toxicity and the development of novel therapeutics is hampered by the lack of robust, reproducible, and cost-effective model systems. Herein, we characterize a novel *Drosophila*-based model of acetaminophen toxicity. We demonstrate that acetaminophen treatment of *Drosophila* results in similar consequences to those observed in mammalian systems, including a robust production of reactive oxygen species, depletion of glutathione, and ultimately death. Genetic manipulations in the *Drosophila* fat body (analogous to the mammalian liver) modifies toxicity consistent with studies in mice. Finally, we utilize this system to investigate the effects of the microbiome and age on acetaminophen toxicity. This model brings to the study of oxidative liver injury all of the myriad benefits of the *Drosophila* model organism, including ease of genetic and microbiome manipulation, availability of transgenic animals, and amenability to high-throughput screening.

### 3.1 INTRODUCTION

The FDA estimates that acetaminophen (APAP) is the most widely used drug in the United States, with approximately 28 billion doses purchased per year<sup>1</sup>. As a consequence, APAP overdose is the leading cause of drug-induced liver injury in the United States<sup>2</sup>. Upon ingestion, APAP is absorbed in the intestine and travels to the liver via the portal circulation where it is rapidly glucuronidated or sulfonated allowing for its harmless excretion<sup>3</sup>. If the liver is exposed to an excess of APAP, however, these detoxification processes are overwhelmed, and APAP is instead metabolized by the cytochrome P450 enzyme Cyp2e1 into the highly reactive and toxic metabolite NAPQI<sup>4</sup>. NAPQI rapidly forms adducts with critical cellular proteins, impairs mitochondrial membrane integrity, and results in a profound production of reactive oxygen species (ROS) within hepatocytes<sup>5</sup>. If these ROS overwhelm the cellular antioxidant response, cell death and tissue necrosis occurs, resulting in severe hepatotoxicity that can lead to death<sup>6</sup>.

Despite the clinical importance of APAP overdose, treatment remains limited<sup>7</sup>. Current therapies include limiting absorption of APAP by administering activated charcoal<sup>8-10</sup>, replenishing glutathione stores by administering the glutathione precursor n-acetylcysteine (NAC)<sup>11,12</sup>, and subsequent supportive care. A complicating factor in clinical trials has been the significant interindividual variability in susceptibility to APAP toxicity<sup>13</sup>. It has been proposed that this variability is due to genetic differences (i.e. altered expression of Cyp2e1 or conjugation enzymes<sup>14,15</sup>) or environmental exposures (alcohol<sup>16</sup>, drugs<sup>13,17</sup>, or microbiome composition<sup>18</sup>). However, investigation of these factors in preclinical studies is complicated due to the time and expense of generating transgenic mice and the variability of the currently available rodent models<sup>19</sup>.

Herein, we present a novel, highly reproducible, *Drosophila*-based system for studying acetaminophen toxicity. Our data demonstrate that acetaminophen accumulates in *Drosophila*, resulting in the generation of ROS in the fat body (an organ analogous to the mammalian liver<sup>20</sup>), a rapid depletion of systemic glutathione, and subsequent mortality. In addition, genetic manipulation of the fat body results in alterations in APAP toxicity, in agreement with existing studies in mice. Finally, we utilized this system to investigate the effect of the microbiome and aging on APAP toxicity, two conditions that are expensive and involved to investigate in murine systems. Our data demonstrate that the presence of the microbiome is protective in the context of APAP toxicity and that age may play a significant role in susceptibility to drug induced liver injury.

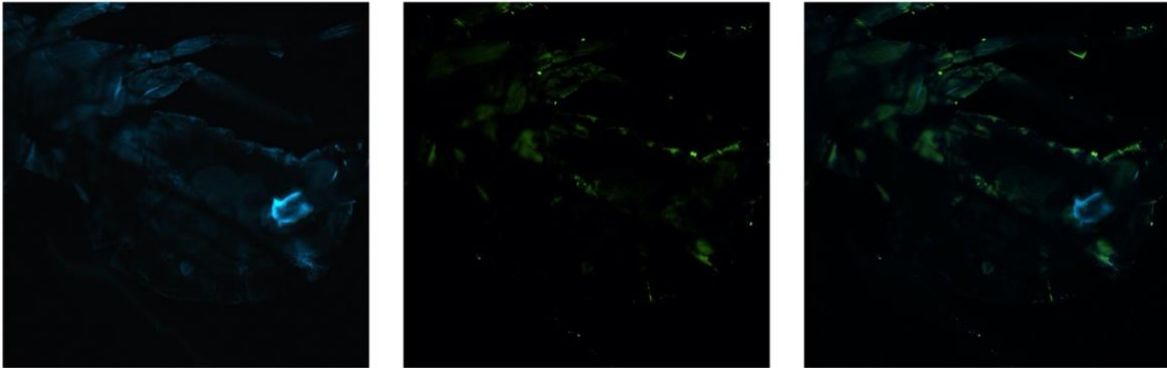
The model presented here brings the immense power of *Drosophila* genetics to the study of APAP toxicity. This will allow for the identification of genetic factors that may modulate susceptibility to APAP. In addition, the high-throughput nature of *Drosophila* will allow for the screening of potential therapeutics against APAP toxicity. These findings can guide subsequent studies in rodent models as well as human disease and lead to an improvement in the understanding of APAP toxicity and the clinical tools available for its treatment.

## 3.2 RESULTS

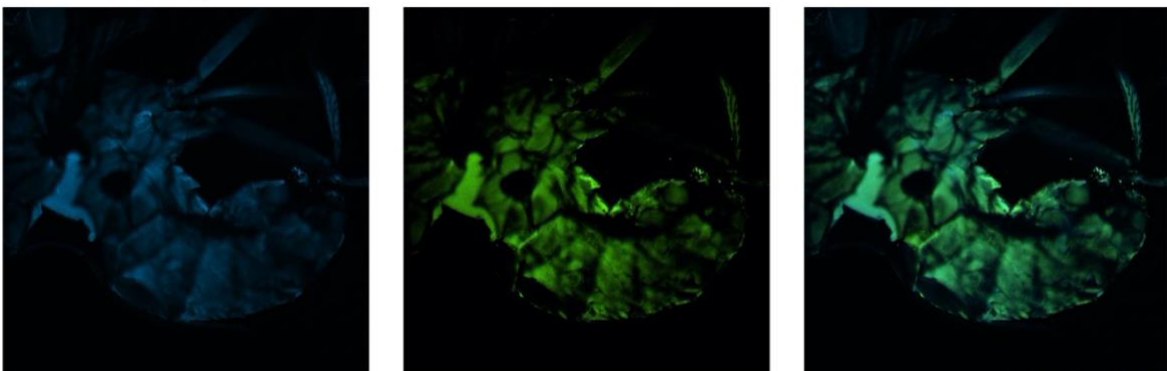
### 3.2.1 Acetaminophen Accumulates in *Drosophila*.

To determine if ingested acetaminophen accumulates in the tissues of *Drosophila*, we transferred 5 day old W1118 *Drosophila* to vials containing 5% sucrose, 1% agar, and either vehicle control or 100 mM APAP. After 12 hours, *Drosophila* were harvested and CLARITY<sub>21</sub> performed for DAPI (nuclear stain) and APAP using an anti-acetaminophen antibody. Vehicle-fed *Drosophila* demonstrated very little background APAP immunoreactivity at 12 hours (Figure 3.1A). In contrast, APAP feeding resulted in a significant increase of APAP immunoreactivity in the abdomen of treated flies, consistent with an accumulation of APAP (Figure 3.1B).

**A. Vehicle Control**



**B. APAP - 12 hours**



APAP DAPI

**Figure 3.1: Accumulation of Acetaminophen in *Drosophila* observed using CLARITY.**

**(A)** Vehicle-treated flies stained for DAPI and APAP. **(B)** *Drosophila* treated for 12 hours with APAP and stained for DAPI and APAP.

### 3.2.2 Acetaminophen exposure results in dose-dependent mortality in WT *Drosophila*.

To determine if this accumulation eventually resulted in toxicity, 5 day old W1118 male (Figure 3.2A) and female (Figure 3.2B) *Drosophila* were administered 100mM, 50 mM, 25mM, 12.5 mM, or vehicle control as described above and survival measured. As shown in Figure 1C-D, APAP feeding resulted in a dose-dependent mortality in both male and female *Drosophila*. Intriguingly, female flies were more resistant to APAP toxicity at all doses.

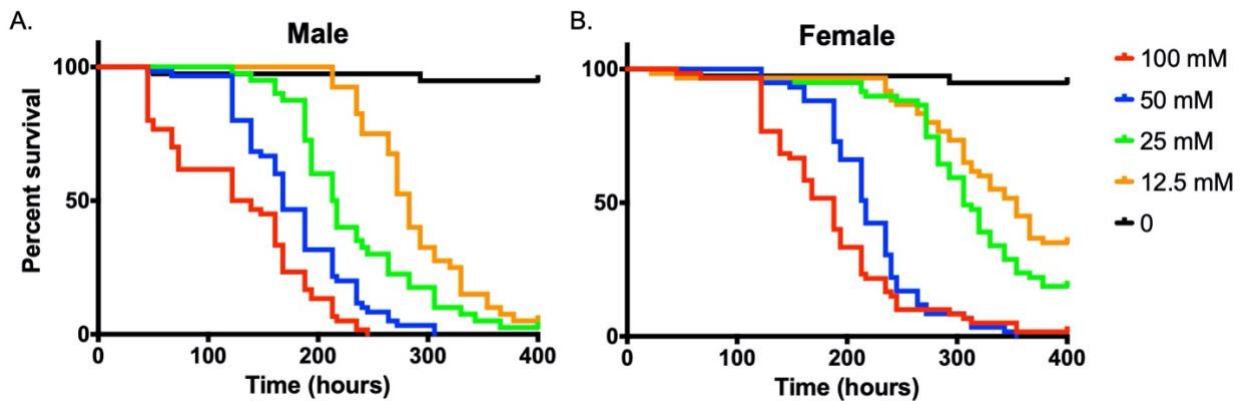


**Figure 3.2: Acetaminophen results in dose-dependent mortality in adult *Drosophila*.**

Mortality observed due to APAP exposure in 5 day old W1118 (A) male and (B) female *Drosophila*. Log-Rank  $p=0.0001$ ,  $n=60$ .

### ***3.2.3 APAP Administration Increases ROS in the Drosophila Fat Body and Depletes Systemic Glutathione.***

In the mammalian liver, APAP is bioconverted into the toxic metabolite NAPQI by the Cytochrome P450 enzyme Cyp2e1<sup>4</sup>. NAPQI is highly reactive and rapidly conjugates with critical cellular enzymes, interfering with normal cellular function and destabilizing the mitochondrial membranes. Due to its impact on mitochondrial function, a hallmark of APAP hepatotoxicity is the robust production of reactive oxygen species (ROS)<sup>22</sup>.

To determine if APAP ingestion resulted in increased ROS in the *Drosophila* Fat Body, early third-instar *Drosophila* larvae were fed for 4 hours on either PBS (vehicle control) or 100 mM APAP along with HydroCy3, a ROS sensitive dye that fluoresces in the presence of superoxide radicals<sup>23</sup>. PBS feeding resulted in minimal ROS production in the fat body (Figure 3.3A). However, APAP feeding significantly increased ROS in the fat body (Figure 3.3B-C).

NAPQI is rapidly conjugated to glutathione, limiting its toxicity while depleting cellular glutathione stores<sup>13,24</sup>. We assessed the effect of APAP feeding on systemic glutathione levels. Under vehicle fed conditions, we observed that female flies had a nearly two-fold higher level of glutathione than male flies (Figure 3.3D). This may partly account for the delayed onset of mortality observed in female flies relative to male flies (Figure 3.2A-B). In both male and female flies, APAP feeding resulted in a decrease in total glutathione relative to vehicle control (Figure 3.3D).

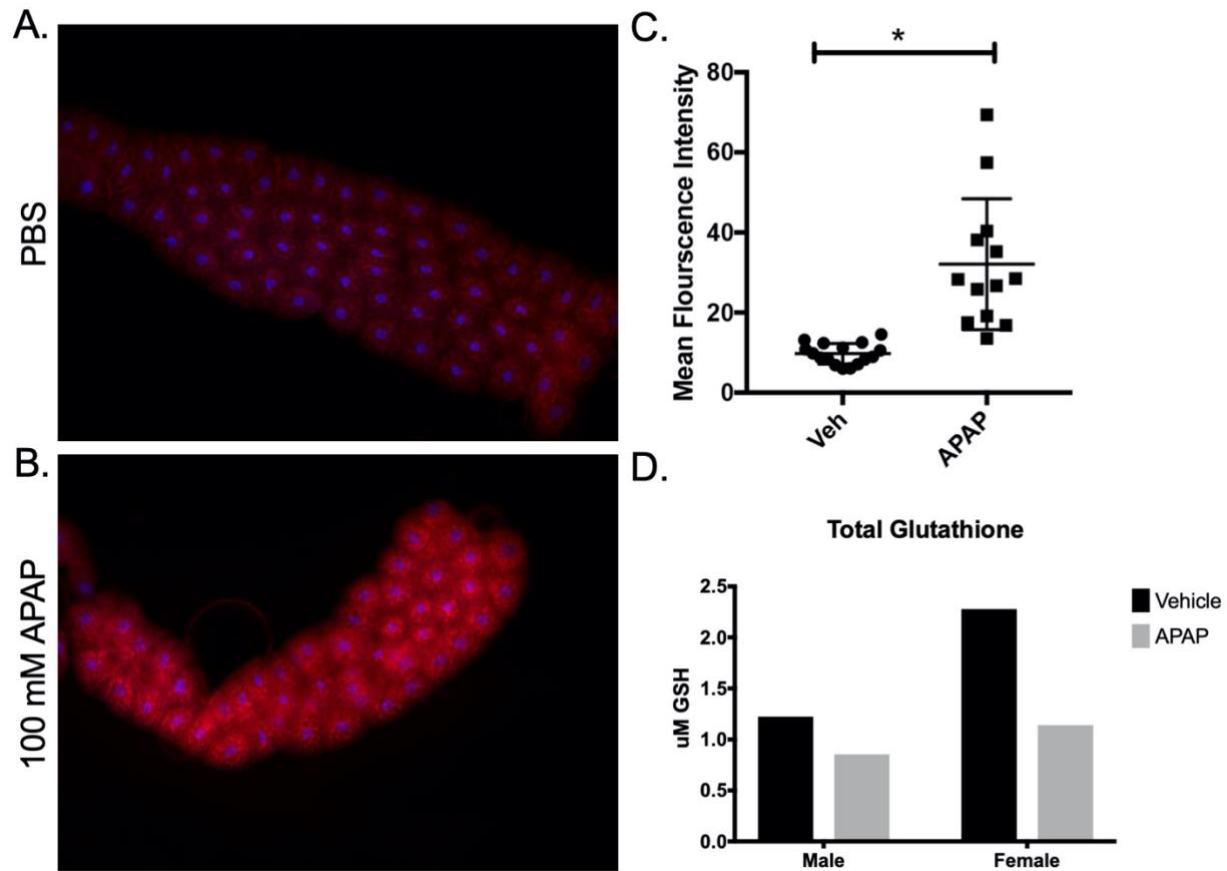


**Figure 3.3: APAP Administration Increases ROS in the *Drosophila* Fat Body and Depletes Systemic Glutathione.**

Representative fluorescent images of fat body of early third instar *Drosophila* larvae after 4 hours of feeding the ROS sensitive dye HydroCy3 and either (A) PBS or (B) 100 mM APAP in PBS. (C) Quantification of fluorescence intensity from imaged fat bodies. \* $p < 0.05$  as determined by t-test.  $n = 13$  flies per condition. (D) Total glutathione content of whole *Drosophila* treated with either vehicle control or 100 mM APAP for 3 days.  $n = 1$ .

### 3.2.4 Fat body-specific depletion of Cyp18a1 attenuates APAP toxicity.

In the mammalian system, APAP requires bioconversion by *cyp2e1* for toxicity. We identified a putative *Drosophila* homologue to *cyp2e1*, Cyp18a1 (Figure 3.4A). Depletion of Cyp18a1 in the fat body rendered these *Drosophila* resistant to APAP-induced mortality (Figure 3.4B), in agreement with murine studies in which *cyp2e1* was knocked out<sup>25</sup>. This protection in *Drosophila* appears to be due to the lack of APAP bioconversion, as metabolomic analysis of whole *Drosophila* reveal an increase in native acetaminophen in fat body-specific Cyp18a1 knockdown animals (Figure 3.4C). Taken together, these data demonstrate that the mechanism of action of APAP-induced toxicity is conserved from *Drosophila* to mammals.

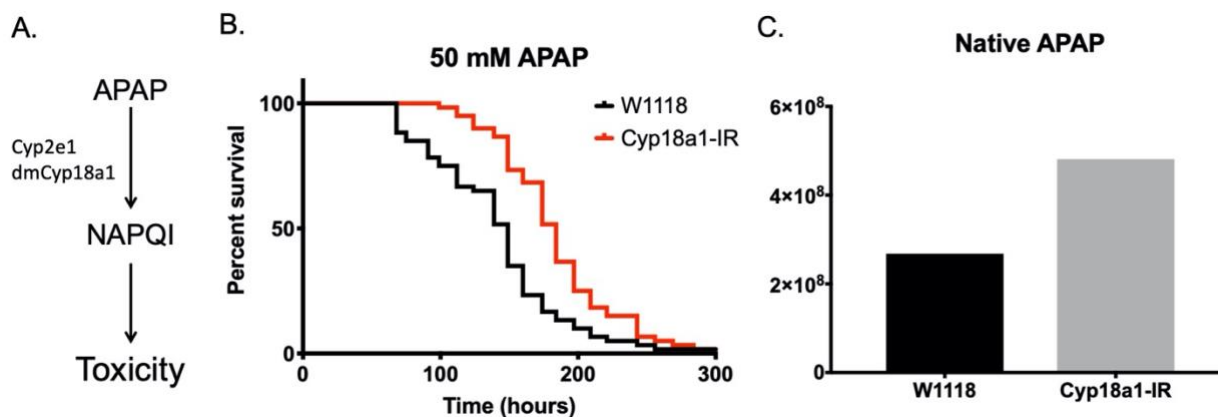


**Figure 3.4: Fat body-specific depletion of Cyp18a1 attenuates APAP toxicity.**

(A) Schematic of APAP metabolism and mechanism of toxicity. (B) Effect of fat body-specific depletion of Cyp18a1 on survival of *Drosophila* treated with 50 mM APAP. Log-Rank test  $p < 0.0001$ ,  $n = 60$ . (C) Measurement of native acetaminophen from whole flies using mass spectrometry.  $n = 1$ .

### 3.2.5 Genetic and pharmacologic modifiers of APAP toxicity in *Drosophila*.

It is well established in murine models of APAP hepatotoxicity that genetic alteration of the cellular antioxidant response can alter the severity of liver injury. The master transcriptional regulator of the host antioxidant response is the transcription factor Nrf2<sup>26</sup>. In mice, overexpression of Nrf2 protects against APAP overdose<sup>27</sup> while knock out results in more severe hepatic injury<sup>28</sup>. The *Drosophila* homologue of Nrf2 is CnCC<sup>29</sup>.

We specifically depleted or overexpressed CnCC in the *Drosophila* fat body and assessed their susceptibility to APAP-induced mortality. In agreement with studies conducted in mice, Cncc overexpression resulted in a significant decrease in mortality in response to APAP. In contrast, Cncc knockdown augmented APAP toxicity and increased mortality (Figure 3.5A). These data demonstrate that the genetic manipulations that alter susceptibility in mice are conserved in *Drosophila*.

N-acetyl cysteine (NAC) is the current standard of care for APAP overdose<sup>12</sup>. It is believed to have benefit in APAP hepatotoxicity by increasing the availability of the glutathione precursor cysteine, thereby driving glutathione synthesis. To test its efficacy in the *Drosophila* model, we treated *Drosophila* concurrently with both NAC and APAP. At 10mM, NAC feeding significantly protected against APAP induced mortality relative to vehicle control (Figure 3.5B). Another small molecule that works to increase glutathione and has shown efficacy in human disease is the amino acid methionine<sup>30</sup>. In agreement with these studies, 10 mM methionine treatment attenuated APAP toxicity in *Drosophila* (Figure 3.5C).

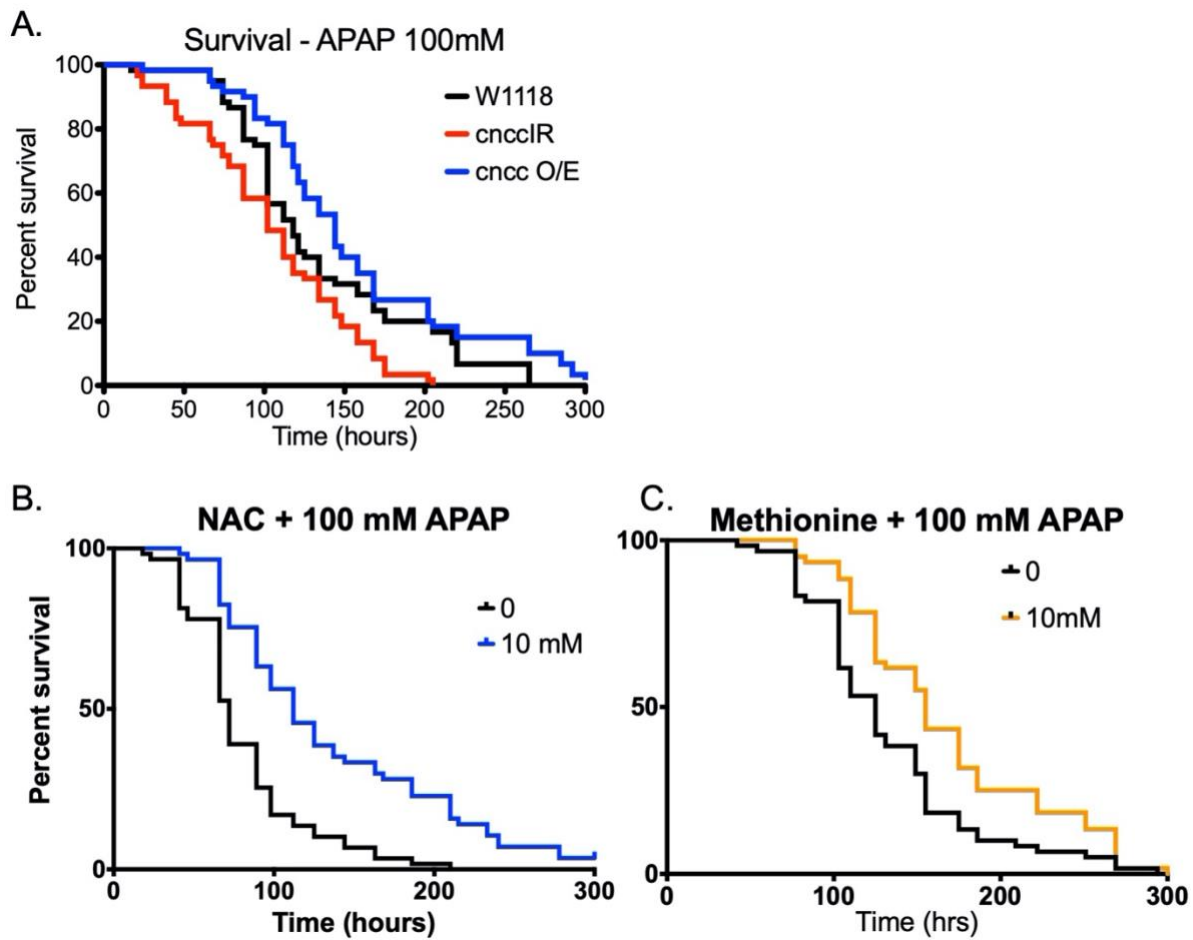


**Figure 3.5: Genetic and pharmacologic modifiers of APAP toxicity in *Drosophila*.**

(A) Survival of wild type (W1118) and fat body specific dNrf2 knockout (*cnccIR*) and overexpressing (*cncc O/E*) flies treated with 100 mM acetaminophen. (B) Effect of 10 mM N-acetylcysteine supplementation on APAP toxicity. (C) Effect of 10 mM Methionine supplementation of APAP toxicity. Log-Rank test  $p < 0.0001$ ,  $n = 60$ .

### ***3.2.6 The microbiome protects against acetaminophen toxicity in *Drosophila*.***

These data demonstrate that studies performed in mice using different genetic or pharmacologic manipulations could be recapitulated in flies. We next wanted to determine if we could utilize our model to pilot studies that are more difficult, time-consuming, and expensive in murine models. It has been proposed that the microbiome may modify susceptibility to APAP toxicity in humans and thereby explain inter-individual susceptibility to drug induced liver injury<sup>18</sup>. Studies investigating the severity of APAP hepatotoxicity in GF vs conventional mice have been inconclusive<sup>31</sup>.

To address this question, we treated 5 day old germ-free or conventional *Drosophila* with 100 mM APAP as describes above. As shown in Figure 3.6A, the presence of a microbiome significantly protected against APAP induced toxicity. To extend these data, we treated conventional *Drosophila* with antibiotics for 3 days to deplete the microbiome. In agreement with the data from GF flies, antibiotic treatment significantly augmented APAP induced mortality (Figure 3.6B).

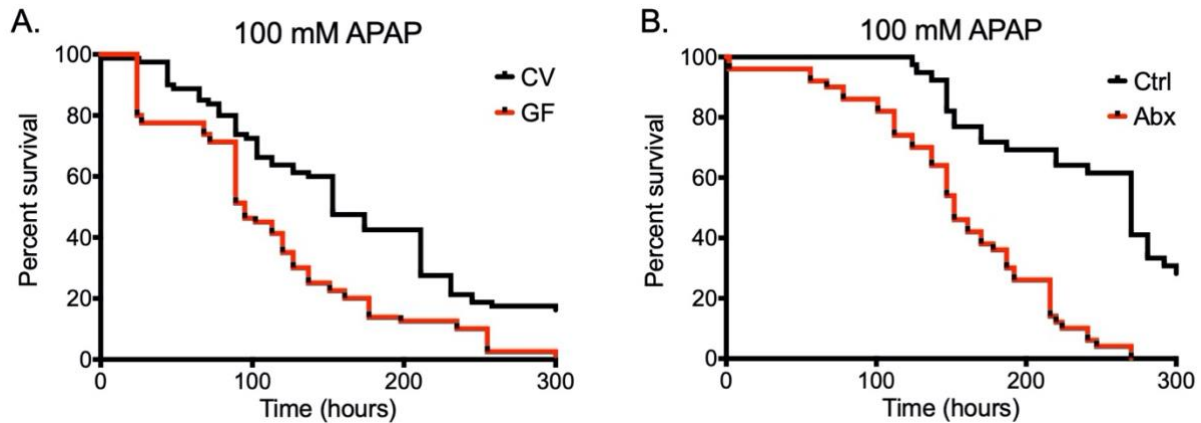


**Figure 3.6: The microbiome protects against acetaminophen toxicity in *Drosophila*.**

(A) Survival of germ-free (GF) and conventional (CV) *Drosophila* exposed to 100 mM APAP.

(B) Effect of antibiotic-mediated depletion of the microbiome on susceptibility to APAP toxicity.

Log-Rank test  $p < 0.0001$ ,  $n = 60$ .

### 3.2.7 Effects of age on APAP-induced mortality

Few human or murine studies exist regarding the influence of aging on susceptibility to drug induced liver injury<sup>32</sup>. Medication use is exponentially greater in the elderly, and complex drug combinations may result in increased unintentional APAP overdose in this population. To determine if aging altered susceptibility to APAP, we followed mortality in 5, 10, and 30 day old flies with and without APAP.

These data reveal a striking age-dependent increase in mortality (Figure 3.7A-B). This effect was most pronounced in the oldest flies (30 days old at time of APAP administration) and was observed in both males and females (Figure 3.7A-B). Future studies in murine models will be necessary to corroborate these findings.

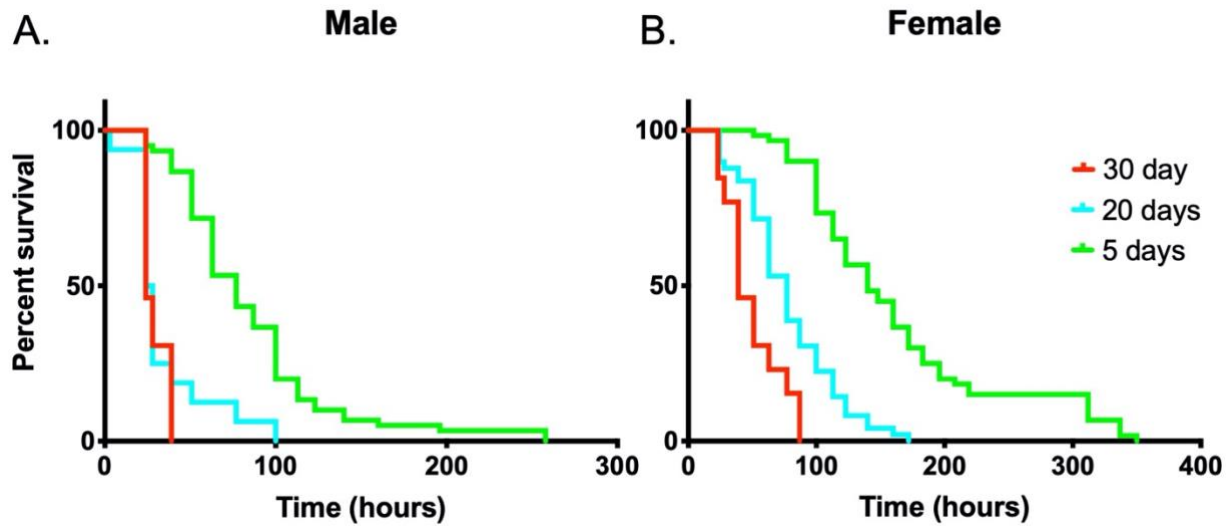


**Figure 3.7: Effects of age on APAP-induced mortality.**

Susceptibility of 5, 20, and 30 day old (A) male and (B) female flies to APAP induced mortality.

Log-Rank test  $p < 0.0001$ ,  $n = 60$ .

### 3.3 DISCUSSION

Acetaminophen overdose is the most common cause of drug induced liver injury in the United States<sup>2</sup>. While some overdoses are intentional, many result from the inadvertent combination of one of innumerable acetaminophen containing drugs. Despite its ubiquity, acetaminophen can cause significant hepatic injury at relatively low doses, and current therapy is limited and primarily supportive<sup>12</sup>.

A major blockade to the study of the pathogenesis of APAP hepatotoxicity and the identification of novel therapeutics is the lack of robust, reproducible experimental models. Many of the cell lines used in hepatic research, such as HepG2 cells, do not express the cytochrome P450 enzymes necessary to bioconvert APAP into its toxic metabolite<sup>33</sup>. While APAP treatment of HepG2 cells does cause cell death, the mechanism is unclear and possibly not relevant *in vivo*. Rodents will develop APAP hepatotoxicity and accompanying histologic changes including centrilobular necrosis, similar to that observed in humans. However, the model requires overnight fasting to deplete hepatic glutathione, and if not done precisely, leads to notoriously variable results<sup>19</sup>. As such, development of novel tools for the study of APAP toxicity is desperately needed.

Herein, we describe the use of *Drosophila melanogaster* as a model for APAP-induced oxidative liver injury. Our data demonstrate that APAP accumulates within flies, results in reactive oxygen species generation within the fat body, and leads to mortality in a dose-dependent manner. Furthermore, APAP toxicity in *Drosophila* can be modified by genetic and pharmacologic manipulations that have been validated in both mice and humans. Finally, we utilized our model to determine the impact of antibiotic use and age on APAP toxicity, which have not been described previously.

*Drosophila* bring to the study of oxidative liver injury many advantages, including ease of genetic manipulation, availability of genetic mutants and constructs, ease of germ-free generation, relatively short lifespan, amenability to high-throughput screening, and overall cost relative to murine models<sup>34</sup>. However, some limitations should be noted. First, the fat body, while analogous, lacks the structural organization and cellular make-up of the mammalian liver. Second, *Drosophila* lack a portal circulation that moves absorbed intestinal metabolites directly to the fat body. Instead, the fat body and other systemic organs are bathed in “hemolymph.” Therefore, it is possible that absorbed acetaminophen may impact other systemic organs as well as the fat body, whereas in mammals APAP toxicity is fairly specific to the liver. Third, *Drosophila* do not have an adaptive immune system, which complicates both the study of tissue restitution after injury and the underlying crosstalk with intestinal microbes.

Despite these limitations, the use of *Drosophila* holds great potential for the study of APAP overdose and potentially other forms of drug-induced liver injury. Genetic screens may help identify previously uncharacterized genetic modifiers of susceptibility. High-throughput compound screens may yield new therapeutics. Germ-free and monocolonization studies may provide some insight into the opaque and complex bidirectional signaling between the microbiome and systemic organs. The model presented here, therefore, shows great promise for the advancement of the study of drug induced liver injury.

### 3.4 METHODS

#### *Drosophila*

*Drosophila* were maintained on standard diets at 25°C with 12 hour light/dark cycles (7 am – 7 pm). Unless otherwise stated, WT flies are of the W1118 background. Tissue specific genetic manipulations were performed using the Gal4 UAS system described previously<sup>35</sup>. Briefly, virgin Yolk or R4-Gal4 *Drosophila* were crossed with male W1118 (control), UAS-CNCC IR (dNrf2 knockdown), UAS-CNCC (dNrf2 overexpression), or UAS-Cyp18a1IR (Cyp18a1 knockdown). Offspring were collected 5 days post-eclosure and used for experiments.

#### *Drosophila* Acetaminophen Model

Acetaminophen was dissolved in 5% sucrose and 1% agar. 3 mls of this mixture was aliquoted into empty vials and allowed to solidify and dry in a fume hood. 20 flies were transferred to each vial and mortality recorded approximately every 12 hours for the duration of the experiment. Control vials containing only 5% sucrose and 1% agar were included in every experiment to account for sporadic death. N-acetylcysteine and methionine (Sigma-Aldrich) were dissolved in the APAP media at the indicated concentrations.

#### CLARITY

Whole *Drosophila* were fixed in 4% PFA for 12 hours at 4°C, then rinsed in 3 changes of PBS with shaking at room temperature for 3 hours. They were then immersed in FlyClear Solution-1 (8% THEED (2,2',2'',2'''- (Ethylenedinitrilo)-tetraethanol) (Sigma-Aldrich), 5% Triton X-100 (Sigma-Aldrich) and 25% Urea (Fisher Scientific, in PBS) for 14 days with shaking at 37°C, as described previously<sup>21</sup>. Cleared *Drosophila* were rinsed in 3 changes of PBS with shaking for 12 hours at room temperature, then immersed in blocking solution (PBS, 5% normal goat serum, 0.1% Triton X-100) at room temperature for 3 hours. The samples were transferred to sheep anti-

acetaminophen primary antibody in blocking solution (1:250, Bio-Rad, 0016-0104 ) for 12 hours at 4°C, followed by 3x 5 minute washes in PBS with 0.1% Triton X-100 with shaking at room temperature. They were then incubated in donkey anti-sheep IgG Alexa Fluor 488 secondary antibody (1:500, Abcam, ab150177) for 3 hours at room temperature followed by a 10 minute counterstain with DAPI. The *Drosophila* were mounted on 1.0 – 1.2 mm cavity slides (Eisco) in VECTASHIELD® Antifade Mounting Medium (Vector Laboratories), coverslipped and sealed with clear nail polish. Samples were allowed to set at room temperature for 12 hours, then imaged using a Nikon A1R HD25 inverted confocal microscope at 40x (Nikon, Apo Fluor, 1.30 NA, WD = 0.24mm).

### **Analysis of fat body ROS**

Early third-instar *Drosophila* larvae were fed for 4 hours on either PBS (vehicle control) or 100mM APAP along with HydroCy3 (ROSstar 550, Li-Cor). Fat bodies were then dissected, whole-mounted on glass microscope slides and imaged using Nikon eclipse 80i microscope fitted with a R1 Retiga Q Imaging camera. Quantification of fluorescence intensity was performed using ImageJ software (NIH).

### **Glutathione measurements**

GSH and GSSG were measured from whole *Drosophila* tissue using a glutathione assay kit (Cayman Chemical) according to manufacturer's instructions. Data are normalized to number of *Drosophila* utilized.

### **Generation of germ-free flies**

Adult flies were placed in vials with fresh food and left overnight (8-14 hours). The vials were emptied and ~5mL dH<sub>2</sub>O was added to each vial. A paintbrush was used to suspend the remaining eggs in the dH<sub>2</sub>O, then the dH<sub>2</sub>O and eggs were poured into 90um cell strainers. In an aseptic

environment, the cell strainers were placed in 50% bleach for 10 minutes, then transferred into sterile dH<sub>2</sub>O for 1 minute three times consecutively. Using a sterile scalpel and forceps, the bottoms of the cell strainers were removed and placed in new, autoclaved vials with germ-free fly food. To verify the absence of bacteria, flies from two different germ-free vials were crushed in ~200uL of sterile dH<sub>2</sub>O in an aseptic environment, then plated on blood agar. The blood agar plate was left overnight at 37 degrees Celsius. No bacteria were observed growing on the plate.

### **Antibiotic treatment**

5 day old *Drosophila* were transferred to media containing 5% sucrose, 1% agar, 100 ug/mL ampicillin, and 50 ug/mL streptomycin (Sigma-Aldrich). 3 days later, *Drosophila* were transferred to fresh vials containing acetaminophen without antibiotics and mortality assessed. Mice were gavaged daily for 5 days with 200 uL PBS containing 1 mg/mL ampicillin, 1 mg/mL gentamicin, 1 mg/mL metronidazole, 1 mg/mL neomycin, and 0.5 mg/mL vancomycin (all obtained from Sigma-Aldrich).

### 3.5 REFERENCES

1. Bunchorntavakul, C. & Reddy, K. R. Acetaminophen (APAP or N-Acetyl-p-Aminophenol) and Acute Liver Failure. *Clin Liver Dis* **22**, 325–346 (2018).
2. Yoon, E., Babar, A., Choudhary, M., Kutner, M. & Pysopoulos, N. Acetaminophen-Induced Hepatotoxicity: a Comprehensive Update. *J Clin Transl Hepatol* **4**, 131–142 (2016).
3. Forrest, J. A., Clements, J. A. & Prescott, L. F. Clinical pharmacokinetics of paracetamol. *Clin Pharmacokinet* **7**, 93–107 (1982).
4. Manyike, P. T., Kharasch, E. D., Kalhorn, T. F. & Slattery, J. T. Contribution of CYP2E1 and CYP3A to acetaminophen reactive metabolite formation. *Clin. Pharmacol. Ther.* **67**, 275–282 (2000).
5. Gemborys, M. W., Mudge, G. H. & Gribble, G. W. Mechanism of decomposition of N-hydroxyacetaminophen, a postulated toxic metabolite of acetaminophen. *J. Med. Chem.* **23**, 304–308 (1980).
6. Nelson, S. D. Molecular mechanisms of the hepatotoxicity caused by acetaminophen. *Semin. Liver Dis.* **10**, 267–278 (1990).
7. Stine, J. G. & Lewis, J. H. Current and future directions in the treatment and prevention of drug-induced liver injury: a systematic review. *Expert Rev Gastroenterol Hepatol* **10**, 517–536 (2016).
8. Gazzard, B. G., Willison, R. A., Weston, M. J., Thompson, R. P. & Williams, R. Charcoal haemoperfusion for paracetamol overdose. *Br J Clin Pharmacol* **1**, 271–275 (1974).
9. Underhill, T. J., Greene, M. K. & Dove, A. F. A comparison of the efficacy of gastric lavage, ipecacuanha and activated charcoal in the emergency management of paracetamol overdose. *Arch Emerg Med* **7**, 148–154 (1990).

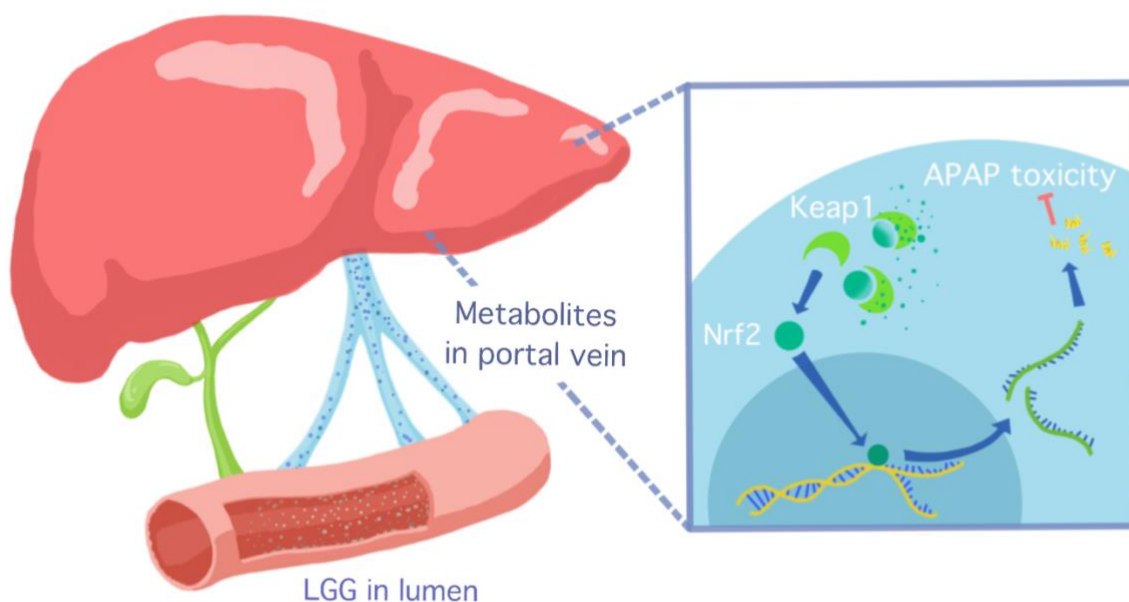
10. Chiew, A. L. *et al.* Massive paracetamol overdose: an observational study of the effect of activated charcoal and increased acetylcysteine dose (ATOM-2). *Clin Toxicol (Phila)* **55**, 1055–1065 (2017).
11. Rumack, B. H., Peterson, R. C., Koch, G. G. & Amara, I. A. Acetaminophen overdose. 662 cases with evaluation of oral acetylcysteine treatment. *Arch. Intern. Med.* **141**, 380–385 (1981).
12. Chiew, A. L., Gluud, C., Brok, J. & Buckley, N. A. Interventions for paracetamol (acetaminophen) overdose. *Cochrane Database Syst Rev* **2**, CD003328 (2018).
13. McGill, M. R. & Jaeschke, H. Metabolism and disposition of acetaminophen: recent advances in relation to hepatotoxicity and diagnosis. *Pharm. Res.* **30**, 2174–2187 (2013).
14. Critchley, J. A., Nimmo, G. R., Gregson, C. A., Woolhouse, N. M. & Prescott, L. F. Inter-subject and ethnic differences in paracetamol metabolism. *Br J Clin Pharmacol* **22**, 649–657 (1986).
15. Zhao, L. & Pickering, G. Paracetamol metabolism and related genetic differences. *Drug Metab. Rev.* **43**, 41–52 (2011).
16. Schmidt, L. E., Dalhoff, K. & Poulsen, H. E. Acute versus chronic alcohol consumption in acetaminophen-induced hepatotoxicity. *Hepatology* **35**, 876–882 (2002).
17. Abebe, W. Herbal medication: potential for adverse interactions with analgesic drugs. *J Clin Pharm Ther* **27**, 391–401 (2002).
18. Klaassen, C. D. & Cui, J. Y. Review: Mechanisms of How the Intestinal Microbiota Alters the Effects of Drugs and Bile Acids. *Drug Metab. Dispos.* **43**, 1505–1521 (2015).
19. Mossanen, J. C. & Tacke, F. Acetaminophen-induced acute liver injury in mice. *Lab. Anim.* **49**, 30–36 (2015).

20. Baker, K. D. & Thummel, C. S. Diabetic larvae and obese flies-emerging studies of metabolism in *Drosophila*. *Cell Metab.* **6**, 257–266 (2007).
21. Pende, M. *et al.* High-resolution ultramicroscopy of the developing and adult nervous system in optically cleared *Drosophila melanogaster*. *Nat Commun* **9**, 4731 (2018).
22. Jaeschke, H., Xie, Y. & McGill, M. R. Acetaminophen-induced Liver Injury: from Animal Models to Humans. *J Clin Transl Hepatol* **2**, 153–161 (2014).
23. Sadlowski, C. M., Maity, S., Kundu, K. & Murthy, N. Hydrocyanines: a versatile family of probes for imaging radical oxidants in vitro and in vivo. *Molecular Systems Design & Engineering* **2**, 191–200 (2017).
24. Mitchell, J. R., Jollow, D. J., Potter, W. Z., Gillette, J. R. & Brodie, B. B. Acetaminophen-induced hepatic necrosis. IV. Protective role of glutathione. *J. Pharmacol. Exp. Ther.* **187**, 211–217 (1973).
25. Lee, S. S., Buters, J. T., Pineau, T., Fernandez-Salguero, P. & Gonzalez, F. J. Role of CYP2E1 in the hepatotoxicity of acetaminophen. *J. Biol. Chem.* **271**, 12063–12067 (1996).
26. Moi, P., Chan, K., Asunis, I., Cao, A. & Kan, Y. W. Isolation of NF-E2-related factor 2 (Nrf2), a NF-E2-like basic leucine zipper transcriptional activator that binds to the tandem NF-E2/AP1 repeat of the beta-globin locus control region. *Proc. Natl. Acad. Sci. U.S.A.* **91**, 9926–9930 (1994).
27. Okawa, H. *et al.* Hepatocyte-specific deletion of the *keap1* gene activates Nrf2 and confers potent resistance against acute drug toxicity. *Biochem. Biophys. Res. Commun.* **339**, 79–88 (2006).

28. Enomoto, A. *et al.* High sensitivity of Nrf2 knockout mice to acetaminophen hepatotoxicity associated with decreased expression of ARE-regulated drug metabolizing enzymes and antioxidant genes. *Toxicol. Sci.* **59**, 169–177 (2001).
29. Kobayashi, M. *et al.* Identification of the interactive interface and phylogenetic conservation of the Nrf2-Keap1 system. *Genes Cells* **7**, 807–820 (2002).
30. Prescott, L. F., Sutherland, G. R., Park, J., Smith, I. J. & Proudfoot, A. T. Cysteamine, methionine, and penicillamine in the treatment of paracetamol poisoning. *Lancet* **2**, 109–113 (1976).
31. Possamai, L. A. *et al.* The role of intestinal microbiota in murine models of acetaminophen-induced hepatotoxicity. *Liver Int.* **35**, 764–773 (2015).
32. Mian, P., Allegaert, K., Spriet, I., Tibboel, D. & Petrovic, M. Paracetamol in Older People: Towards Evidence-Based Dosing? *Drugs Aging* **35**, 603–624 (2018).
33. Guo, L. *et al.* Similarities and differences in the expression of drug-metabolizing enzymes between human hepatic cell lines and primary human hepatocytes. *Drug Metab. Dispos.* **39**, 528–538 (2011).
34. Ugur, B., Chen, K. & Bellen, H. J. Drosophila tools and assays for the study of human diseases. *Dis Model Mech* **9**, 235–244 (2016).
35. Duffy, J. B. GAL4 system in Drosophila: a fly geneticist's Swiss army knife. *Genesis* **34**, 1–15 (2002).

# Chapter 4

## Gut-Resident *Lactobacilli* Activate Hepatic Nrf2 and Protect Against Oxidative Liver Injury



This chapter is adapted from:

Bejan J. Saeedi<sup>1,4</sup>, Ken H. Liu<sup>2,4</sup>, Joshua A. Owens<sup>2</sup>, Sarah Hunter-Chang<sup>1</sup>, Mary C. Camacho<sup>1</sup>, Richard U. Eboka<sup>1</sup>, Bindu Chandrasekharan<sup>1</sup>, Nusaiba F. Baker<sup>1</sup>, Trevor M. Darby<sup>3</sup>, Brian S. Robinson<sup>1</sup>, Rheinallt M. Jones<sup>3</sup>, Dean P. Jones<sup>2,5</sup>, Andrew S. Neish<sup>1,5</sup>. Gut-Resident *Lactobacilli* Activate Hepatic Nrf2 and Protect Against Oxidative Liver Injury. (2020) *Cell Metabolism*

<sup>1</sup>Department of Pathology, <sup>2</sup>Division of Pulmonary, Allergy and Critical Care Medicine, <sup>3</sup>Division of Pediatric Gastroenterology, Hepatology, and Nutrition, Department of Pediatrics, Emory University School of Medicine, Atlanta GA, 30322, USA.

<sup>4</sup>These authors contributed equally, <sup>5</sup>Senior author

## ABSTRACT

Many studies have suggested a role for gut-resident microbes (the “gut microbiome”) in modulating host health, however the mechanisms by which they impact systemic physiology remain largely unknown. In this study, metabolomic and transcriptional profiling of germ-free and conventionalized mouse liver revealed an upregulation of the Nrf2 antioxidant and xenobiotic response in microbiome-replete animals. Using a *Drosophila*-based screening assay, we identified members of the genus *Lactobacillus* capable of stimulating Nrf2. Indeed, the human commensal *Lactobacillus rhamnosus* GG (LGG) potently activated Nrf2 in the *Drosophila* liver analog and the murine liver. This activation was sufficient to protect against two models of oxidative liver injury, acetaminophen overdose and acute ethanol toxicity. Characterization of the portal circulation of LGG-treated mice by tandem mass spectrometry identified a small molecule activator of Nrf2, 5-methoxyindoleacetic acid, produced by LGG. Taken together, these data demonstrate a mechanism by which intestinal microbes modulate hepatic susceptibility to oxidative injury.

## 4.1 INTRODUCTION

The microorganisms that reside within the human gut comprise over 100 trillion bacteria, along with myriad fungi and viruses <sup>1</sup>. Until relatively recently, little was known about the functional consequences of this diverse and dynamic community on the host. With the advent of nucleic acid based taxonomic profiling and the development of germ-free model systems, substantial progress has been achieved in understanding the effects of the gut microbiome on host physiology and homeostasis <sup>2</sup>. Initial investigations of host-microbiome interactions focused on the physiology and pathology of the intestine, the tissue with which these microbes are in direct contact. Multiple studies have demonstrated that intestinal disorders of diverse etiology, including inflammatory bowel disease <sup>3,4</sup>, irritable bowel syndrome <sup>5,6</sup>, celiac disease <sup>7</sup>, and colon cancer <sup>8–10</sup>, are profoundly influenced by the microbiome. Recently, however, investigators have begun to appreciate that the effects of gut-resident bacteria are not limited to intestinal tissue, but can have far-reaching effects on distal organs, including the liver, pancreas, heart, and even the brain <sup>11</sup>.

Of these systemic organs, the liver is situated in a unique position to receive signals from the intestinal microbiome. Ingested small molecules and peptides derived from non-self foreign substances in the gut (xenobiotics) are both passively and actively absorbed by the intestinal epithelium and transported into the portal circulation. This component of the circulatory system collects blood from the majority of the intestine and delivers it directly to the liver, the principal metabolic and detoxification hub of the mammalian organism. The liver, therefore, serves a critical gatekeeper function at the interface between a flood of foreign –xenobiotic- substances and a finely tuned systemic milieu.

It has long been appreciated that the xenobiotic detoxification functions of the liver evolved to deal with this exposure to diet-derived foreign material arriving from the intestine. Several

transcriptional regulators, including pregnane X receptor (PXR), constitutive active/androstane receptor (CAR), aryl hydrocarbon receptor (AHR), among others, can acutely sense the presence of xenobiotic ligands and mediate the subsequent cellular response <sup>12,13</sup>. Additionally, recent studies have revealed that these pathways are not only sensitive to changes in the diet but may be altered by peptides and small molecules derived from the gut-resident microbiota <sup>14</sup>. This is due to the diverse biochemical activities encoded in microbial genomes that play key roles in the biotransformation and detoxification of ingested nutrients and pharmacological agents <sup>15</sup>. Multiple signaling pathways, including those involved in bile acid biosynthesis <sup>16–18</sup>, the urea cycle <sup>19</sup>, and choline metabolism <sup>20–22</sup>, have been shown to be sensitive to changes to the microbial communities of the gut. Consistently, the microbiome appears to modify susceptibility to several hepatic diseases, including non-alcoholic fatty liver disease (NAFLD) <sup>23,24</sup>, alcoholic liver disease (ALD) <sup>25</sup>, hepatocellular carcinoma (HCC) <sup>26,27</sup>, among others. Thus, the microbiome-gut-liver relationship is emerging as an important factor in multiple physiological and pathological states.

In this study, we took a global approach to identify the signaling pathways in the liver that are modified by the microbiome. We performed metabolomic analysis on hepatic tissue from germ-free or conventionalized (microbiome-replete) mice. In conventionalized animals, we observed a significant increase in metabolites associated with antioxidant and xenobiotic response pathways. A highly conserved master regulator of these responses is the basic leucine zipper transcription factor Nuclear factor erythroid-derived 2-like 2 (Nrf2) <sup>28</sup>. Indeed, subsequent transcriptomic analysis of liver from the same animals revealed significant inductions of a number of canonical Nrf2 target transcripts, but not of other classical regulators of the detoxification response such as PXR, CAR, or AHR.

To determine the microbial populations responsible for the observed activation of hepatic Nrf2, we utilized a transgenic Nrf2 reporter *Drosophila melanogaster* screening assay <sup>29</sup>. Our results reveal that members of the genus *Lactobacillus* were capable of activating systemic Nrf2 signaling. Furthermore, oral gavage of the representative *Lactobacillus*, *Lactobacillus rhamnosus* GG (LGG), induced Nrf2 in the liver of conventional mice and this activation was sufficient to protect against two different models of acute oxidative liver injury. Finally, we performed ultra-high resolution LC MS/MS to characterize the small molecule complement present in the portal circulation of mice treated with LGG and identified 5-methoxyindoleacetic acid (5-MIAA) as a novel LGG-derived small molecule capable of activating hepatic Nrf2. These data address key gaps in our understanding of the commensal-liver axis and provide further insight into the role of the intestinal microbiome in hepatic health and homeostasis.

## 4.2 RESULTS

### *4.2.1 Conventionalization of germ-free mice alters the hepatic metabolome*

Given the taxonomic complexity of the microbiome and the diverse functional consequences of dysbiosis on host hepatic physiology, we utilized a non-biased metabolomics-based approach to outline the broad impact of commensal-liver interactions. Germ-free (GF) mouse littermates were separated at weaning (3 weeks of age) into two groups with one group maintained in sterile isolators, while the other group was transferred to cages with bedding obtained from conventionally raised specific pathogen free (SPF) mice (Figure 4.1A). These mice were then allowed three weeks to acquire and establish a microbiome (“conventionalization”) (CV) before sacrifice and metabolomic analysis<sup>30,31</sup> of mitochondrial fractions obtained from liver tissue from both groups (Figure 4.1B-C). Pathway analysis of altered features using Mummichog analysis<sup>32</sup> revealed that conventionalization elicited distinct shifts in metabolic pathways previously shown to be modulated by the microbiota (Figure 4.1D). More specifically, pathways for hepatic amino acid metabolism<sup>33</sup>, bile acid biosynthesis<sup>16,18</sup>, and the urea cycle<sup>19,34</sup> were altered by the microbiome. These analyses also revealed an induction of regulatory networks involved in drug metabolism and the antioxidant response, including alterations in cytochrome P450 metabolites and glutathione synthesis (Figure 4.1D).

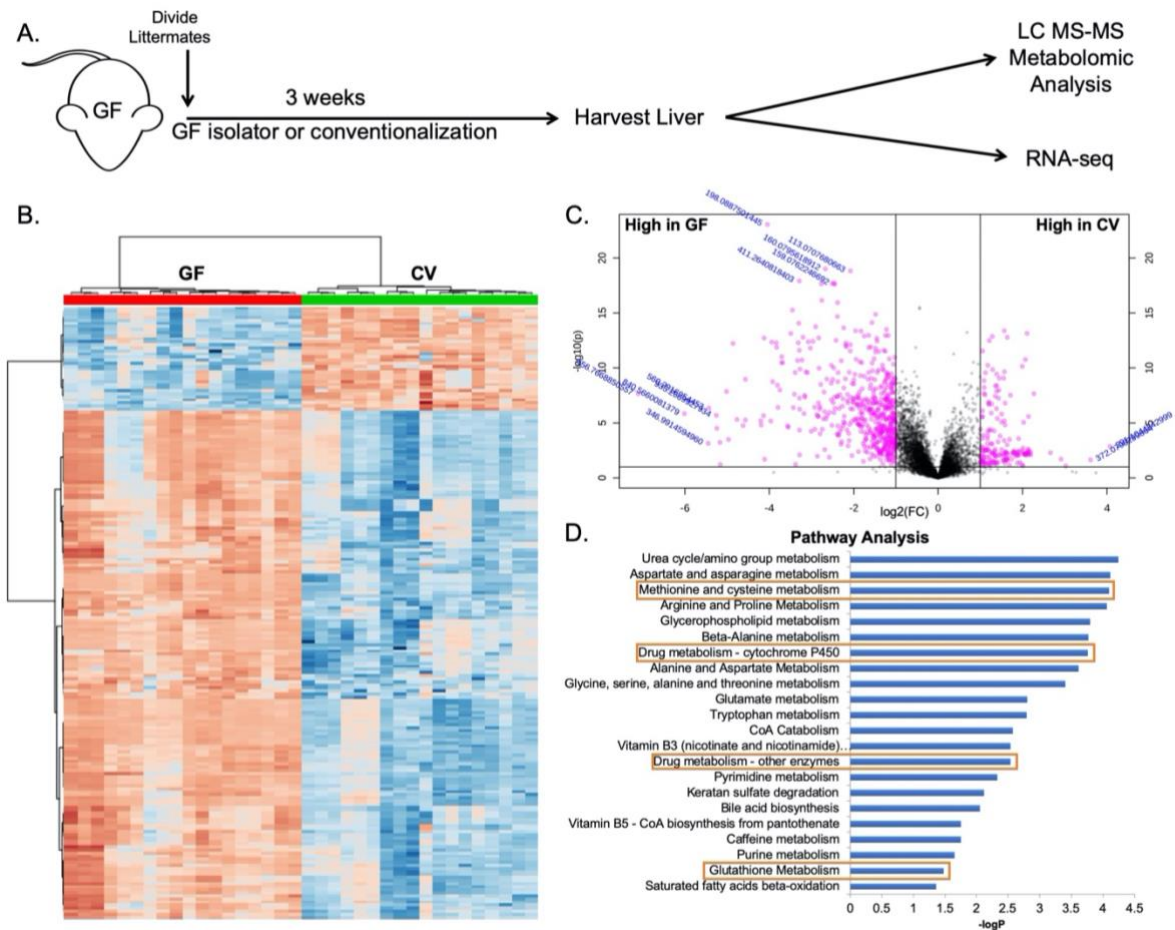


**Figure 4.1: Conventionalization of germ-free mice alters the hepatic metabolome.**

(A) Schematic of experimental design. Germ-free (GF) littermates were separated at weaning and either maintained GF or conventionalized (CV) with bedding from conventionally raised Specific pathogen free (SPF) mice for three weeks prior to sacrifice and harvest of liver tissue. (B) Hierarchical clustering of the top 200 altered features identified from ultra-high resolution LC-MS analysis of liver tissue from experiment described in (A). (C) Volcano plot of features identified in LC-MS analysis of liver tissue from experiment described in (A), where pink indicates  $p < 0.05$  as calculated by t-test. (D) Mummichog pathway analysis for the identification of pathways induced in CV relative to GF. Red boxes highlight pathways involved in antioxidant and xenobiotic metabolism.  $n=6$  mice per condition (GF or CV), 3 male and 3 female.

#### ***4.2.2 Conventionalization of germ-free mice induces the hepatic Nrf2 antioxidant response pathway***

Parallel transcriptomic analysis using RNAseq on the same liver tissue demonstrated a significantly altered profile in the hepatic transcriptome of CV mice relative to GF (Figure 4.2A). Analysis of upstream transcriptional regulators of the altered transcripts by Ingenuity Pathway Analysis showed an induction of genes in CV mice known to be regulated by Nrf2, a master regulator of the cellular antioxidant response (Figure 4.2B). Further analysis of the transcriptional profiles of CV and GF livers revealed an induction of many Nrf2 target transcripts in CV mice involved in the hepatic antioxidant and xenobiotic response (Figure 4.2C). Collectively, these data demonstrate that colonization with gut-resident microbes has significant influences on hepatic oxidative metabolic processes, and by inference, gut-liver signaling.

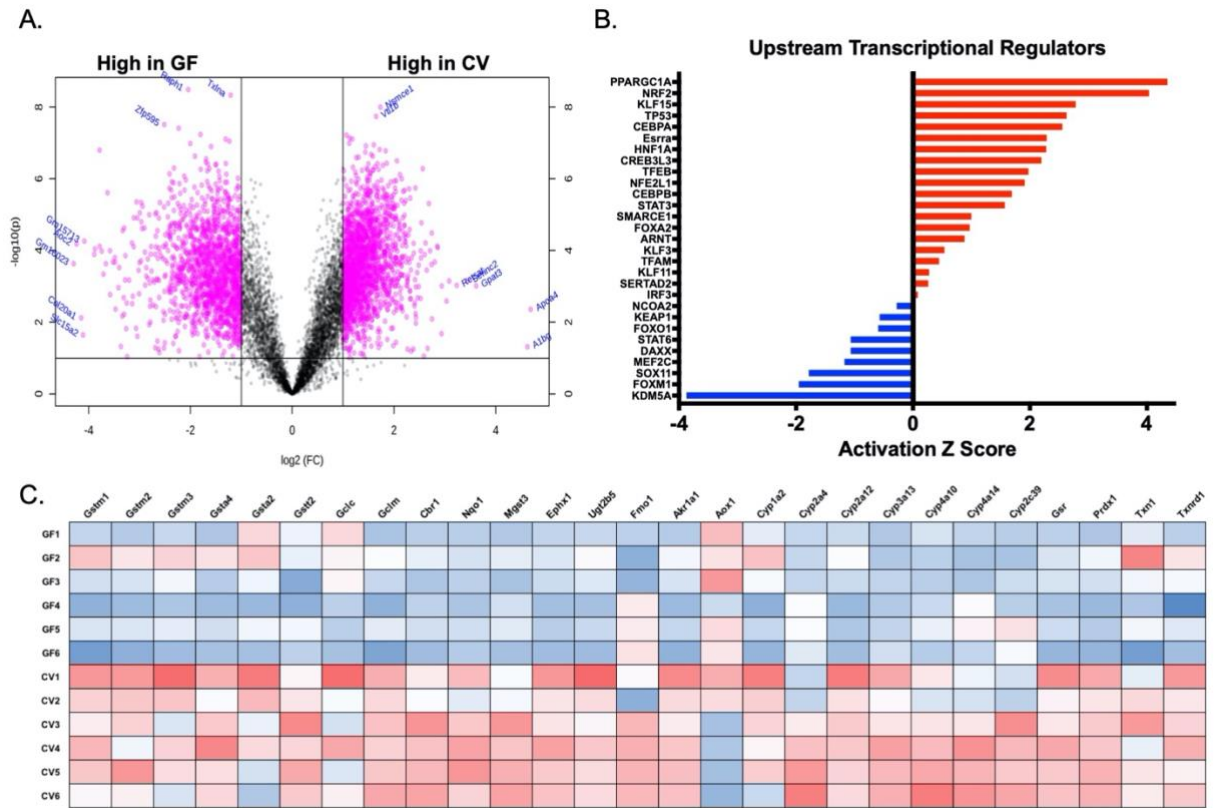


**Figure 4.2: Conventionalization of germ-free mice induces the hepatic Nrf2 antioxidant response pathway.**

(A) Volcano plot of transcript enrichment detected by RNAseq analysis of liver tissue of GF and CV mice. Pink data points denote transcripts that were significantly enriched in GF or conventional mice to a confidence level of  $p < 0.05$  as determined by t-test. (B) Ingenuity Pathway Analysis of RNAseq identifies activated (red) and repressed (blue) transcriptional regulators in CV relative to GF mice. (C) Heatmap of genes under the transcriptional control of Nrf2 identified in RNAseq analysis.  $n = 6$  mice per condition (GF or CV), 3 male and 3 female.

### ***4.2.3 Symbiotic Lactobacilli sp. activate the Nrf2 pathway in the Drosophila melanogaster fat body***

Next, we sought to determine which bacterial members of the microbiome were responsible for the observed induction of Nrf2 signaling. Because of the multi-dimensional nature of the gut-liver axis, we utilized the model organism *Drosophila melanogaster* to screen for Nrf2 inducing bacteria. *Drosophila* have an intestinal system similar to that of vertebrates, with a single layer of epithelium lining the gut lumen <sup>35</sup> and also possess an organ analogous to the vertebrate liver known as the fat body <sup>36</sup>.

Using a transgenic Nrf2 reporter fly (*gstD1-GFP*) <sup>29</sup>, in which GFP is expressed in response to Nrf2 activation and binding to a consensus ARE (Figure 4.3A), we assessed the capacity of candidate Gram-positive and Gram-negative commensal bacteria to activate Nrf2 signaling in the *Drosophila* fat body (Figure 4.3B). Early third-instar germ-free larvae were allowed to feed on either sterile food or food inoculated with 2x10<sup>8</sup> CFU/gram of bacteria. 16 hours later, the fat body was dissected and analyzed using fluorescence microscopy. Of the bacteria assayed, *Lactobacilli* were the most robust inducers of Nrf2 in the fat body (Figure 4.3C-D). These included the *Drosophila* commensal *Lactobacillus plantarum* and the human commensal and probiotic *Lactobacillus rhamnosus* GG (LGG). These data are in agreement with previous reports from our research group showing that oral administration of *L. plantarum* or LGG can activate Nrf2 in the intestinal epithelium of both flies and mice <sup>37</sup>. Moreover, these *Drosophila* data demonstrate that a specific subset of bacteria can exert effects on Nrf2 beyond the confines of the gut in tissues that do not experience direct cell-microbe contact.

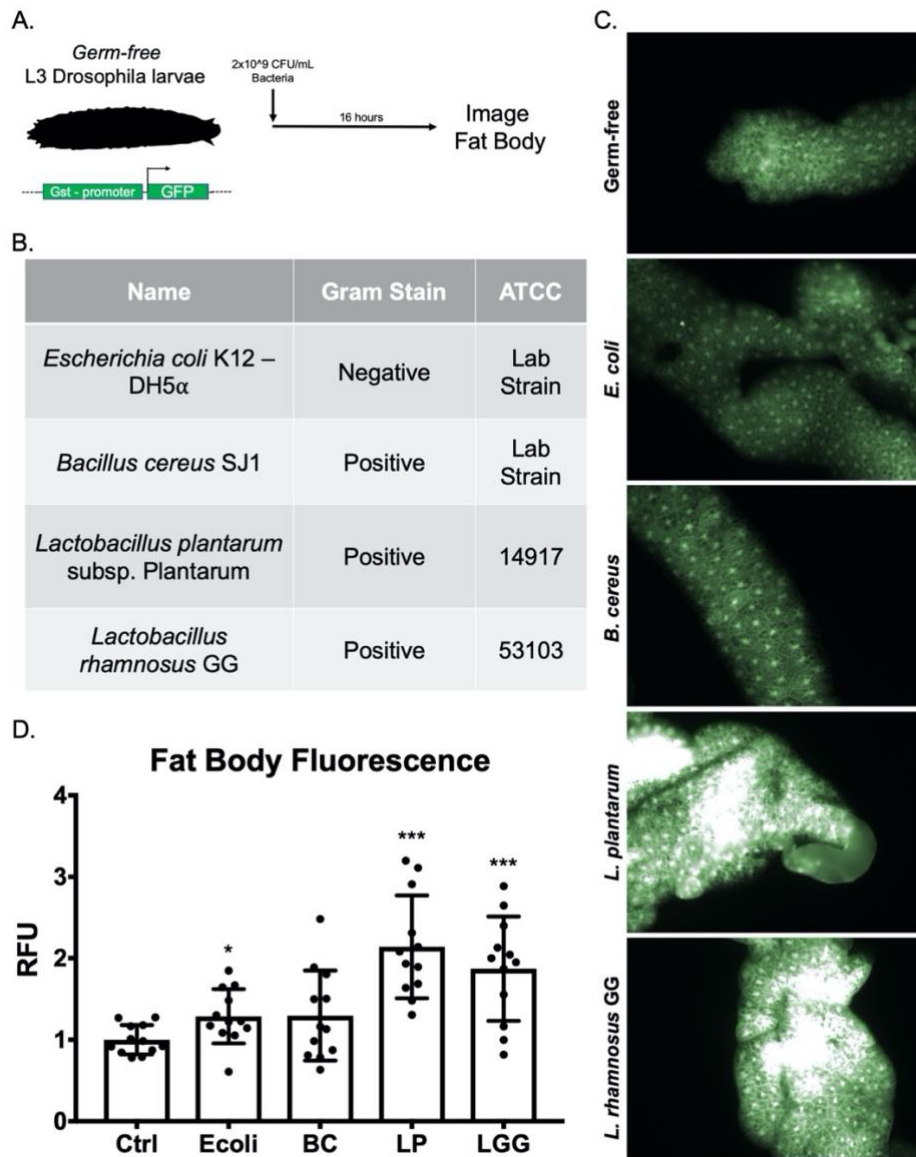


**Figure 4.3: Symbiotic *Lactobacilli* sp. activate the Nrf2 pathway in the *Drosophila melanogaster* fat body.**

**(A)** Schematic of experimental system. **(B)** Identities and characteristics of assayed bacteria. **(C)** Fluorescent images of *Drosophila* fat body from transgenic flies described in (A) after 16-hour treatment with the indicated bacteria. **(D)** Quantification of fat body fluorescence detected in (C) by Image J software analysis. \* $p < 0.05$ , \*\* $p < 0.01$ , \*\*\* $p < 0.002$  as determined by one-way ANOVA and post-hoc t-test.  $n = 12$  flies per condition.

#### ***4.2.4 Oral administration of Lactobacillus rhamnosus GG activates Nrf2 signaling in the murine liver***

To corroborate these findings in vertebrates, we performed a two week regimen of daily oral gavage of conventional (microbiome-replete) C57BL/6 mice with vehicle (HBSS), LGG, or *Bacillus cereus* (BC), a Gram-positive commensal that does not induce Nrf2 in the intestine <sup>38</sup>. Immunofluorescence for Nrf2 in hepatic sections from these animals reveals a faint signal in both the HBSS and BC treated animals (Figure 4.4A). The LGG treatment group, however, demonstrated a significant increase in Nrf2 immunoreactivity as well as a prominent punctate staining pattern that colocalized with the nuclear stain DAPI (Figure 4.4A-B). These data indicate an overall stabilization and subsequent nuclear translocation of Nrf2 in hepatocytes in response to daily gavage of LGG. Furthermore, this response appears to be specific to LGG, as BC had no effect on levels of Nrf2 immunofluorescence or DAPI colocalization (Figure 4.4A-B). To determine if the observed Nrf2 stabilization results in increased Nrf2 activity, we performed RT-PCR for known Nrf2 target transcripts in livers from HBSS, LGG, or BC treated mice. In agreement with the immunofluorescence, HBSS and BC had similar steady state mRNA levels of the Nrf2 target transcripts *Nqo1*, *Trx1*, *Gsta1*, and *Gclc*. LGG treatment, however, led to a significant increase in the levels of all of the analyzed targets (Figure 4.4C). These data support our findings in *Drosophila* that implicate *Lactobacilli* in systemic activation of Nrf2.

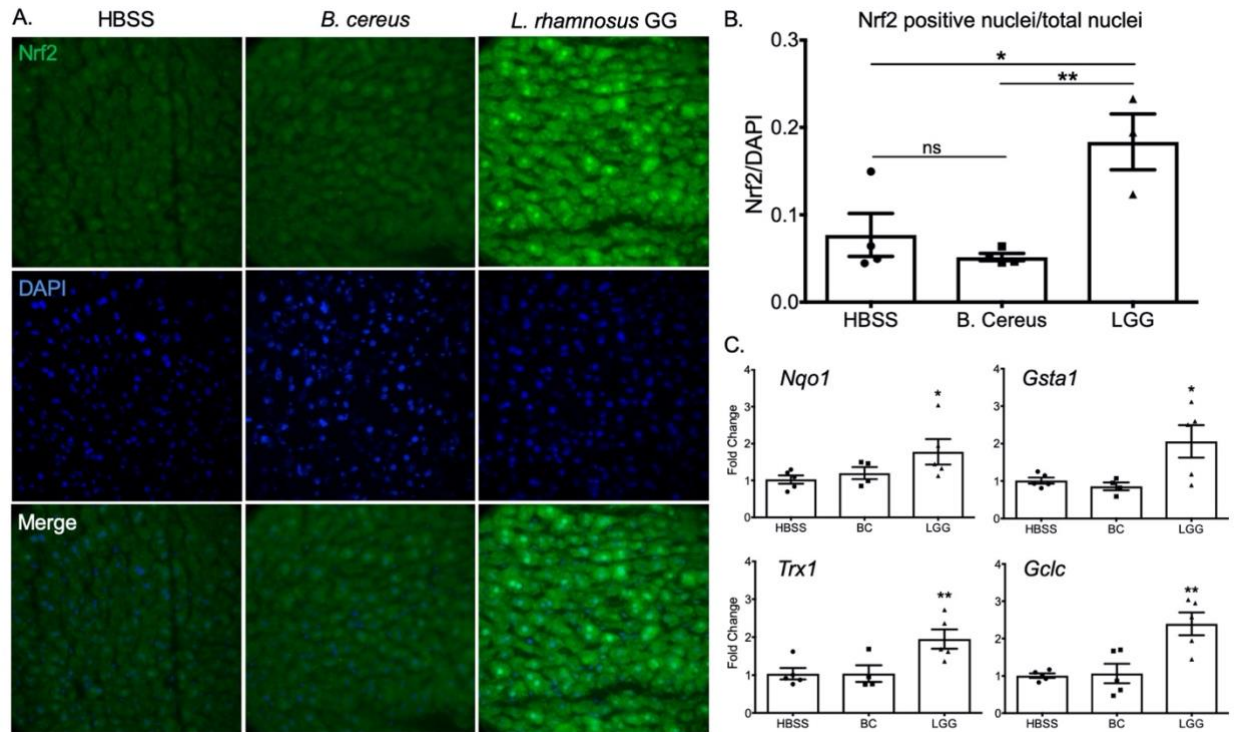


**Figure 4.4: Oral administration of *Lactobacillus rhamnosus* GG activates Nrf2 signaling in murine liver.**

(A) Immunofluorescence analysis using an antibody against Nrf2 on liver histological sections prepared from animals orally administered HBSS (vehicle), or  $2 \times 10^8$  CFU BC or LGG daily for two weeks. Images were acquired at 60x magnification. (Green=Nrf2) (Blue=DAPI). (B) Quantification of nuclear co-localization from images in A.  $n=3$  animals per treatment. (C) RT-PCR of liver tissue for the steady state transcript levels of Nrf2 targets involved in the cellular antioxidant and xenobiotic response. Each experiment included a minimum of  $n=3$  per treatment. \* $p < 0.05$ , \*\* $p < 0.01$ , \*\*\* $p < 0.002$  as determined by one-way ANOVA and post-hoc t-test.  $n=3$  mice per condition.

#### ***4.2.5 Lactobacillus rhamnosus GG protects the Drosophila fat body against toxicity in a Nrf2-dependent manner***

Given the effect of LGG administration on Nrf2 activity and expression of key antioxidant enzymes, we hypothesized that LGG would be protective against acute oxidative liver injury. First, we utilized a *Drosophila* model of oxidative injury. Five-day old adult *Drosophila* were fed acetaminophen (APAP), an acute oxidative stressor in mammals <sup>39</sup>, or the herbicide paraquat (PQ) which is known to induce oxidative stress in the fly <sup>40</sup>. We demonstrate that feeding of either PQ or APAP resulted in dose-dependent mortality in adult *Drosophila* (Figure 4.5A). To determine the effect of these compounds on fat body signaling, we again utilized the *gstDI-GFP* Nrf2 reporter fly. Third-instar larvae were fed either 15 mM PQ or 100 mM APAP overnight, followed by dissection and fluorescent evaluation of the fat body. Indeed, both PQ and APAP robustly induced dNrf2 signaling in the fat body at this time point, relative to vehicle controls (Figure 4.5B), consistent with a production of ROS and subsequent activation of dNrf2.

We next sought to determine the effect of LGG colonization on PQ or APAP toxicity. Five-day old germ-free flies were collected and fed for 3 days on germ-free food or LGG colonized food, followed by challenge with PQ or APAP. LGG treatment significantly attenuated PQ and APAP toxicity (Fig 4.6A). To determine the involvement of dNrf2 signaling in LGG-mediated protection, we specifically depleted dNrf2 in the fat body and maintained GF or mono-colonized with LGG. In this context, there was no significant difference between the mortality rates of GF and LGG treated flies in response to APAP or PQ (Figure 4.6B). These data demonstrate that LGG mediated dNrf2 activation is the mechanism by which LGG protects against oxidative fat body injury in *Drosophila*.

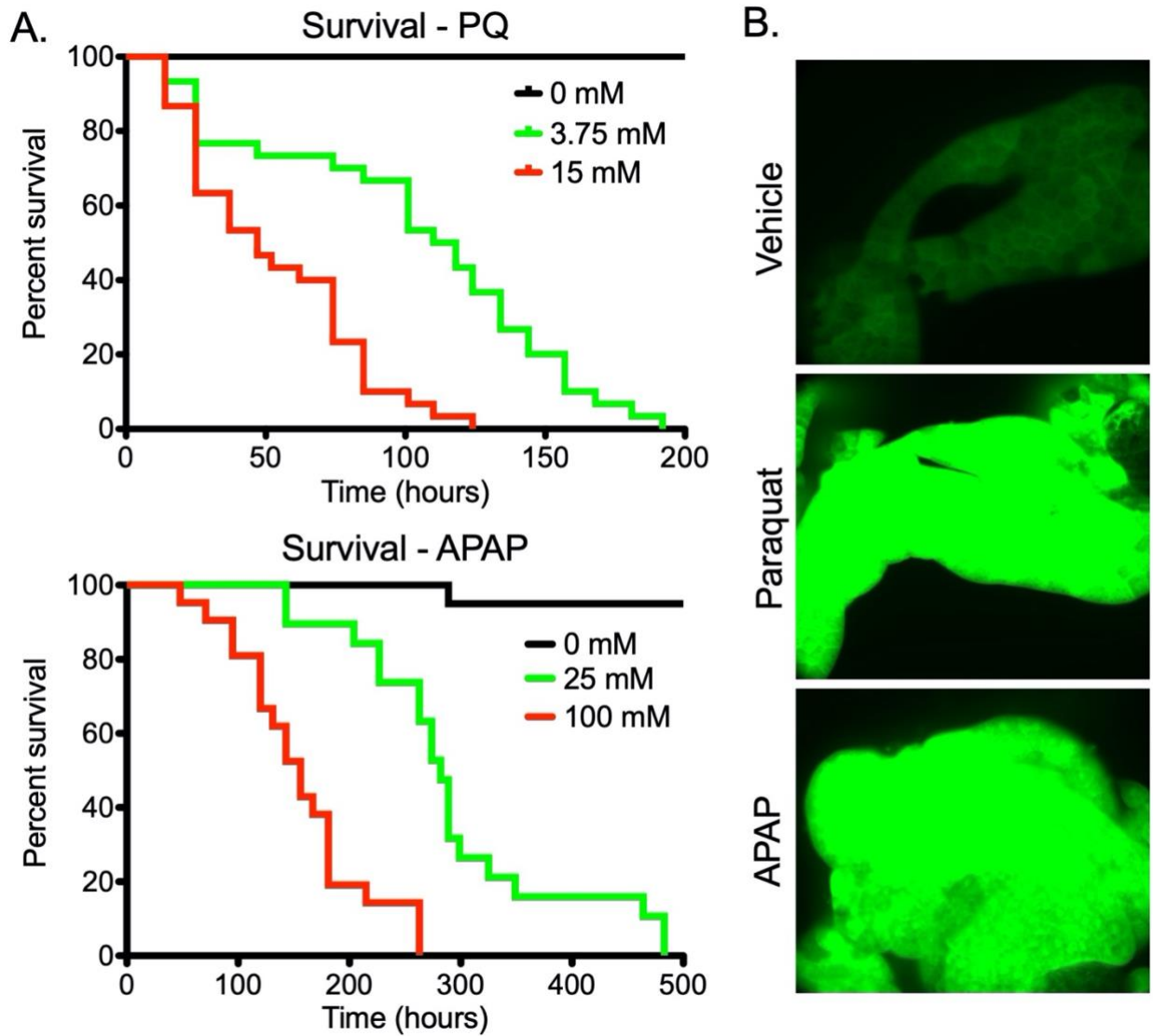


**Figure 4.5: *Drosophila* model of oxidative liver injury.**

(A) Survival of adult *Drosophila* exposed to the indicated doses of either paraquat (PQ) or acetaminophen (APAP). Log-Rank test  $p < 0.0001$ ,  $n = 20$ . (B) Fluorescent imaging of fat bodies of *gstD1-gfp* larvae following 16 hours exposure to 15 mM PQ or 100 mM APAP.

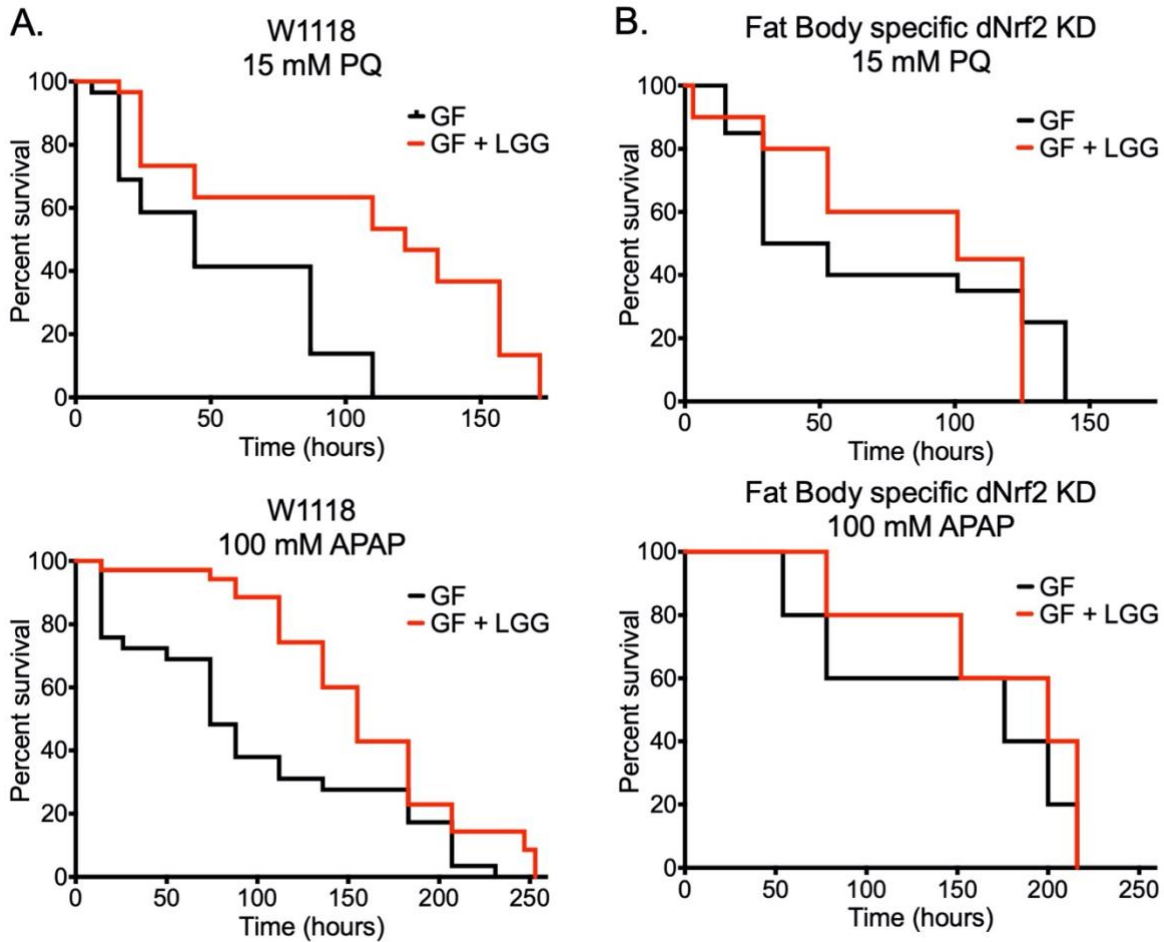


**Figure 4.6** *Lactobacillus rhamnosus* GG protects the *Drosophila* fat body against toxicity in a Nrf2 dependent manner.

(A) Survival of either germ-free (GF) or *Lactobacillus rhamnosus* GG (LGG) mono-associated adult *Drosophila* exposed to 15 mM PQ or 100 mM APAP. PQ: Log-Rank  $p < 0.0001$ ,  $n = 30$ . APAP: Log-Rank  $p < 0.01$ ,  $n = 30$ . (B) Survival of GF or LGG mono-associated adult female *Drosophila* of the genotype *yolk-GAL4 UAS-cncCIR* (Fat body specific *Drosophila* (d)Nrf2 knockdown) exposed to 15 mM PQ or 100 mM APAP. PQ: Log-Rank  $p = 0.7799$ ,  $n = 20$ . APAP: Log-Rank  $p = 0.4765$ ,  $n = 20$ .

#### ***4.2.6 Lactobacillus rhamnosus GG administration attenuates acetaminophen hepatotoxicity in conventional mice***

We next sought to corroborate these findings in a mammalian model of acetaminophen hepatotoxicity. To this end, conventionally raised C57BL/6 mice were orally administered either vehicle (HBSS) or LGG for 2 weeks. These treatments had no discernable effect on overall liver histology as assessed by H&E (Figure 4.7A). To determine the effect of LGG treatment on histologic hallmarks of APAP toxicity, HBSS and LGG pretreated mice were given a sub-lethal oral dose of 300 mg/kg APAP. HBSS-treated animals 24 hours after APAP had significant centrilobular necrosis, whereas liver injury in the LGG-treated groups was significantly attenuated (Figure 4.7A-B). In agreement with these results, serum ALT (a marker of hepatocyte injury) was elevated in the HBSS group after acetaminophen overdose but was markedly diminished in LGG treated animals (Figure 4.7C). To evaluate hepatic oxidative stress, we determined the ratio of total (GSH) to oxidized (GSSG) glutathione in the liver 24 hours after APAP overdose. Liver tissues from LGG pretreated animals had a significantly higher ratio of GSH to GSSG than those from HBSS pretreated animals (Figure 4.7D), indicating diminished hepatocellular oxidative stress. These data demonstrate the protective effect of LGG administration against the oxidative liver injury induced by acetaminophen. Of note, this protection does not appear to be due to altered APAP metabolism, as the mRNA levels of the cytochrome P450 enzymes responsible for its bioconversion were unchanged by LGG administration (Figure 4.8).

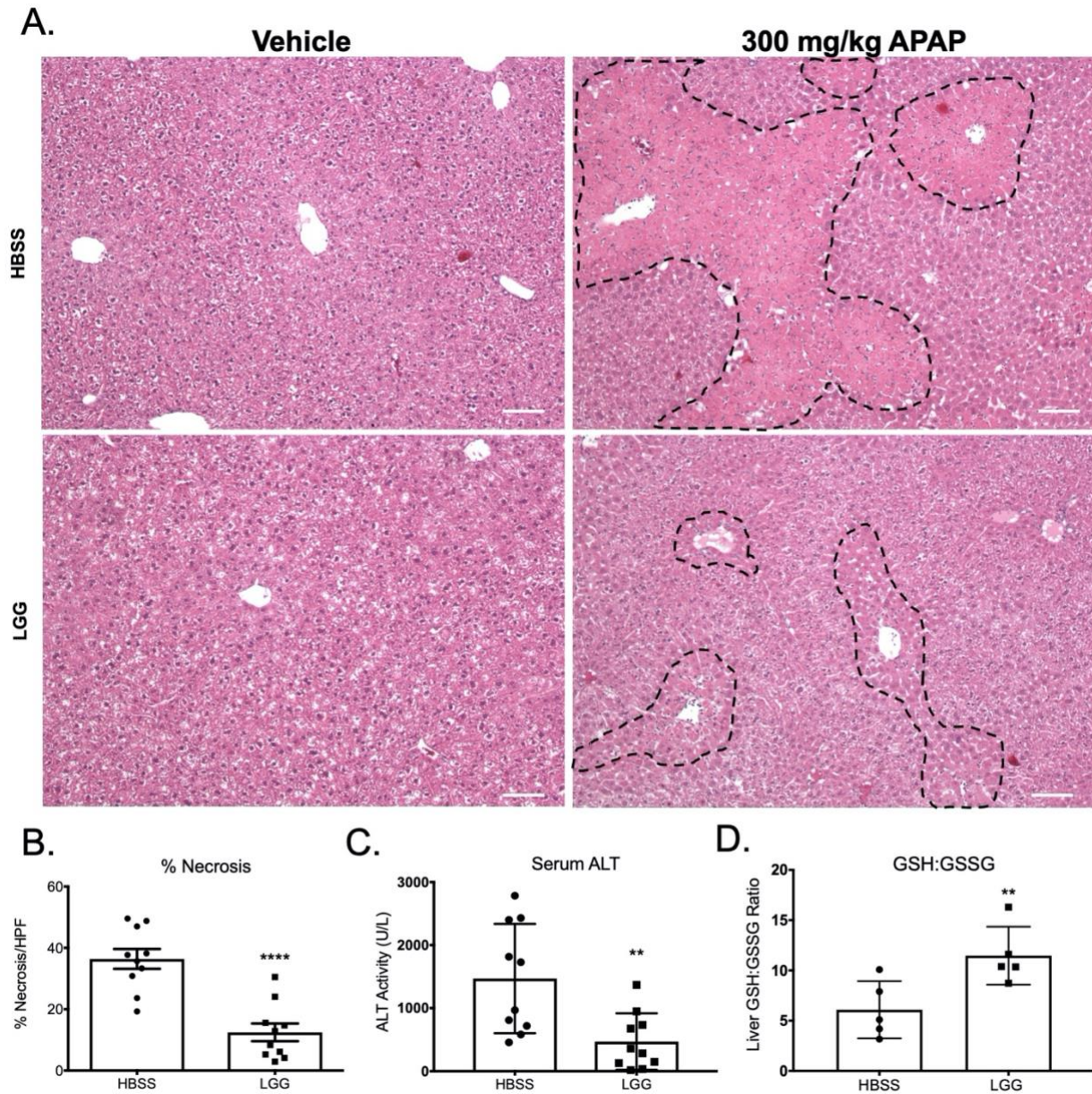


**Figure 4.7: *Lactobacillus rhamnosus* GG administration attenuates acetaminophen hepatotoxicity in conventional mice.**

(A) Representative H&E images of mouse livers 24 hours after oral administration of 300 mg/kg APAP or vehicle control. Where indicated, mice received a daily oral gavage of either HBSS (vehicle) or  $2 \times 10^8$  CFU *Lactobacillus rhamnosus* GG (LGG) for two weeks prior to APAP administration. Characteristic centrilobular necrosis is outlined by dashed lines. (B) Quantification

of percent necrosis per high power field of histology from (A). n=5 mice per group. (C) Serum ALT levels at 24 hours after oral administration of 300 mg/kg APAP or vehicle control of mice described in (A). (D) Ratio of hepatic GSH to GSSG of livers 24 hours post APAP overdose as described in (A). \*\*p<0.01 \*\*\*\*p<0.0001 as determined by t-test. n=10 mice per group (A-C). Scale bar (white) = 100  $\mu$ m.

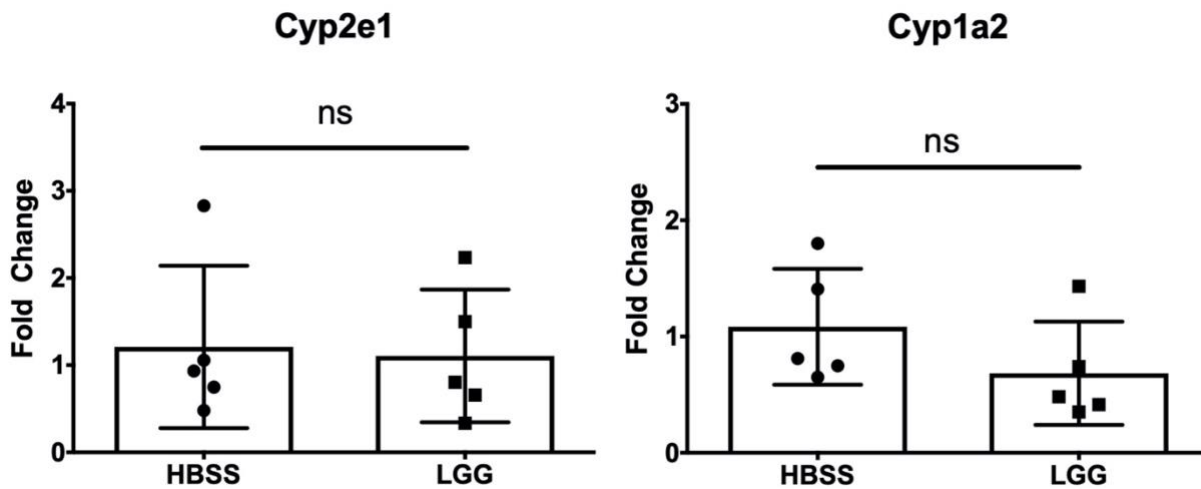


**Figure 4.8: Steady-state mRNA levels of acetaminophen metabolizing enzymes.**

RT-PCR for the mRNA levels of cytochrome P450 2e1 and 1a2 in liver tissue after 2 weeks of oral HBSS or LGG gavage. ns=not significant as determined by t-test. n=5 mice per group.

#### ***4.2.7 Hepatic Nrf2 mediates Lactobacillus rhamnosus GG protection against acetaminophen hepatotoxicity***

Our findings agree with an existing body of literature that describes the protective effects of LGG against oxidative liver injury<sup>23,41–45</sup>. The mechanisms proposed for this protection vary from an improvement in barrier function<sup>41,42,45</sup> to alterations in bile acid signaling<sup>43</sup>. To specifically investigate the role of LGG-mediated Nrf2 activation in facilitating the observed hepatoprotection, we generated liver-specific Nrf2 knockout mice using Albumin-Cre<sup>+/-</sup> x Nrf2<sup>fl/fl</sup> mice. WT (Nrf2<sup>fl/fl</sup>) and KO (Albumin-Cre x Nrf2<sup>fl/fl</sup>) mice were gavaged with either HBSS or LGG as described above for 2 weeks, followed by oral administration of 300 mg/kg APAP. Histologic analysis of Nrf2<sup>fl/fl</sup> animals 24 hours after APAP administration revealed significant centrilobular necrosis in HBSS treated animals that was attenuated in LGG treated animals (Figure 4.9A). However, in Albumin-Cre<sup>+/-</sup> x Nrf2<sup>fl/fl</sup> mice, both HBSS and LGG treated animals exhibited similar tissue necrosis (Figure 4.9A, quantified in Figure 4.9B). Consistently, serum ALT levels and hepatic GSH:GSSG ratio from Albumin-Cre x Nrf2<sup>fl/fl</sup> animals were not different between HBSS and LGG treated mice. (Figure 4.9C-D).

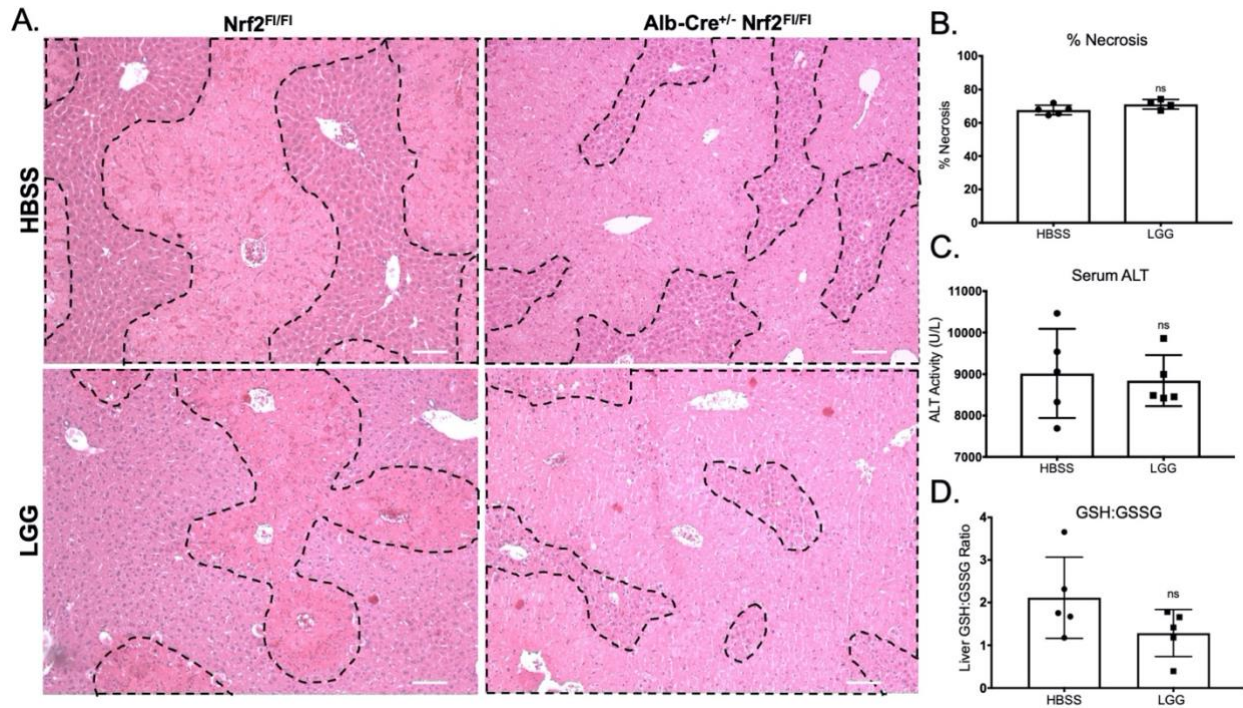


**Figure 4.9: Hepatic Nrf2 mediates *Lactobacillus rhamnosus* GG protection against acetaminophen hepatotoxicity.**

(A) Representative H&E of mouse livers 24 hours after oral administration of 300 mg/kg APAP or vehicle control from WT or littermate albumin-Cre x *Nrf2<sup>fl/fl</sup>* liver-specific Nrf2 knockout mice. Where indicated, mice received a daily oral gavage of either HBSS (vehicle) or  $2 \times 10^8$  CFU *Lactobacillus rhamnosus* GG (LGG) for two weeks prior to APAP administration. (B) Quantification of percent necrosis/HPF from histology in (A). (C) Serum ALT activity at 24 hours post overdose of mice described in (A). (D) Ratio of hepatic GSH to GSSG 24 hours post overdose as described in (A). \* $p < 0.05$  \*\* $p < 0.01$  ns=not significant as determined by t-test.  $n = 5$  mice per group. Scale bar (white) = 100  $\mu\text{m}$ .

#### ***4.2.8 Hepatic Nrf2 mediates Lactobacillus rhamnosus GG protection against acute alcohol induced injury***

Several studies have implicated the microbiome in susceptibility to acute ethanol toxicity and demonstrated efficacy of LGG administration in this model of acute hepatic oxidative stress<sup>46,47</sup>. As Nrf2 has also been implicated in the pathogenesis of alcohol induced liver injury, we sought to determine the role of Nrf2 in mediating the protective effects of LGG in this system. Nrf2<sup>fl/fl</sup> and Albumin-Cre<sup>+/-</sup> x Nrf2<sup>fl/fl</sup> were treated with oral HBSS or LGG for two weeks as described above, followed by a single oral dose of 6g/kg ethanol. Livers harvested from HBSS pretreated mice 6 hours post ethanol administration exhibited significant steatosis, a histologic hallmark of acute ethanol hepatotoxicity, as visualized by Oil red O staining (Figure 4.10A). LGG pretreatment in Nrf2<sup>fl/fl</sup> animals significantly reduced the amount of hepatic steatosis and serum ALT (Figure 4.10B-C). However, no difference was observed in either steatosis or serum ALT between HBSS and LGG treated groups in the Albumin-Cre<sup>+/-</sup> x Nrf2<sup>fl/fl</sup> mice (Figure 4.10B-C). These data demonstrate that Nrf2 is required for the hepatoprotective effects of LGG in the setting of acute oxidative stress in two distinct modes of injury, APAP overdose and ethanol toxicity.

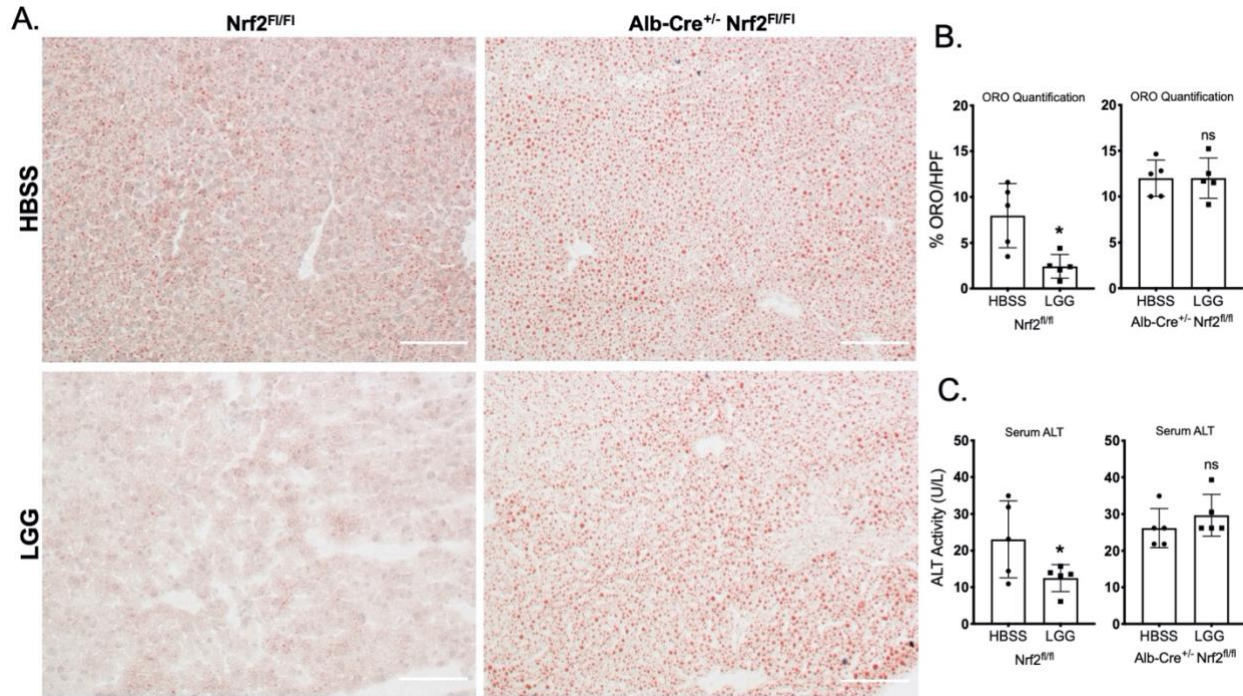


**Figure 4.10: Hepatic Nrf2 mediates *Lactobacillus rhamnosus* GG protection against acute alcohol induced injury.**

(A) Representative Oil red O staining for lipid content of mouse livers pretreated with HBSS or LGG by daily oral gavage for 2 weeks, 6 hours after a single oral dose of 6 g/kg ethanol, in WT or littermate albumin-Cre x Nrf2<sup>fl/fl</sup> liver-specific Nrf2 knockout mice. (B) Quantification of Oil red O staining from histologic images from (E). (C) Serum ALT activity after ethanol overdose from mice in (A). \*p<0.05 \*\*p<0.01 ns=not significant as determined by t-test. n=5 mice per group. Scale bar (white) = 100 μm.

#### 4.2.9 *Lactobacillus rhamnosus* GG alters the small molecule milieu of portal serum.

To determine the mechanism by which gut-resident LGG activates Nrf2 at a distance, we characterized the small molecule milieu present in the portal circulation of LGG-treated animals relative to HBSS treated controls. Portal blood was collected 12 hours after oral administration and mass spectrometry performed (Figure 4.11A). Subsequent tandem mass spectrometry identified candidate small molecules that were significantly enriched in the portal circulation of LGG-treated animals, of which 6 were positively identified (Figure 4.11B).

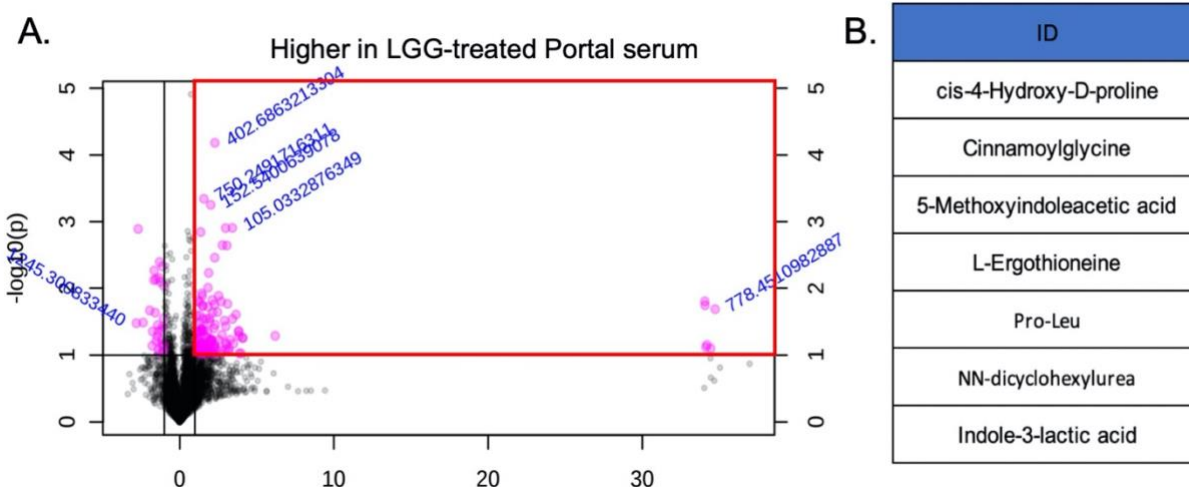


**Figure 4.11: *Lactobacillus rhamnosus* GG alters the small molecule milieu of portal serum.**

(A) Features identified by ultra-high resolution mass spectrometry of serum collected from the hepatic portal vein of mice at 12 hours after oral administration of *Lactobacillus rhamnosus* GG (LGG) or vehicle control. Red box outlines features increased by >2 fold in portal serum from LGG treated mice relative to vehicle treated. (B) List of matched metabolites from MS2 spectra increased in the portal serum of mice administered LGG as described in (A).

#### ***4.2.10 Lactobacillus rhamnosus GG mediated generation of 5-methoxyindoleacetic acid activates hepatic Nrf2***

To determine the effect of these small molecules on Nrf2 activation, we utilized a stably-transduced ARE-Luciferase HepG2 cell line as a Nrf2 reporter system. Of the small molecules enriched in the portal serum of LGG treated animals, only 5-Methoxyindoleacetic acid (5-MIAA) resulted in an increase in reporter activity (Figure 4.12). To corroborate these findings, we determined the steady state mRNA levels of the known Nrf2 target transcripts *NQO1*, *HMOX1*, and *GCLC* after a 12-hour stimulus with 5-MIAA. We observed a significant induction of all of these targets in response to 5-MIAA relative to methanol (vehicle control) (Figure 4.13A). To confirm that this response was due to an increase in Nrf2 stabilization and nuclear translocation, we treated HepG2 cells with 5 mM 5-MIAA for 6 hours and western-blotted for Nrf2 in the nuclear fraction (Figure 4.13B-C). Indeed, 5-MIAA treatment significantly increased the levels of nuclear Nrf2 relative to methanol control (Figure 4.13B-C). Using mass spectrometry-based quantification of the portal circulation of LGG-treated animals, 5-MIAA was found at a concentration of 2 uM (Figure 4.14A-B). A similar concentration of 5 uM resulted in an increase in ARE-luciferase *in vitro* of 1.6-2 fold (Figure 4.12), which is similar to the increase in Nrf2 target genes observed *in vivo* after LGG gavage (Figure 4.4A).

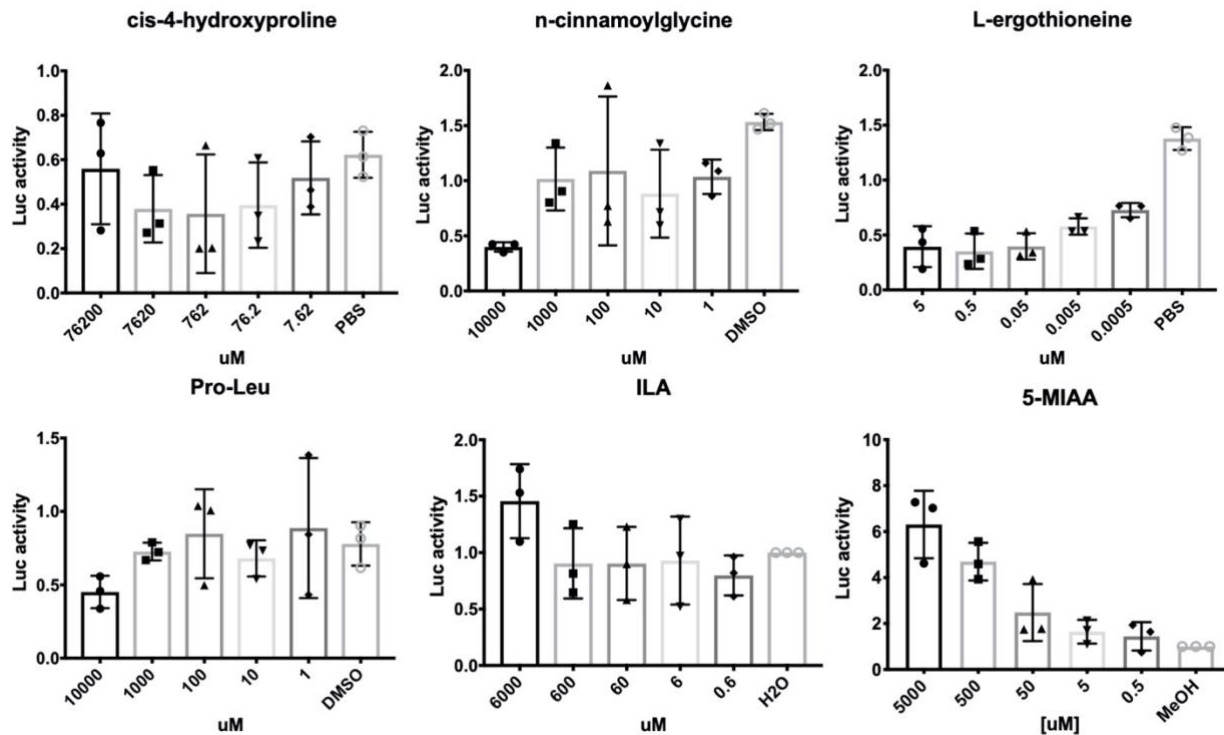


**Figure 4.12: Effect of LGG-induced small molecules on Nrf2 activity in HepG2 cells.**

(A) Luciferase activity in extracts of HepG2 cells which harbors a Nrf2 responsive promoter transcriptionally fused to *luc* upon exposure to the indicated compounds for 12 hours.

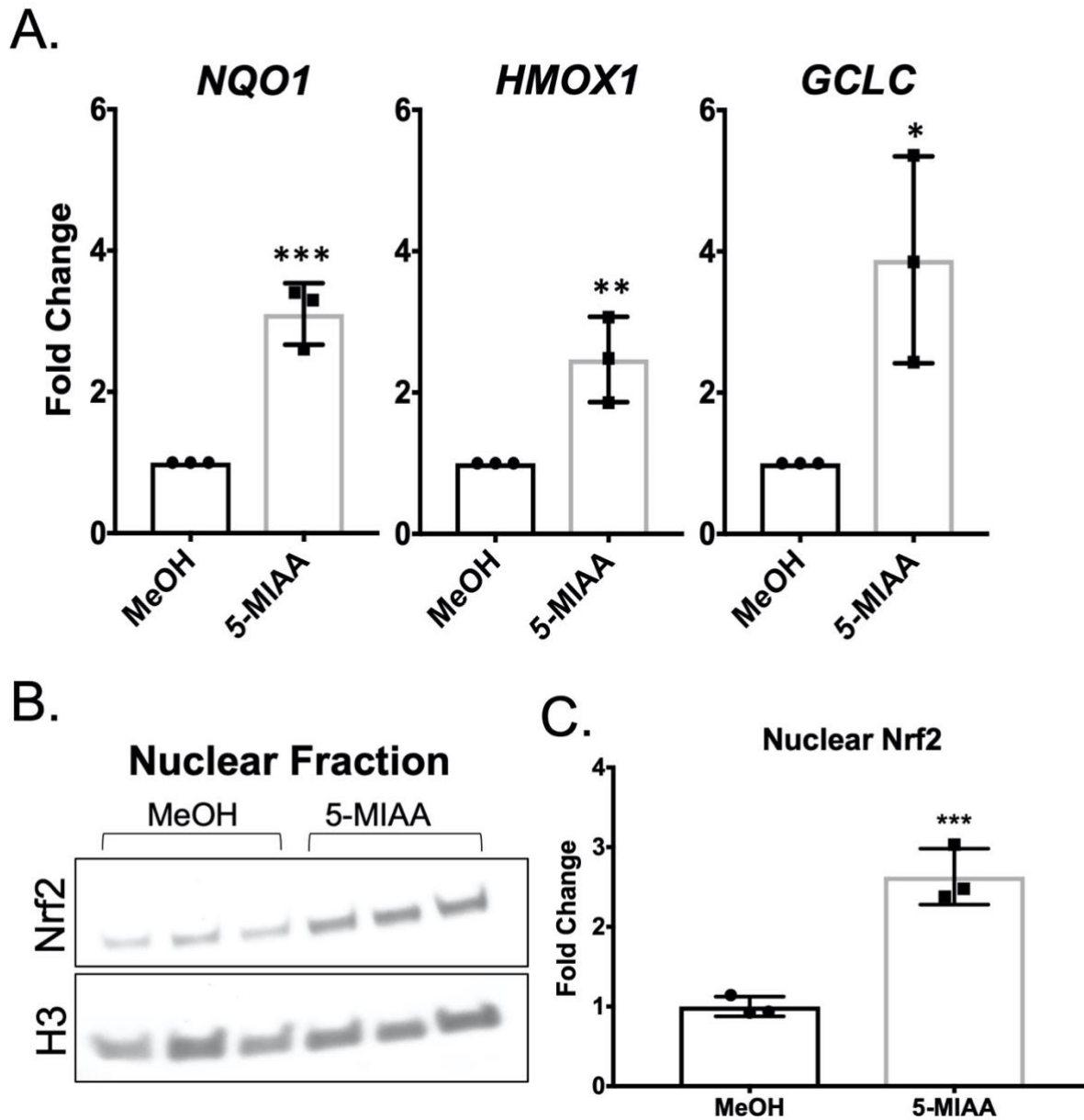


**Figure 4.13: LGG-derived 5-methoxyindoleacetic acid activates hepatic Nrf2.**

(A) RT-PCR for steady state mRNA levels of genes under the transcriptional control of Nrf2 after a 12-hour exposure of HepG2 cells to 5-MIAA or methanol (vehicle control). (B) Immunoblot analysis using antibodies against Nrf2 or Histone H3 (loading control) in nuclear fractions purified from HepG2 cells +/- 5-MIAA for 6 hours. (C) Densitometry analysis of data in (E). \* $p < 0.05$ , \*\* $p < 0.01$ , \*\*\* $p < 0.002$  as determined by t-test.  $n = 3$  independent replicates.

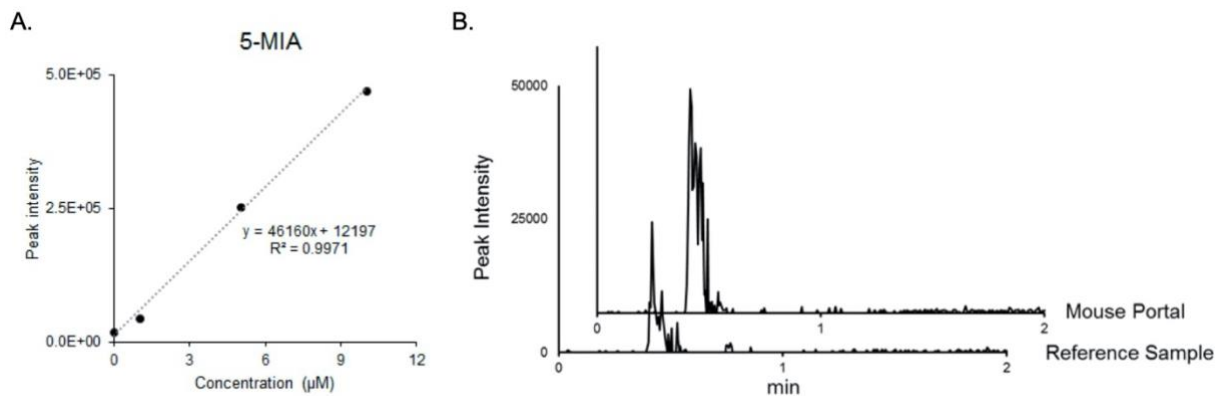


**Figure 4.14: 5-MIAA quantification in portal serum of LGG treated mice.**

(A) Method of standards addition to determine concentration of 5-MIAA in plasma reference sample. (B) Reference standardization shows that 5-MIAA in mouse portal circulation is 2 µM.

#### 4.2.11 *Lactobacilli* produce 5-MIAA *in vitro*

Finally, to determine the microbial origin of 5-MIAA we cultured an array of representative gut microbes for 18 hours under appropriate growth conditions. Subsequent targeted mass spectrometry for 5-MIAA showed an accumulation of 5-MIAA in LGG, LP, and all of the other *Lactobacillus* culture supernatants tested over the course of 18 hours, while the Gram negative commensal *E. coli*, the Gram negative pathogen *S. Typhimurium*, and several strains of the genus *Lactococcus* did not produce 5-MIAA in this time frame (Figure 4.15G). Together, these data demonstrate that the *Lactobacillus*-derived small molecule 5-MIAA can activate hepatic Nrf2 and promote transcription of genes involved in the cellular antioxidant response.

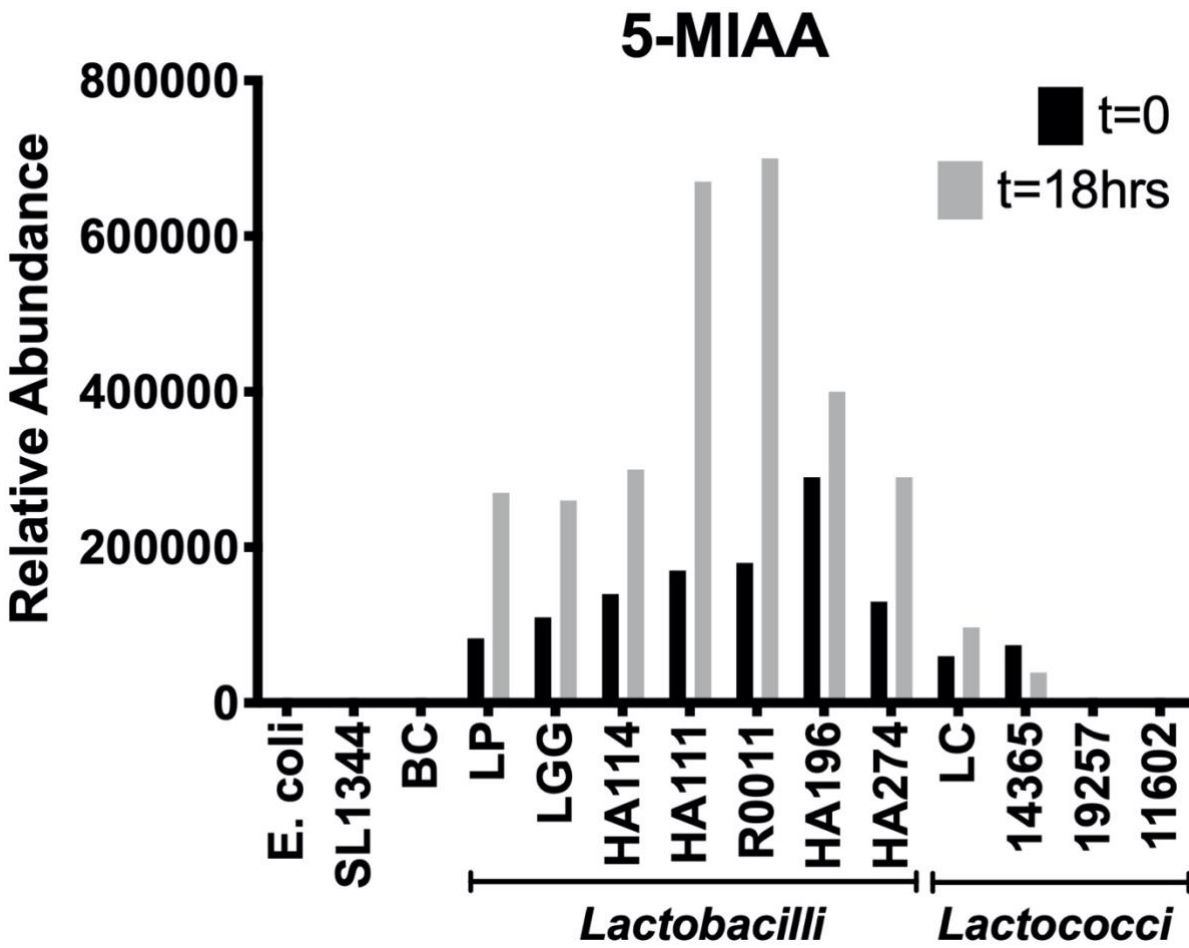


Figure 4.15: Lactobacilli produce 5-MIAA *in vitro*.

Relative abundance of 5-MIAA in culture supernatants of the listed bacteria at t=0 hours (black columns) and t=18 hours (grey columns) of culture.

### 4.3 DISCUSSION

In this study, we demonstrate a previously unappreciated role for the microbiome in altering hepatic xenobiotic and antioxidant responses via activation of the transcription factor Nrf2. Furthermore, we identify *Lactobacilli sp.* as mediators of this effect in part due to their production of 5-methoxyindole acetic acid, which we detected in both culture supernatant from *in vitro* cultures of *Lactobacilli sp.* and in serum extracted from the portal circulation of LGG gavaged animals. Activation of Nrf2 by LGG *in vivo* was functionally protective against oxidative liver injury, as administration of exogenous LGG protected against both acetaminophen-induced hepatotoxicity and acute ethanol toxicity in a Nrf2 dependent manner.

Our data demonstrate commensal-mediated activation of a highly conserved xenobiotic response pathway in two model organisms, *Drosophila melanogaster* and *Mus musculus*. Insects and mammals are highly evolutionarily divergent, yet this signaling is mechanistically conserved, providing further evidence for the importance of gut-resident microbes in modulating systemic health and susceptibility to disease. Our group has demonstrated that ingested microbes can induce activation of Nrf2 and confer cytoprotection of the gut epithelium of both flies and mice when directly contacted by bacteria <sup>37</sup>, suggesting the Nrf2 pathway may have evolved a secondary role in perception and response to the microbiota. The present work shows microbes can stimulate cytoprotective effects systemically and affect a central nexus of biochemical processing with profound effects on host metabolism of ingested xenobiotics.

Recent research has established a role for the gut microbiome in influencing human health and homeostasis, even in organs anatomically distant from the intestine. Indeed, many systemic human diseases affecting hepatic, cardiovascular, and even neuronal tissues can be modulated by the collective microbial structure within the gut (and likely other tissues) <sup>11</sup>. This realization has

prompted attempts to modulate the microbiome therapeutically through the use of probiotics, antibiotics, and fecal microbiota transplant (FMT). Of these, probiotics hold significant promise, with fewer negative sequelae than antibiotics and without the cost and invasiveness of FMT. However, the likely diverse mechanisms by which specific bacteria and their products elicit their distinct beneficial effects remain unknown. Additionally, probiotics have only been shown to be efficacious in very specific clinical scenarios. Therefore, identification of discrete molecular pathways affected by probiotic administration would allow for the more targeted use of probiotics or exploitation of microbial derived small molecules.

Previous studies in mice have shown that the commercially available probiotic *Lactobacillus rhamnosus* GG can improve outcomes in several clinically relevant models of liver injury, including NAFLD <sup>24,43,44</sup> and ALD <sup>41,42,45</sup>. Mechanistically, these effects were attributed to the ability of LGG to alter bile acid signaling and promote barrier function. Indeed, we and others have shown *Lactobacilli* are quite effective at enhancing intestinal epithelial barrier function <sup>48</sup>, suppressing innate inflammatory signaling pathways <sup>49</sup>, and stimulating proliferation <sup>38</sup>, which clearly could contribute to the widely known beneficial effects of treating mice with this microbe. The data presented here add to this body of literature by establishing a novel mechanism by which LGG can alter hepatic networks and consequently modify susceptibility to disease. We identify 5-MIAA as a LGG-derived small molecule inducer of Nrf2, though it is likely that many other small molecules are present within the portal circulation in response to LGG that we could not identify using our specific metabolomic platform. Future studies investigating the proteome, lipidome, and transcriptome of the portal circulation of mice exposed to a range of bacteria will be necessary for us to gain a full understanding of the microbiome-gut-liver axis.

We utilized acetaminophen toxicity, an acute model of oxidative liver injury, to demonstrate the functional importance of LGG-mediated hepatic Nrf2 activation. These data demonstrate that Nrf2 mediates the hepatoprotection observed in LGG pretreated animals after APAP overdose. Importantly, LGG administration does not alter the expression of the cytochrome P450 enzymes necessary for the conversion of APAP to its toxic metabolic byproduct, NAPQI. Additionally, while no significant alteration in hepatocyte proliferation (as measured by PCNA immunohistochemistry) was observed between vehicle and LGG treated mice at 24 hours post-APAP, there was a trend toward more proliferation in LGG-treated animals. These data raise the possibility that hepatic repair mechanisms may be altered and may play a role in models of chronic liver injury. While acetaminophen hepatotoxicity is a clinically important problem <sup>39,50</sup>, the necessity for pretreatment with LGG largely diminishes its therapeutic potential. Nrf2 is protective against many liver insults, and is implicated in the pathogenesis of more chronic conditions such as non-alcoholic fatty liver disease <sup>51</sup>, ALD <sup>52</sup>, and HCC <sup>53</sup>. As these injuries occur over a much longer time frame than acetaminophen overdose, it is possible that probiotics can be used to therapeutically boost Nrf2 activity and the subsequent cytoprotective responses after diagnosis. Several studies have begun to elucidate the utility of LGG in protection from these chronic liver injuries, however the mechanistic importance of Nrf2 has not been investigated. More generally, our observation that specific bacteria can induce hepatic detoxification pathways has additional implications for clinical medicine. It is well known that specific bacterial members of the microbiota can directly metabolize specific ingested pharmacological agents and xenobiotics, resulting in inactivation (or transformation to a toxic form) <sup>15</sup>. Our results suggest that composition of the microbiota, or supplemented bacteria can alter host bioprocessing of xenobiotics with

potentially greater global effects individual pharmacological agents given the wide spectrum of activities induced by the Nrf2 pathway.

In summary, these findings add to our understanding of the functional consequences of the microbiome-gut-liver axis. Furthermore, we establish *Lactobacilli* as potent drivers of hepatic Nrf2 and add to the significant body of literature supporting its potential as a hepatoprotective agent. These data also indicate that the microbiota, aside from specific intrinsic encode biocatalytic activities, are capable of inducing host bioprocessing pathways, with potential consequences on ingested xenobiotics and pharmacological agents.

#### Limitations of Study

While we demonstrate in this study that *Lactobacilli* are capable of activating Nrf2 at a distance via the production of the small molecule 5-MIAA, there are several key limitations that should be noted. First, we only tested a few representative microbes for systemic Nrf2 activation in our *Drosophila* model. These microbes do not cover the gut microbiome as a whole, and it would be interesting to determine what other bacterial taxa have this capability. *Drosophila* have a much more limited microbiome than mammals, with an abundance of aerobes and facultative anaerobes present in the gut and a complete absence of anaerobes<sup>35</sup>. This discrepancy prevents a full screen of all the critical bacterial species present in the murine or human intestine. Another limitation of this study is that analysis of portal serum from LGG treated mice revealed 133 differentially abundant features, of which only 6 were identified. It will be interesting to identify those other small molecules and characterize their Nrf2 activating capacity. Additionally, we only assessed small molecules in this study. Future studies should include analysis of other components of the portal circulation via proteomics and lipidomics.

## **ACKNOWLEDGEMENTS**

**Funding:** This work was supported by the National Institute for Diabetes and Digestive and Kidney Diseases (R01 award AI64462, F30 award DK117570).

## **4.4 METHODS**

### **Mice**

Germ-free C57BL/6 animals were obtained from Taconic and maintained in germ-free isolators under the care of the Emory Gnotobiotic core. Conventional animals were obtained from Jackson Laboratories. Nrf2<sup>fl/fl</sup> animals were obtained from Taconic (Model 13107) and crossed with Alb-Cre hemizygous mice from Jackson Laboratories (Stock #003574). Nrf2 KO mice were Alb-Cre<sup>+/-</sup>, Nrf2<sup>fl/fl</sup> and WT controls were littermate Alb-Cre<sup>-/-</sup>, Nrf2<sup>fl/fl</sup>. Gavage of commensals and probiotics was performed as described previously<sup>37</sup>. Briefly,  $2 \times 10^8$  CFU of LGG or BC was prepared as described below and resuspended in 100  $\mu$ L HBSS and administered via oral gavage to mice. This was performed daily for 14 days prior to sacrifice or administration of APAP or EtOH. All conventional mice utilized for this study were male, 8-10 weeks of age. Mice were maintained as per the approved protocol by the Emory University Animal Care and Use Committee. Mice were maintained at an average temperature of 22° C and a standard 12 hour light/dark cycle (7 am – 7 pm). Mice were fed a standard chow diet (Purina Lab Diets Cat# 5001). Health Status checks were performed daily by veterinary technicians.

### **Conventionalization**

GF Littermates were divided at weaning (3 weeks of age) and half (3 males, 3 females) were maintained in the germ-free isolators for three weeks. The other half of the litter (3 males, 3 females) was transferred out of the isolators and placed in cages containing dirty bedding from the

specific pathogen free (SPF) colony within the same mouse facility. These mice were given three weeks to acquire a microbiome prior to sacrifice and analysis of liver tissue. As all follow up studies in conventional mice were performed in males, no analysis of the sex-specific effects of conventionalization was performed for this study.

### ***Drosophila***

Germ-free *Drosophila* were generated by collecting freshly laid eggs, then incubating in 50% bleach for 5 minutes followed by three 5 minute washes in sterile water. 5 days post-eclosure, GF *Drosophila* were allowed to feed on either GF food or food containing  $2 \times 10^8$  CFU LGG/mL for 3 days. Monocolonized *Drosophila* were then used for experiments. dNrf2 knockdown *Drosophila* were generated using the Gal4 UAS system described previously<sup>54</sup>. Briefly, virgin Yolk-Gal4/cyo *Drosophila* were crossed with male W1118 (control), or UAS-CNCC IR (dNrf2 knockdown). Straight-winged female offspring were collected 5 days post-eclosure and used for experiments. *gstD1-GFP Drosophila* were made germ-free, and early third instar larvae were allowed to feed on GF, *E. coli*, *B. cereus*, LGG, or *L. plantarum* colonized food for 16 hours. All studies in adult *Drosophila* were initiated at 5 days post-eclosure. *Drosophila* were maintained on a 12 hr light/dark cycle (7 am – 7 pm) at 25° C.

### **Cell lines and Culture**

HepG2 cells stably transduced with the ARE-Luciferase construct were purchased from BPS Bioscience. These cells are male in origin. Cells were cultured in Growth medium 1K (MEM medium supplemented with 10% FBS, 1% non-essential amino acids, 1 mM Na-pyruvate, 1% Penicillin/Streptomycin) at 37° C and 5% CO<sub>2</sub>.

### **Mass spectrometry**

Liver samples were collected from GF and CV animals (n = 6 per group), weighed, and metabolites extracted by protein precipitation using acetonitrile (10x volume:tissue). Untargeted metabolomics profiling was performed using liquid chromatography (HILIC or C18 analytical separation) coupled to a Thermo Scientific High-Field Qexactive mass spectrometer (HILIC/ESI+, C18/ESI-, 85-1,275 *m/z*, 120k resolution). Spectral features (*m/z*, retention time) corresponding to identified and uncharacterized metabolites were integrated and aligned using apLCMS/xMSanalyzer software. Statistical analysis was performed using Metaboanalyst<sup>55</sup> and pathway enrichment analysis using Mummichog software<sup>32</sup> and used in combination with a library of > 500 chemicals verified by *m/z*, retention time and MS/MS by authenticated standards. Candidate molecule were identified following ion dissociation experiments on a Thermo Scientific Fusion mass spectrometer, and spectral library matching to the mzCloud library using Compound Discoverer 3.0.

### **RNAsequencing**

RNA-Seq analyses were conducted at the Yerkes NHP Genomics Core on GF (n = 6) and CV liver (n = 6). RNA was isolated from snap frozen liver tissues using the Qiagen RNeasy mini kit (Qiagen) and assessed for integrity and quantity using an Agilent Bioanalyzer (Agilent Technologies) and a NanoDrop 2000 spectrophotometer (Thermo Fisher Scientific). Libraries were prepared using the Illumina TruSeq mRNA stranded kit as per the manufacturer's instructions. Briefly, 500–1,000 ng of Globin-depleted RNA was used for library preparation. ERCC synthetic spike-in controls 1 or 2 (Ambion) were added to each total RNA sample and processed in parallel. Amplified libraries were validated using the Agilent 4200 TapeStation and quantified using a Qubit fluorometer. Libraries were normalized, pooled, followed by clustering on a HiSeq 3000/4000 flowcell using the Illumina cBot. The clustered flowcell was then sequenced

on the Illumina HiSeq 3000 system employing a single-end 101-cycle run, with multiplexing to achieve approximately 20 million reads per sample. Transcript abundance was estimated using htseq-count v0.6.1p1 and differential expression analyses were performed using DESeq2. The upstream transcriptional regulator module in the Ingenuity Pathway Analysis software was used to determine potential transcription factors involved in the observed transcriptional profiles from GF and CV mouse livers.

### **Bacterial cultures and growth conditions**

*Lactobacillus sp.* and *Lactococcus sp.* were grown in de Man, Rogosa, and Sharpe (MRS) broth at 37 degrees Celsius without shaking. *Bacillus cereus* was grown in brain heart infusion (BHI) media with shaking at 37 degrees Celsius. *Escherichia coli* K12 and *Salmonella typhimurium* were grown in LB media with shaking at 37 degrees Celsius for 16 hours prior to administration. For oral gavage, all bacteria were cultured for 16 hours, centrifuged at 3000xg for 5 minutes, the supernatant aspirated, and the pellet washed with one volume HBSS. This was repeated for a total of 3 washes. The bacteria were then resuspended to a final concentration of  $2 \times 10^9$  CFU/mL and 100  $\mu$ L of this was gavaged to animals as described above. For *Drosophila* monocolonization, bacteria were resuspended in food at a final concentration of  $2 \times 10^8$  CFU/mL.

### ***Drosophila* fat body challenge**

For evaluation of dNrf2 activation in the fat body in response to paraquat (PQ) and acetaminophen (APAP), early third instar GST-GFP larvae were fed food containing either H<sub>2</sub>O (vehicle), 15 mM PQ, or 100 mM APAP. 16 hours later, fat bodies were dissected, fixed, and imaged as described above. For survival assays, 5 day old GF, CV, or LGG monocolonized *Drosophila* were transferred to fresh vials containing either H<sub>2</sub>O (vehicle), 15 mM PQ, or 100 mM APAP dissolved in 5% sucrose and 1% agar. Flies were maintained at 25 degrees Celsius and mortality recorded.

## **Immunofluorescence**

Liver samples for immunofluorescence were embedded in OCT (Sakura Rinetek USA) and snap frozen. 5  $\mu$ M sections were fixed in 4% paraformaldehyde. Samples were permeabilized in 0.5% triton-X 100 in PBS and blocked with 5% bovine serum albumin (Sigma Aldrich). The Nrf2 polyclonal rabbit antibody was used at 1:100 in PBS with 0.1% Triton-X and 5% BSA. Samples were incubated in primary antibody overnight at 4 degrees Celsius. Samples were then washed three times and incubated for 1 hour in Alexa-fluor 488 goat anti-rabbit (Invitrogen). Samples were again washed and incubated with DAPI at a concentration of 1:10000 in PBS for 5 minutes. Samples were mounted using Prolong diamond antifade and imaged on Nikon eclipse 80i microscope fitted with a R1 Retiga Q Imaging camera. The images in Figure 4.4 were obtained at 60x magnification at an excitation/emission of 493/519 (Alexa-fluor 488 for Nrf2) and 358/461 (DAPI for nuclei). Colocalization analysis was performed using ImageJ (NIH). For imaging of *Drosophila* fat body, fat bodies were dissected, fixed in 4% PFA and 0.1% NP40 in PBS for 5 minutes, followed by 3 PBS washes. Fat bodies were whole-mounted on glass microscope slides and imaged using Nikon eclipse 80i microscope fitted with a R1 Retiga Q Imaging camera. Quantification of fluorescence intensity was performed using ImageJ software (NIH).

## **Transcriptional analysis**

For transcriptional analysis, whole liver was dissected and snap frozen in liquid nitrogen. Liver was then homogenized using a liquid nitrogen cooled mortar and pestle. 50 mg of liver tissue was mechanically disrupted in Trizol (Invitrogen) using a MagnaLyser with MagnaLyser beads (Roche). For *in vitro* samples from HepG2 cells, cells were lysed directly into Trizol. RNA was prepared according to Trizol manufacturer's instructions. RT-PCR was performed using

SybrGreen supermix (Bio-Rad) using the primers listed in Table S1. Fold change determined using  $2^{-\Delta\Delta Ct}$  method <sup>56</sup>.

### **Acetaminophen challenge**

Mice were fasted overnight (16 hours) with free access to water. Mice were then gavaged with 300 mg/kg or 600 mg/kg acetaminophen dissolved in HBSS with 50% polyethylene glycol. Mice were monitored for distress throughout the course of the assay. At 24 hours post treatment, mice were sacrificed, serum collected for biochemical assays (see below), and liver harvested for histology (FFPE). Histologic analysis of H&E stained sections was performed in a blinded fashion by a board-certified pathologist (BSR). ALT activity was assayed using the ALT Infinity assay (Thermo Scientific) according to manufacturer's instructions. GSH and GSSG were measured from liver tissue using a glutathione assay kit (Cayman Chemical) according to manufacturer's instructions. Formalin-fixed paraffin embedded samples were stained with haematoxylin and eosin and imaged at 10x. 5 images were obtained from each section and percent necrosis calculated by a board-certified pathologist (Brian Robinson, MD/PhD).

### **Ethanol challenge**

Ethanol challenge was carried out as described previously <sup>46,47</sup>. Briefly, mice were fasted overnight (16 hours) with free access to water. Mice were then given an oral gavage of 6 mg ethanol per kg body weight. 6 hours later animals were sacrificed, serum collected for ALT activity assay as described above, and liver harvested. For histologic analysis of steatosis, 5 um thick liver cryosections were formalin fixed and stained with Oil red O. Images were obtained at 20X.

### **ARE-Luciferase Assay**

HepG2 cells stably transduced with the ARE-Luciferase construct were purchased from BPS Bioscience. Cells were exposed to serial dilutions of the indicated compounds for 12 hours and

luciferase detected using the One-Step Luciferase assay system (BPS Bioscience) on a HTX Synergy plate reader (BioTek). Data are represented relative to vehicle control.

### **Western blot analysis**

For analysis of Nrf2 nuclear translocation, HepG2 cells were exposed to 5 mM 5-MIAA for 6 hours. Nuclei were prepared using the NE-PER kit (Thermo-Fisher) according to manufacturer's instructions. Equal protein (as determined by BCA assay (Thermo Scientific)) was run on 4-20% gradient gels and transferred to nitrocellulose membranes. Primary antibodies were incubated in 5% non-fat dry milk in TBS + 0.1% Tween overnight at 4 degrees Celsius at a dilution of 1:1000. The Nrf2 antibody used was rabbit anti-Nrf2 (Abcam). HRP-conjugated anti-rabbit secondary antibodies (GE Healthcare) were used along with Pico substrate (Thermo Scientific). Blots were imaged using KwikQuant digital imager. Densitometry analysis was performed using Image-J software (NIH). Data were normalized to H3 signal.

### **QUANTIFICATION AND STATISTICAL ANALYSIS**

Values are presented as mean +/- SEM. Statistical analyses were performed using GraphPad Prism software. For comparisons of two groups, t-test was used. For *Drosophila* survival studies, the Log-Rank test was used to determine statistical significance. For comparisons of groups of 3 or more, one-way ANOVA was used, followed by Dunnett's multiple comparison test. For unpaired t-tests, F tests were performed to determine equal variances between groups. For one-way ANOVA, the Brown-Forsythe test was performed to determine equal variances between groups. Statistical parameters are stated within the figure legends.

### **DATA AND CODE AVAILABILITY**

The RNA sequencing data generated in this study are available in the Gene Expression Omnibus repository under the accession number GSE145012.

#### 4.5 REFERENCES

1. Human Microbiome Project Consortium. Structure, function and diversity of the healthy human microbiome. *Nature* **486**, 207–214 (2012).
2. Integrative HMP (iHMP) Research Network Consortium. The Integrative Human Microbiome Project. *Nature* **569**, 641–648 (2019).
3. Sartor, R. B. Microbial influences in inflammatory bowel diseases. *Gastroenterology* **134**, 577–594 (2008).
4. Tamboli, C. P., Neut, C., Desreumaux, P. & Colombel, J. F. Dysbiosis as a prerequisite for IBD. *Gut* **53**, 1057 (2004).
5. Carroll, I. M., Ringel-Kulka, T., Siddle, J. P. & Ringel, Y. Alterations in composition and diversity of the intestinal microbiota in patients with diarrhea-predominant irritable bowel syndrome. *Neurogastroenterol. Motil.* **24**, 521–530, e248 (2012).
6. Carroll, I. M. *et al.* Molecular analysis of the luminal- and mucosal-associated intestinal microbiota in diarrhea-predominant irritable bowel syndrome. *Am. J. Physiol. Gastrointest. Liver Physiol.* **301**, G799-807 (2011).
7. Girbovan, A., Sur, G., Samasca, G. & Lupan, I. Dysbiosis a risk factor for celiac disease. *Med. Microbiol. Immunol.* **206**, 83–91 (2017).
8. Couturier-Maillard, A. *et al.* NOD2-mediated dysbiosis predisposes mice to transmissible colitis and colorectal cancer. *J. Clin. Invest.* **123**, 700–711 (2013).
9. Sobhani, I. *et al.* Microbial dysbiosis in colorectal cancer (CRC) patients. *PLoS ONE* **6**, e16393 (2011).

10. Zhan, Y. *et al.* Gut microbiota protects against gastrointestinal tumorigenesis caused by epithelial injury. *Cancer Res.* **73**, 7199–7210 (2013).
11. Ho, J. T. K., Chan, G. C. F. & Li, J. C. B. Systemic effects of gut microbiota and its relationship with disease and modulation. *BMC Immunol.* **16**, 21 (2015).
12. Timsit, Y. E. & Negishi, M. CAR and PXR: the xenobiotic-sensing receptors. *Steroids* **72**, 231–246 (2007).
13. Larigot, L., Juricek, L., Dairou, J. & Coumoul, X. AhR signaling pathways and regulatory functions. *Biochim Open* **7**, 1–9 (2018).
14. Macpherson, A. J., Heikenwalder, M. & Ganal-Vonarburg, S. C. The Liver at the Nexus of Host-Microbial Interactions. *Cell Host Microbe* **20**, 561–571 (2016).
15. Klaassen, C. D. & Cui, J. Y. Review: Mechanisms of How the Intestinal Microbiota Alters the Effects of Drugs and Bile Acids. *Drug Metab. Dispos.* **43**, 1505–1521 (2015).
16. Dawson, P. A. & Karpen, S. J. Intestinal transport and metabolism of bile acids. *J. Lipid Res.* **56**, 1085–1099 (2015).
17. Jiang, C. *et al.* Intestinal farnesoid X receptor signaling promotes nonalcoholic fatty liver disease. *J. Clin. Invest.* **125**, 386–402 (2015).
18. Foley, M. H., O’Flaherty, S., Barrangou, R. & Theriot, C. M. Bile salt hydrolases: Gatekeepers of bile acid metabolism and host-microbiome crosstalk in the gastrointestinal tract. *PLoS Pathog.* **15**, e1007581 (2019).
19. Stewart, G. S. & Smith, C. P. Urea nitrogen salvage mechanisms and their relevance to ruminants, non-ruminants and man. *Nutr Res Rev* **18**, 49–62 (2005).
20. Wang, Z. *et al.* Gut flora metabolism of phosphatidylcholine promotes cardiovascular disease. *Nature* **472**, 57–63 (2011).

21. Romano, K. A., Vivas, E. I., Amador-Noguez, D. & Rey, F. E. Intestinal microbiota composition modulates choline bioavailability from diet and accumulation of the proatherogenic metabolite trimethylamine-N-oxide. *MBio* **6**, e02481 (2015).
22. Schugar, R. C., Willard, B., Wang, Z. & Brown, J. M. Postprandial gut microbiota-driven choline metabolism links dietary cues to adipose tissue dysfunction. *Adipocyte* **7**, 49–56 (2018).
23. de Faria Ghetti, F. *et al.* Influence of gut microbiota on the development and progression of nonalcoholic steatohepatitis. *Eur J Nutr* **57**, 861–876 (2018).
24. Perumpail, B. J. *et al.* The Therapeutic Implications of the Gut Microbiome and Probiotics in Patients with NAFLD. *Diseases* **7**, (2019).
25. Cassard, A.-M. & Ciocan, D. Microbiota, a key player in alcoholic liver disease. *Clin Mol Hepatol* **24**, 100–107 (2018).
26. Roderburg, C. & Luedde, T. The role of the gut microbiome in the development and progression of liver cirrhosis and hepatocellular carcinoma. *Gut Microbes* **5**, 441–445 (2014).
27. Wan, M. L. Y. & El-Nezami, H. Targeting gut microbiota in hepatocellular carcinoma: probiotics as a novel therapy. *Hepatobiliary Surg Nutr* **7**, 11–20 (2018).
28. Moi, P., Chan, K., Asunis, I., Cao, A. & Kan, Y. W. Isolation of NF-E2-related factor 2 (Nrf2), a NF-E2-like basic leucine zipper transcriptional activator that binds to the tandem NF-E2/AP1 repeat of the beta-globin locus control region. *Proc. Natl. Acad. Sci. U.S.A.* **91**, 9926–9930 (1994).
29. Sykiotis, G. P. & Bohmann, D. Keap1/Nrf2 signaling regulates oxidative stress tolerance and lifespan in *Drosophila*. *Dev. Cell* **14**, 76–85 (2008).

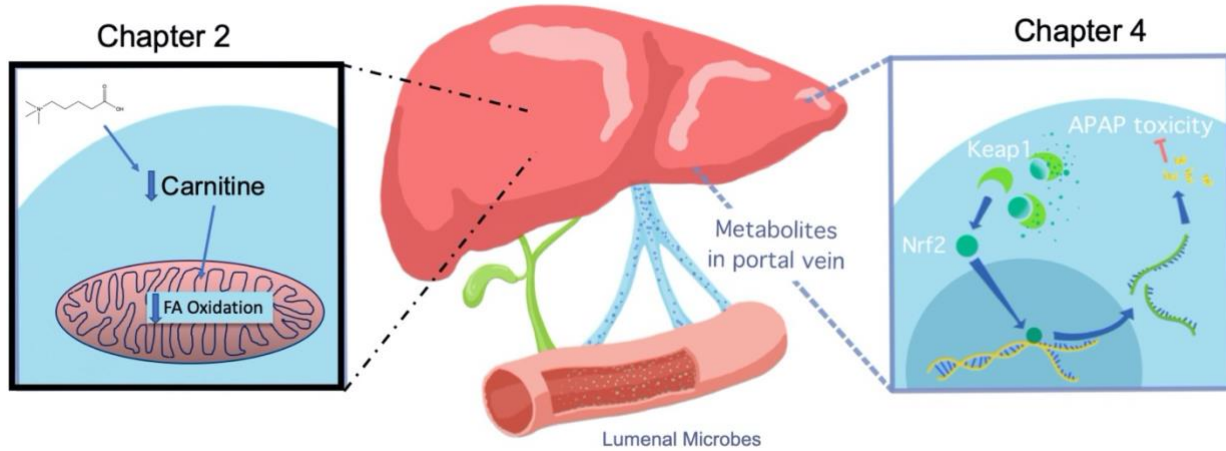
30. Liu, K. H. *et al.* High-Resolution Metabolomics Assessment of Military Personnel: Evaluating Analytical Strategies for Chemical Detection. *J. Occup. Environ. Med.* **58**, S53-61 (2016).
31. Go, Y.-M. *et al.* Mitochondrial metabolomics using high-resolution Fourier-transform mass spectrometry. *Methods Mol. Biol.* **1198**, 43–73 (2014).
32. Li, S. *et al.* Predicting network activity from high throughput metabolomics. *PLoS Comput. Biol.* **9**, e1003123 (2013).
33. Lin, R., Liu, W., Piao, M. & Zhu, H. A review of the relationship between the gut microbiota and amino acid metabolism. *Amino Acids* **49**, 2083–2090 (2017).
34. Ramezani, A. *et al.* Role of the Gut Microbiome in Uremia: A Potential Therapeutic Target. *Am. J. Kidney Dis.* **67**, 483–498 (2016).
35. Douglas, A. E. The *Drosophila* model for microbiome research. *Lab Anim (NY)* **47**, 157–164 (2018).
36. Søndergaard, L. Homology between the mammalian liver and the *Drosophila* fat body. *Trends Genet.* **9**, 193 (1993).
37. Jones, R. M. *et al.* Lactobacilli Modulate Epithelial Cytoprotection through the Nrf2 Pathway. *Cell Rep* **12**, 1217–1225 (2015).
38. Jones, R. M. *et al.* Symbiotic lactobacilli stimulate gut epithelial proliferation via Nox-mediated generation of reactive oxygen species. *EMBO J.* **32**, 3017–3028 (2013).
39. Bunchorntavakul, C. & Reddy, K. R. Acetaminophen (APAP or N-Acetyl-p-Aminophenol) and Acute Liver Failure. *Clin Liver Dis* **22**, 325–346 (2018).
40. Hosamani, R. & Muralidhara. Acute exposure of *Drosophila melanogaster* to paraquat causes oxidative stress and mitochondrial dysfunction. *Arch. Insect Biochem. Physiol.* **83**, 25–40 (2013).

41. Chen, R.-C. *et al.* Lactobacillus rhamnosus GG supernatant promotes intestinal barrier function, balances Treg and TH17 cells and ameliorates hepatic injury in a mouse model of chronic-binge alcohol feeding. *Toxicol. Lett.* **241**, 103–110 (2016).
42. Forsyth, C. B. *et al.* Lactobacillus GG treatment ameliorates alcohol-induced intestinal oxidative stress, gut leakiness, and liver injury in a rat model of alcoholic steatohepatitis. *Alcohol* **43**, 163–172 (2009).
43. Kim, B. *et al.* Protective effects of Lactobacillus rhamnosus GG against dyslipidemia in high-fat diet-induced obese mice. *Biochem. Biophys. Res. Commun.* **473**, 530–536 (2016).
44. Ritze, Y. *et al.* Lactobacillus rhamnosus GG protects against non-alcoholic fatty liver disease in mice. *PLoS ONE* **9**, e80169 (2014).
45. Wang, Y. *et al.* Lactobacillus rhamnosus GG treatment potentiates intestinal hypoxia-inducible factor, promotes intestinal integrity and ameliorates alcohol-induced liver injury. *Am. J. Pathol.* **179**, 2866–2875 (2011).
46. Chen, P. *et al.* Microbiota Protects Mice Against Acute Alcohol-Induced Liver Injury. *Alcohol. Clin. Exp. Res.* **39**, 2313–2323 (2015).
47. Wang, Y. *et al.* Lactobacillus rhamnosus GG culture supernatant ameliorates acute alcohol-induced intestinal permeability and liver injury. *Am. J. Physiol. Gastrointest. Liver Physiol.* **303**, G32-41 (2012).
48. Swanson, P. A. *et al.* Enteric commensal bacteria potentiate epithelial restitution via reactive oxygen species-mediated inactivation of focal adhesion kinase phosphatases. *Proc. Natl. Acad. Sci. U.S.A.* **108**, 8803–8808 (2011).

49. Collier-Hyams, L. S., Sloane, V., Batten, B. C. & Neish, A. S. Cutting edge: bacterial modulation of epithelial signaling via changes in neddylation of cullin-1. *J. Immunol.* **175**, 4194–4198 (2005).
50. Larson, A. M. *et al.* Acetaminophen-induced acute liver failure: results of a United States multicenter, prospective study. *Hepatology* **42**, 1364–1372 (2005).
51. Chambel, S. S., Santos-Gonçalves, A. & Duarte, T. L. The Dual Role of Nrf2 in Nonalcoholic Fatty Liver Disease: Regulation of Antioxidant Defenses and Hepatic Lipid Metabolism. *Biomed Res Int* **2015**, 597134 (2015).
52. Lamlé, J. *et al.* Nuclear factor-eythroid 2-related factor 2 prevents alcohol-induced fulminant liver injury. *Gastroenterology* **134**, 1159–1168 (2008).
53. Yates, M. S. & Kensler, T. W. Keap1 eye on the target: chemoprevention of liver cancer. *Acta Pharmacol. Sin.* **28**, 1331–1342 (2007).
54. Duffy, J. B. GAL4 system in Drosophila: a fly geneticist's Swiss army knife. *Genesis* **34**, 1–15 (2002).
55. Xia, J. & Wishart, D. S. Using MetaboAnalyst 3.0 for Comprehensive Metabolomics Data Analysis. *Curr Protoc Bioinformatics* **55**, 14.10.1-14.10.91 (2016).
56. Schmittgen, T. D. & Livak, K. J. Analyzing real-time PCR data by the comparative C(T) method. *Nat Protoc* **3**, 1101–1108 (2008).

# Chapter 5

## Discussion and Future Directions



## 5.1 DISCUSSION

The gut microbiome has been called the “forgotten organ<sup>1</sup>.” While not essential to the survival of the host, it does fine-tune host fitness. The metabolic activities intrinsic to intestinal bacteria improve nutrient harvest from the diet<sup>2</sup>, produce myriad small molecules that affect host signaling<sup>3</sup>, and may even detoxify caustic ingested compounds<sup>4</sup>. These activities have immense physiological consequences, which have been teased out in studies utilizing germ-free mice and other model organisms. In support of these findings, dysbiosis is frequently observed in human disease and has been proposed as a potential disease modifying factor in cases in which no other genetic or environmental factors appear to be at play<sup>5</sup>. With this in mind, clinicians and researchers have deployed a host of microbiome-modifying therapies to attempt to treat human diseases.

Antibiotics can eliminate pathogenic bacteria or tamp down bacterial overgrowth and are beneficial in many clinical scenarios. However, they also deplete beneficial bacteria and interfere with the complex community architecture of the intestinal microbiome<sup>6</sup>. This can, at its worst, open a niche for the bloom of pathogenic bacteria, such as *C. difficile*<sup>7</sup>.

Fecal microbiota transplant (FMT) is a therapeutic modality with immense promise that has gained surprising traction in popular culture. Beyond its use for the treatment of *C. difficile*, it has been proposed (within the scientific community) as a potential therapy for other intestinal disorders associated with dysbiosis, such as irritable bowel syndrome and inflammatory bowel diseases. Outside of mainstream microbiome research (no pun intended), FMT has been touted as a cure-all for intractable medical maladies. Blogs are dedicated to the benefits of FMT for indications well outside of the narrow diagnosis of recurrent *C. difficile*<sup>9</sup>. And while clinicians may be limited in their ability to dole out FMTs, there is a small, dark corner of the web that provides instructions for the avid Do-It-Yourselfer. Despite this bolus of testimonials, controlled clinical

trials have found mostly mixed and negative results when it comes to the use of FMT outside of treatment of recurrent *C. difficile*s.

Probiotics are another potential mode by which clinicians can modify the microbial communities in our gut<sup>10</sup>. Probiotics can be given orally and in pill form, making them more cost effective than FMT, and have relatively few negative sequelae compared to antibiotic use. However, their efficacy, just like FMT, does not measure up to the hype<sup>11</sup>.

Despite its moniker as “the forgotten organ,” study of the microbiome comes with more challenges than that of a classical organ system. Far from being a discrete set of genetically homogenous cells, like host tissues, the microbiome is a dynamic and ever-changing community of microbes, fungi, and viruses<sup>12</sup>. Microbes compete and rely on each other for resources, in addition to being tamed against the onslaught of neutralizing antibodies and antimicrobial peptides secreted by the host. This interplay complicates the use of any of the microbiome-based therapies outlined above. Without detailed molecular insight into the mechanisms behind the observed functional effects of the microbiome, it is unlikely that we can reproduce a clinical scenario in which modulation of the microbiome would have benefit in humans. The studies included herein add to that understanding in 3 distinct ways.

In Chapter 2, we identified a discrete microbiome-derived small molecule and characterized its effect on hepatic metabolism. In Chapter 3, we developed a model of oxidative liver injury in *Drosophila*, providing a high-throughput system for the identification of disease-modifying effects of the microbiome. In Chapter 4, we characterized the effects of the microbiome on hepatic signaling, identified the microbial species responsible, and demonstrated a therapeutic benefit of exogenous administration of those species. Together, these studies represent a small contribution to a burgeoning field and can be significantly extended as outlined below.

## 5.2 FUTURE DIRECTIONS

In Chapter 2 we identified the microbiome-derived small molecule  $\delta$ -valerobetaine, which is absent in germ-free mice and acts on the host to lower circulating and cellular carnitine. This, in turn, inhibits systemic hepatic fatty acid oxidation and exacerbates hepatic steatosis after an overnight fast. Historically, this may have been an evolutionary advantage as food was scarce and preservation of adipose stores was paramount. Indeed, conventional mice are more resistant to starvation than genetically identical germ-free animals<sup>13</sup>. However, high levels of VB and the consequent brake on fatty acid oxidation may contribute to metabolic syndrome, fatty liver disease, diabetes, and other pathologies associated with our current epidemic of obesity. In support of this hypothesis we found that circulating VB was correlated with central adiposity and severity of fatty liver disease in humans.

A major weakness of this study is the lack of a clear mechanism. We currently do not understand how VB decreases carnitine levels. Preliminary data suggest that it may inhibit carnitine reuptake in the kidney, as VB treated animals have an increase in urinary carnitine. However, it may also be acting at the level of carnitine synthesis. Given its structural similarity to the carnitine precursor butyrobetaine, VB may be inhibiting carnitine synthesis by interacting with BBOX, the enzyme that converts butyrobetaine into carnitine. Further experiments are necessary to determine the relative contribution of these mechanisms to the carnitine lowering effects of VB.

Mechanism aside, it is clear that VB alters host fatty acid oxidation. This is likely a negative metabolic outcome in obese patients that are trying to burn fat to lose weight. The obvious approach to deplete VB is to deplete the microbiome. This could be done in an untargeted way, i.e. through the use of antibiotics. However, for all of the reasons stated above, antibiotic therapy is likely not the most viable path forward. Furthermore, broad-spectrum antibiotic treatment of

mice did not decrease circulating VB levels. This is likely due to the promiscuous production of VB by diverse bacteria (illustrated in Figure 2.3B).

Instead of targeting and depleting distinct bacterial species, it may be possible to target and inhibit the conserved metabolic pathway for the production of VB. This would require the elucidation of steps required for VB production by bacteria, followed by rational drug design to inhibit those steps in all responsible bacteria. Alternatively, it may be possible to perform a high-throughput compound screen on known VB producing bacteria. These culture supernatants could be screened for VB production as shown in Figure 2.3. Finally, our data demonstrate that the effects of VB could be rescued by addition of exogenous carnitine. Perhaps the most pragmatic approach, if not the most scientifically satisfying, is to stratify patients based on VB status and simply treat with exogenous carnitine. Indeed, this approach has already shown promise<sup>14</sup>.

In Chapter 3 we characterized a novel *Drosophila* model of acetaminophen toxicity. We demonstrate for the first time that acetaminophen (APAP) causes dose-dependent mortality in *Drosophila*. Similar to mammalian systems, APAP resulted in a rapid production of reactive oxygen species in the fat body. Toxicity could be attenuated or augmented using genetic or pharmacologic approaches that have been validated in murine models. Finally, we used this model to pilot an investigation of the effect of antibiotics and age on APAP toxicity.

This represents steps toward validation of this APAP model in *Drosophila*. However, further use of this system will be essential to determine its utility in modeling mammalian disease. For example, while fat body specific depletion of certain antioxidant genes (Nrf2, Trx1) did augment mortality, it is unclear if the fat body is the only organ affected by APAP. Analysis of intestinal tissue, as well as other systemic tissues, will be important.

Other exciting future directions include performing deficiency screens to identify novel genetic modifiers of APAP susceptibility. This will deepen our understanding of the exact mechanisms of APAP toxicity, which are still incompletely understood. Current treatment for APAP overdose is limited and mainly centered on supportive care. This model can easily be adapted for screening of compound libraries to identify potential therapeutics for APAP. Finally, *Drosophila* are a powerful tool for untangling the complex effects of the microbiome on host susceptibility to disease. The data presented in Chapter 3 already demonstrate that the microbiome is protective against APAP toxicity. To assess the impact of individual microbes, a more comprehensive monocolonization study can be performed.

In Chapter 4, we identify a previously uncharacterized role for gut-resident *Lactobacilli* in activating hepatic Nrf2 and the subsequent antioxidant response pathway. This activation was sufficient to protect against two different models of acute oxidative liver injury, namely acetaminophen overdose and acute ethanol toxicity. Furthermore, Nrf2 was necessary for this protection. We characterized the small molecules present in the portal circulation of LGG-treated mice and identified 5-methoxyindole acetic acid as a *Lactobacillus*-derived metabolite capable of activating Nrf2. Several key aspects of this study require further investigation.

First, while only *Lactobacilli* produced 5-MIAA, it is unclear if they are wholly responsible for the increase in Nrf2 signaling observed in conventional animals relative to germ-free. Monocolonization of germ-free animals with representative *Lactobacilli*, such as LGG, would be helpful in clarifying this point. While the screen of bacterial supernatants performed in Figure 4.15 did include several diverse representatives of the host microbiome, it was by no means an exhaustive screen. Analysis of other intestinal microbes, especially anaerobes that were not investigated in this study, may be revealing.

Second, the small molecule precursor and metabolic pathway necessary for 5-MIAA production was not identified. It would be interesting to increase precursor abundance (i.e. through dietary supplementation) and see if Nrf2 activation can be driven in this manner. Additionally, we could genetically manipulate LGG to mutate the pathway necessary for 5-MIAA production and determine the effect on hepatic Nrf2 activation and protection from liver injury.

Third, of the 136 features increased in the portal serum by LGG administration, we only positively identified 6 compounds. The identities and activities of those other features should be investigated. Furthermore, we only utilized small molecule metabolomics to characterize the portal serum. Future studies using lipidomics, transcriptomics, and proteomics may reveal dramatic changes that we missed using our narrow approach.

Finally, it is likely that there are many more effects of exogenous *Lactobacillus* administration on the host. We focused on the liver due to its close proximity to the intestine, but there are already myriad studies that demonstrate that gut microbes alter host physiology in nearly every organ. A more detailed mechanistic understanding of how these effects are elicited may make the use of probiotics in clinical practice a viable option.

### 5.3 REFERENCES

1. O'Hara, A. M. & Shanahan, F. The gut flora as a forgotten organ. *EMBO Rep.* **7**, 688–693 (2006).
2. Krajmalnik-Brown, R., Ilhan, Z.-E., Kang, D.-W. & DiBaise, J. K. Effects of gut microbes on nutrient absorption and energy regulation. *Nutr Clin Pract* **27**, 201–214 (2012).
3. Lee, W.-J. & Hase, K. Gut microbiota-generated metabolites in animal health and disease. *Nat. Chem. Biol.* **10**, 416–424 (2014).
4. Nichols, R. G., Peters, J. M. & Patterson, A. D. Interplay Between the Host, the Human Microbiome, and Drug Metabolism. *Hum. Genomics* **13**, 27 (2019).
5. Carding, S., Verbeke, K., Vipond, D. T., Corfe, B. M. & Owen, L. J. Dysbiosis of the gut microbiota in disease. *Microb. Ecol. Health Dis.* **26**, 26191 (2015).
6. Becattini, S., Taur, Y. & Pamer, E. G. Antibiotic-Induced Changes in the Intestinal Microbiota and Disease. *Trends Mol Med* **22**, 458–478 (2016).
7. Leffler, D. A. & Lamont, J. T. Clostridium difficile infection. *N. Engl. J. Med.* **372**, 1539–1548 (2015).
8. D'Haens, G. R. & Jobin, C. Fecal Microbial Transplantation for Diseases Beyond Recurrent Clostridium Difficile Infection. *Gastroenterology* **157**, 624–636 (2019).
9. Fecal Transplant Resources Guide: 40+ Articles, Podcasts, and Sites.  
<https://designershitdocumentary.com/fmt-resources-guide/>.
10. Plaza-Diaz, J., Ruiz-Ojeda, F. J., Gil-Campos, M. & Gil, A. Mechanisms of Action of Probiotics. *Adv Nutr* **10**, S49–S66 (2019).
11. Suez, J., Zmora, N., Segal, E. & Elinav, E. The pros, cons, and many unknowns of probiotics. *Nat. Med.* **25**, 716–729 (2019).

12. Human Microbiome Project Consortium. Structure, function and diversity of the healthy human microbiome. *Nature* **486**, 207–214 (2012).
13. Tennant, B., Malm, O. J., Horowitz, R. E. & Levenson, S. M. Response of germfree, conventional, conventionalized and *E. coli* monocontaminated mice to starvation. *J. Nutr.* **94**, 151–160 (1968).
14. Askarpour, M. *et al.* Beneficial effects of l-carnitine supplementation for weight management in overweight and obese adults: An updated systematic review and dose-response meta-analysis of randomized controlled trials. *Pharmacol. Res.* **151**, 104554 (2020).